

**IN-VITRO OPTICALLY AIDED ROBOTIC MANIPULATION (IVOARM)
SYSTEM AND ALGORITHM DEVELOPMENT**

CHENG CHIA LOON

UNIVERSITI TUNKU ABDUL RAHMAN

DECLARATION

I hereby declare that this project report is based on my original work except for citations and quotations which have been duly acknowledged. I also declare that it has not been previously and concurrently submitted for any other degree or award at UTAR or other institutions.

Signature : _____

Name : CHENG CHIA LOON

ID No. : 08UEB07098

Date : 15 April 2011

APPROVAL FOR SUBMISSION

I certify that this project report entitled “**IN-VITRO OPTICALLY AIDED ROBOTIC MANIPULATION**” was prepared by **CHENG CHIA LOON** has met the required standard for submission in partial fulfilment of the requirements for the award of Bachelor of Engineering (Hons.) Mechatronics Engineering at Universiti Tunku Abdul Rahman.

Approved by,

Signature : _____

Supervisor: Dr.Tan Ching Seong

Date : 15 April 2011

The copyright of this report belongs to the author under the terms of the copyright Act 1987 as qualified by Intellectual Property Policy of University Tunku Abdul Rahman. Due acknowledgement shall always be made of the use of any material contained in, or derived from, this report.

© 2011, Cheng Chia Loon. All right reserved.

Specially dedicated to
my beloved grandmother, mother and father

ACKNOWLEDGEMENTS

I would like to express my deep and sincere gratitude to my supervisor Dr. Tan Ching Seong, His wide knowledge and logical way of thinking have been of great value for me. His understanding, encouraging and personal guidance have provided a good basis for the present thesis.

In addition, I would also like to express my gratitude to my loving parent and friends who had helped and given me encouragement to successfully complete my final year project in less a year.

Beside that, I would like to say thousand thanks to main organiser for Innovate Malaysia Competition – Agilent Track, Agilent Technologies Malaysia. Who given us technical supports and provide necessary Instruments made us to complete our final year project and competition.

I warmly thank Mr. Lim See Wei, Experienced Electronics Engineer from DDMan Sdn Bhd. for his valuable advice and friendly help in my algorithms development and circuit design. His extensive discussions around my work and interesting explorations in operations have been very helpful for this project.

Here, I would like to thanks to Mr.Chia Kok Siang for the past 10 months for co-operation in our Final Year Project. I am also indebted to University Tunku Abdul Rahman (UTAR) for its administrative work for making the final year project so successful.

IN-VITRO OPTICALLY AIDED ROBOTIC MANIPULATION (IVOARM) SYSTEM AND ALGORITHM DEVELOPMENT

ABSTRACT

In-Vitro Optically Aided Robotic Manipulation (IVOARM) constitutes a blind grasping concept using two anthropomorphic fingers with the aid of the directional force sensors and infra-red sensors mounted on it. This manipulator is controlled by an embedded system with high DSP compatibility. The infra-red sensors are mounted on the surface of the finger gripper to detect the presence of the object in the area of the grasping. The physical information of the object such as size and Centroid of the object is determined using the algorithm developed with the aid by the infra red sensors. The purpose of determining the Centroid is to determine the size and method to grasp the object. The result of the object size determination using the IVOARM has been obtained. Based on the size of the object obtained from the calculation, the object will be decided to be gripped in either full envelope gripping or finger tip gripping. Force will be calculated to ensure proper force to be applied.

TABLE OF CONTENTS

DECLARATION	I
APPROVAL FOR SUBMISSION	II
ACKNOWLEDGEMENTS	III
ABSTRACT	IV
TABLE OF CONTENTS	V
LIST OF TABLES	VI
LIST OF FIGURES	VII
LIST OF SYMBOLS / ABBREVIATIONS	VIII
LIST OF APPENDICES	IX

CHAPTER

1	INTRODUCTION	1
	1.1 Background	1
	1.2 Aims and Objectives	2
	1.3 Outline of the Final Year Project	3
2	LITERATURE REVIEW	4
	2.1 Introduction	4
	2.2 Robot Grasping of Unkown objects, Description and Validation of the Funciton with Quadriplegic People	5
	2.2.1 Flow chart	6
	2.2.2 Distance Estimation	6
	2.2.3 Feature extraction	7

	2.2.4	Matching and localization	8
	2.2.3	Evaluation	9
2.3		High Performance Robotic Gripper Based on Choice of Feedback Variables	9
	2.3.1	Mechanical design	10
	2.3.2	Sensors	10
		2.3.2.1 Force sensor	10
		2.3.2.2 Slip sensor	11
		2.3.2.3 Evaluation	11
2.3		Design and Construction of a Robotic Gripper for Activities of Daily Living for People with Disabilities	11
	2.4.1	Mechanical Design	12
		2.4.1.1 Mechanical Movement	12
	2.4.2	Evaluation	14
3		METHODOLOGIES	15
	3.1	Project Design Overview	15
	3.2	The System	16
	3.3	Project Management	18
		3.3.1 Gantt chart	19
	3.4	List of Tools	20
		3.4.1 List of hardware	20
		3.4.2 List of software	21
4		ELECTRONIC CIRCUIT SYSTEMS	22
	4.1	Electronic Components Selection	22
		4.1.1 Selection of distance sensor	22
		4.1.2 Selection of force sensor	23

4.2	Electronic circuit system design	24
4.2.1	Infra-Red Distance Detector	24
4.2.2	Infra-Red Object Detector	26
4.2.3	Force Sensing Resistor	27
4.3	Circuit Design	28
4.3.1	Main Board	28
	4.3.1.1 Servo Controlling using the NPN Transistor	29
4.3.2	FSR board	31
	4.3.2.1 Working Principles of the FSR board	31
	4.3.2.2 Voltage Divider Formula	32
	4.3.2.3 Voltage Follower	32
4.3.3	Infra-Red Object Detector Board	33
	4.3.3.1 Working principles of the IROD board	34
4.4	Imprint on PCB Board	36
4.4.1	Fabrication Process of PCB	37
5	ALGORITHM DEVELOPMENT	38
5.1	Problem Identification	38
5.2	Selection of Embedded System	38
	5.2.1 Selection of Compiler	40
5.3	System Architecture	41
5.4	Algorithm	41
	5.4.1 Search Algorithm	41
	5.4.1.1 Exploring Mode	42
	5.4.1.2 Grasping Mode	42
	5.4.2 Formulate the Searching Algorithm on Draft Paper	45
	5.4.3 Object Centroid and Diameter Calculation by using Forward Kinematics	46
5.5	Equation Formulation	47
	5.5.1 FSR Equation Formulation	47

5.5.2	IRDD Equation Formulation	48
5.6	Servo Motor Control	49
5.6.1	Initial design of Servo Control Signal	49
5.6.2	RTC PWM Generator	50
5.7	Collision Prevention System	52
5.8	Test and Validate	53
6	RESULT AND DISCUSSION	54
6.1	Results	54
6.1.1	Object Colour Detection	55
6.1.2	Detection of Object at Different Temperatures	56
6.1.3	Colour Intensity response on Infra-Red Object Detector	59
6.1.4	Experiment and Result on Object Diameter Estimation	60
6.2	Discussions	62
6.2.1	FSR Respond	62
6.2.2	Suggestion of Noise Filtering	63
6.2.3	Problem of circuits constructed with Veroboard	63
6.2.4	Problem of using Agilent VEE Pro	65
6.3	Precautions	66
6.3.1	Wire Selection	66
6.3.2	Wiring covered by Cable Protector	67
6.3.3	Labelling each wire with suitable name	67
6.3.4	Programming separate into main program and sub program	68
6.3.5	Soldering Techniques	69
6.3.6	Component Selection	69
6.3.7	Power Supply Management	70
6.2.2	Testing and Troubleshooting	70

7	CONCLUSION	71
7.1	Conclusion	71
7.2	Recommendations	72
7.2.1	High speed Grasping with Force Control	72
7.2.2	Implement a Colour Sensor	72
7.2.3	Implement Artificial Intelligence on Search Algorithm	73
7.2.3	Shape Recognition for IVOARM	73
7.3	Publication on Symposium (6 th MCSOCs)	73
	REFERENCES	80
	APPENDICES	83

LIST OF TABLES

TABLE	TITLE	PAGE
Table 3.1:	List of the hardwares'	20
Table 3.2:	Functions of software	21
Table 4.1:	Comparison of Ultrasonic Range Finder and the SHARP GP2D120.	23
Table 4.2:	Comparison of Force Sensors' Characteristic	24
Table 5.1:	The comparison of Embedded System	38
Table 5.2:	Mode descriptions	44
Table 6.1:	Distance detected on different colour	59
Table 6.2:	Experimental result on White Can Diameter	60
Table 6.3:	Experimental results on Black Can Diameter	61

LIST OF FIGURES

FIGURE	TITLE	PAGE
Figure 2.1:	The flow chart on the MADEUS operation (adopted from Christophe Leroux, et al, 2007)	6
Figure 2.2:	The feature extraction on the MADEUS operation (adopted from Christophe Leroux, et al, 2007)	7
Figure 2.3:	The matching and localization (adopted from Christophe Leroux, et al, 2007)	8
Figure 2.4:	The mechanical desgin of the HPRG gripper (adopted from Christopher Leroux, et al, 2007)	10
Figure 2.5:	Manus gripper internal mechanical part (adopted from Redwan Alqasemi, et al, 2007)	11
Figure 2.6:	Manus gripper internal mechanical part movement (adopted from Redwan Alqasemi, et al, 2007)	12
Figure 2.7:	Various finger tip of the Manus Gripper (adopted from Redwan Alqasemi, et al, 2007)	13
Figure 3.1:	Flowchart of electronic circuit system desgin	15
Figure 3.2:	Flowchart of algorithm desgin	16
Figure 3.3:	IVOARM system overview	17
Figure 3.4:	POLC process flow	18
Figure 3.5:	Part of hardware's in project	20
Figure 3.6:	List of software	21
Figure 4.1:	Distance detection on object colour intensity (Adopted from <i>Sharpsma</i> , 2011)	25

Figure 4.2: The TCRT5000 outlook and internal diagram (Adopted from Vishay Semiconductor, 2011)	26
Figure 4.3: Force resistor internal layout structure (Adopted from Versa Point Technology, 2011)	27
Figure 4.4: Force applied on the FSR (Adopted from Versa Point Technology, 2011)	27
Figure 4.5: Complete schematic view of the main board	28
Figure 4.6: Voltage supply and voltage regulator in main board	29
Figure 4.7: The simplified NPN working principle	30
Figure 4.8: Virtual testing on the designed circuit using NI Multisim virtual multimeter	30
Figure 4.9: Complete schematic view of the FSR board	31
Figure 4.10: Voltage divider with voltage follower	31
Figure 4.11: Simplified voltage divider	32
Figure 4.12: Simplified voltage follower	32
Figure 4.13: Virtual measurement on virtual circuit of FSR using NI Multisim	33
Figure 4.14: FSR circuit desgin with breadboard	33
Figure 4.15: Complete schematic view of Infra-Red Object Detector board	34
Figure 4.16: Working principle of Infra-Red Object Detector circuit	34
Figure 4.17: PCB desing in Altium Designer, blue colour indicates connection routes, yellow colour indicates components and green colour indicates components pin holes	36
Figure 4.18: Procedure of PCB fabrication process	37
Figure 5.1: Explorer 16 Development Board for dsPIC	39
Figure 5.2: System Architecture of IVOARM	41
Figure 5.3: Algorithm of IVOARM	42

Figure 5.4: Draft and proof the algorithm concept on graph paper	45
Figure 5.5: Centroid calculation method	46
Figure 5.6: Average FSR response	48
Figure 5.7: Initial servo control signal	50
Figure 5.8: RTC PWM servo control	51
Figure 5.9: The signal sequence input controlled by RTC timer	51
Figure 5.10: Collision Prevention System	52
Figure 5.11: Diameter of object display through LED	53
Figure 6.1: Study affection of IRDD	54
Figure 6.2: White colour detection	54
Figure 6.3: Black colour detection	55
Figure 6.4: The photo taken during experiment	56
Figure 6.5: Detection of empty beaker at normal temperature	57
Figure 6.6: Detection of beaker filled with cold water of 0 degree Celsius	57
Figure 6.7: Detection of beaker filled with hot water of 76 degree Celsius	57
Figure 6.8: Screenshot of Exploring Mode and Grasping Mode	60
Figure 6.9: Force response of the IVOARM finger gripper on the surface object	62
Figure 6.10: Noise disturbance in force response	63
Figure 6.11: Loose connectivity of Veroboard	64
Figure 6.12: Electronic circuit soldered in Veroboard	64
Figure 6.13: Development of program in Agilent VEE Pro	65
Figure 6.14: Suspected problem of Agilent VEE Pro serial communication	66
Figure 6.15: Solid core wire (left) and Stranded wire	67

Figure 6.16: Wire covered by cable protector	67
Figure 6.17: Labelling wire with suitable name	68
Figure 6.18: Separate program into main program and sub program	68
Figure 6.19: Proper soldering techniques (adopted from Fred Martin, 1998)	69
Figure 6.20: Improper soldering techniques (adopted from Fred Martin, 1998)	69
Figure 7.1: Implement colour response to IVOARM	72

LIST OF SYMBOLS / ABBREVIATIONS

AI	Artificial Intelligence
ALU	Arithmetic Logic Unit
°C	Celsius
CAD	Computer Aided Design
CAN	Controller Area Network
<i>cm</i>	centimetre
CNC	Computer Numerical Control
DAQ	Data Acquisition
DC	Direct Current
DSC	Digital Signal Controller
DSP	Digital Signal Processing
dsPIC	digital signal Programmable Interface Controller
FSR	Force Sensing Resistor
GUI	Graphical User Interface
<i>g</i>	force, in unit gram(s)
Hz	Hertz
INSTR	Instruments symbol in Agilent Technologies equipment
I/O	Input/ Output
IRDD	Infra-Red Distance Detector
IROD	Infra-Red Object Detector
IVOARM	In-Vitro Optical Aided Robotic Manipulation
JTAG	Joint Test Action Group
LED	Light Emitting Diode
<i>m</i>	meter
MCLR	Master Clear of instruction
MCU	Microcontroller
<i>mm</i>	millimetre

<i>ms</i>	millisecond(s)
N	Newton
NI	National Instruments
PCB	Printed Circuit Board
PC	Personal Computer
POLC	Planning, Organizing, Leading and Controlling
PWM	Pulse Width Modulation
RAM	Random Access Memory
RTC	Real Time Control
SMPS	Switch Mode Power Supply
UART	Universal asynchronous receiver/transmitter
V	Voltage
VEE Pro	Virtual Engineering Environment
VISA	Virtual Instrument Soft Architecture

LIST OF APPENDICES

APPENDIX	TITLE	PAGE
A	Gantt Chart	84
B	Program Source Code	85
C	PCB Layout	99

CHAPTER 1

INTRODUCTION

1.1 Background

Most of the industrial robot today employs unique method to grab and grip the object with the specific gripper, depending on the requirement. Most of them have actively employed the vision image to aid the gripping process. These give the information such as size, location, object type and others to the gripper. However, not all situations can employ the usage of machine vision as the guidance to the gripping process. The following describe the challenges faced by the machine vision in industries.

The main component used by NASA for the assembly of the International Space Station is the space machine vision. Video camera based system, are attractive because of their ease of use, low maintenance and simplicity of integration to existing equipment (Blais, 2001). However, not all the machine vision can be employed to supervise the gripper. Presence of sun and other strong source of light adversely affect the quality of the conventional methods that rely on standard video images, e.g. the camera on board the Space Shuttle. This has given poor disadvantage to the machine vision where light reflection on the surface of the components or material captured in the video will gives poor view to the engineer when assembling because the engineer need to uses the gripper to move the grip the material and component at exact location. The moment of disturbance from the other source of

light might causes wrong grip or collision at that moment which in turn will delay the time and damage the component as well as incurring high cost.

The Northern Digital Incorporate (Northern Digital Industry, 2010), a company specialize in medical field has stated in their website that “Although machine vision looks appealing from the perspective of minimal impact (with the exception of line-of-sight), there are many difficult implementation and environmental problems. These problems prevent machine vision from being broadly applicable. It is rare to find a machine vision solution that considers usability and minimizes application interference.” The interferences that stated by the Northern Digital Incorporate are the weakness of the machine vision such as line of sight between tracker and target, less intrusive system typically means less robustness or system flexibility, lighting conditions and background interference (complexity) can cause tracking problems.

1.2 Aims and Objectives

The aim of this research is to develop a gripper known as Design of In-Vitro Optically Aided Robotic Manipulation (IVOARM) and a new method which can perform ‘blind grasping’ without the aid of the machine vision and expected to achieve the following objectives:

- I. To design and develop an algorithm for robotic manipulator that is able to perform “contactless detection” – detect object’s distance from the gripper and size estimation before robotic manipulator grasping it.
- II. Monitor the responses from the gripper sensors using suitable measurement tools such as Agilent Measurement Manager and its measurement device such as Agilent U2352A Data Acquisition (DAQ).

- III. Design and develop a circuit system for sensor to detect the object's distance from the gripper and size estimations, cost effectively.

1.3 Outlines of the Final Year Project

Chapter 2, literature Review, studies of robotic manipulator which is done by other researchers. The detail of robot grasping mechanism on unknown object, algorithms of grasping and system architecture of intelligent robotic manipulator will be discussed

In Chapter 3, Methodology is about the overview of project title, the project management, and flow chart to show overall process from the beginning till the end of the project.

In Chapter 4, Sensors and Circuit Systems, details about the selection of sensors in IVOARM, design procedure of circuit system, Fabrication process of circuits will discussed in detail.

In Chapter 5, Algorithm Development and Implementation, system architecture of IVOARM, selection of embedded system, software development and search algorithm development, equations formulation and implementation are topics in this chapter.

In Chapter 6, Result and Discussion, the outcome and problem faced when carrying out this project will be discussed.

In Chapter 7, Conclusion and recommendation, concludes the thesis paper based on the objectives and achievements in this final year thesis. Future improvements will be discussed and provided

CHAPTER 2

LITERATURE REVIEW

2.1 Introduction

Locating and determining the distance of the object from the gripper and using the proper way to grip the object is a major challenge to the industries which operates in variable environment such as space, medical field and others as mentioned in Chapter 1. Machine vision has proven to solve such problems by capturing the image of the object and calculating its distance from the gripper as well as the size of the object to let the gripper to use an appropriate way to grip on it.

However, there are several drawbacks on the machine vision system where its distance estimation and its disturbance of other source of light intensity as well as proper angle of viewing are the main concerns. In machine vision, distance determination is done by extracting the size of the object at its location relative to the camera position. This might create error if there is disturbance and lack of resolution. The light intensity of other source such as the sun which is strong enough will create the disturbance or noise during image capturing in space, as mentioned in Chapter 1. The angle of viewing of the camera and also its viewing path must be clear and no blocking is required so that image capturing can be done.

Force of the gripper's actuator onto object's surface is also considered a major concern where appropriate force will enable the gripper to lift up the objects. Last generation of robotic arms are lacked of force sensors. Excessive force being

employed will damage the objects or leave the gripping mark on the objects surface (Xu DeZhang, et al, 2005). Proper force should be applied with the use of strain gauge sensors to obtain ensure there is no excessive force.

Many studies have been performed on the method to locate, size determination and grasp the objects. Notable research such as **“Robot Grasping of Unknown objects, Development of the robot gripper for a Home Service Robot (Christophe Leroux, et al, 2007); Design and Construction of a Robotic Gripper for Activities of Daily Living for People with Disabilities (Redwan Alqasemi, et al, 2007); High Performance Robotic Gripper Based on Choice of Feedback Variables (Zaki A.M, et al, 2010)”** have been referred to overcome the problem.

2.2 Robot Grasping of Unknown objects, Description and Validation of the Function with Quadriplegic People

Robot Grasping of Unknown objects, Description and Validation of the Function with Quadriplegic People (Christophe Leroux, et al, September 2007) employs the tactics of using machine vision attached to the gripper to detect the distance of the object relative to the video camera. On the gripper, stereoscopic video cameras are attached on it. These camera will capture the image and send to the user by displaying the real time image on the screen. The operator will then control the gripper with the body part which is still functioning well such as hand or leg. There are three phase for this gripping method. Using the only information which is being displayed on the screen, the operator try to control the movement of the arm to adjust the location of the gripper close to the object target. This corresponds to the designation phase. After he or she has determine the object to be grip, the gripper will approach the object via robot arm movement, with the 2-D real time displayed on the screen. This corresponds to the approaching phase. Once the gripper is in position, gripping is triggered and the object is brought back near the operator which is the final phase.

2.2.1 Flow chart

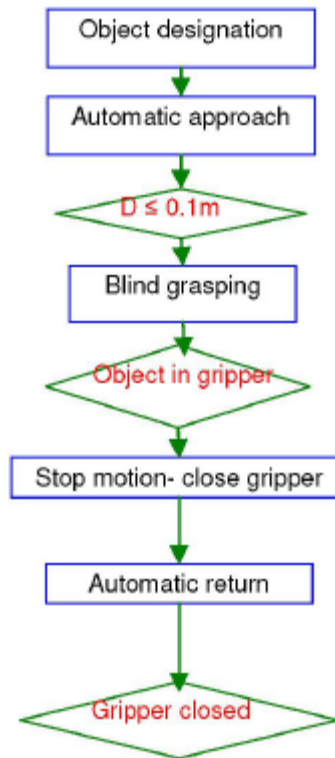


Figure 2.1: The flow chart on the MADEUS operation (adopted from Christophe Leroux, et al, 2007)

The flow chart in the Figure 2.1 shows the MADEUS gripper operation in details. The object in the screen is selected by the users. Once the object is determined, the arm will automatically approach to the object, with the aid of the stereoscopic video camera. When the object is within the 0.1m in the gripper, the gripper will proceed with blind grasping without considering the object actual position in gripper. Once the gripper has grip, the motor will stop to hold on the position. Then, the arm will retract and bring the object back to the user. Once the object is retrieved, the gripper will close to protect its mechanism.

2.2.2 Distance Estimation

The distance estimation of the object relative to the video camera is obtained by extracting the size of the object in the image captured by the video camera. Based on the size of the object in the video camera, the arm will move the gripper to the object using the estimated distance value from the system.

2.2.3 Feature extraction



Figure 2.2: The feature extraction on the MADEUS operation (adopted from Christophe Leroux, et al, 2007)

An image of area will be selected by the user via the focusing program. Once the area in the image defined, it is necessary to locate and "identify" the object truly indicated by the operator. The location is determined by estimate the size and resolution of the object which in turn dominate the whole image. The method uses to select the correct object to be grasped is the 4 buttons in the image. If the first location of the object desired is wrongly indentified by the system, the users will click on one of the button to shift the box concentration on other objects defined in

the image for the system correction. For this stage, interest points are computed using Harris and Stephens feature detector.

2.2.4 Matching and localization

When extracting the features, the selected object on the screen have to be matched with the actual object for the arm identification. The matching process started with the point to characteristic point matching.

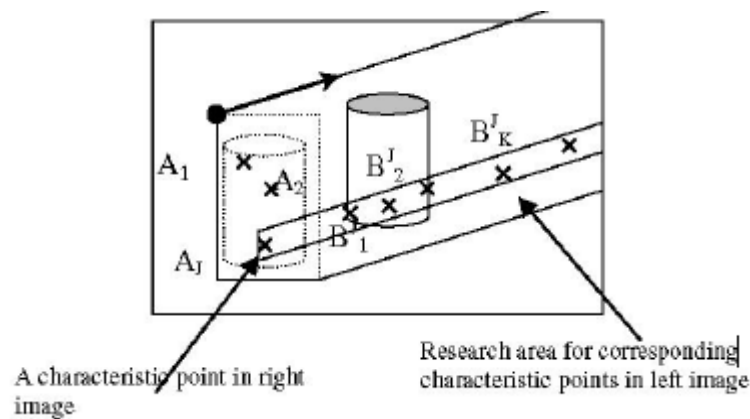


Figure 2.3: The matching and localization (adopted from Christophe Leroux, et al, 2007)

The process (Christophe Leroux, 2007) in this system is explained as following:

1. For each feature point A of image I , we look for feature points B of image I_r which satisfy the epipolar constraint with a given error (see figure 2. 3)
2. Eventually some points B_r^J are eliminated with a i_k correlation measure. Selection using this measure is very weak (high threshold adjusted among experiences) and very small time consuming. This stage is not fundamental but it can improve the statistical matching performances in "limit" cases: when there are few corner points or a great number of corner points.
3. For each point B_r^J we compute the i_k displacement $A_l = A(A_i, B^J)$ expressed in pixels with respect to point A_f . In our case $A(A_l, B^J)$ is simply the Euclidian distance between the two pixels along the epipolar line.

4. We then look for the most frequent value A_m for the A.
5. We then define the matching point for A_I as being the point B having the closest A_I value to A_m in a predefined limit. If no A is found within this limit, we consider that point A_f of freque image I, does not have any correspondent in image 'r

Once all the matching assumptions carried out, the selection of the object consists in retaining the most frequent distance computed. This distance is corresponded to the indicated object. Using the barycentre of the matching points, the direction of the object is located and the distance is estimated.

2.2.5 Evaluation

The gripper Madues relies heavily on machine vision system to indentify and calculate the distance which is all in approximation based on the image obtained. If the image is distorted by noise at the moment of calculation, the calculation will have big error. The robot arm have to repeating to approach the objects on several time before able to determine the exact location to confirm the estimated value.

2.3 High Performance Robotic Gripper Based on Choice of Feedback Variables

The High Performance Robotic Gripper Based (HPRG) on Choice of Feedback Variables (Zaki, A.M. ,et al, 2010) uses the simple mechanical design with 2 fingers parallel design without considering its flexibility. One of the finger is fixed and the other is movable and both shape is rectangular shape as shown in figure 2.4 The movable finger is derieved on a lead screw and guided by a linear bearing system. It is has self locking capability by stoping the lead screw from turning. The sensors being employed in this gripper are Flexiforce A201 to detect the force applied and

Phidget vibrator sensor to be used to detect slip. Permanent magnet BLDC brushless dc motor is used in this gripper due to its low rotor inertia.

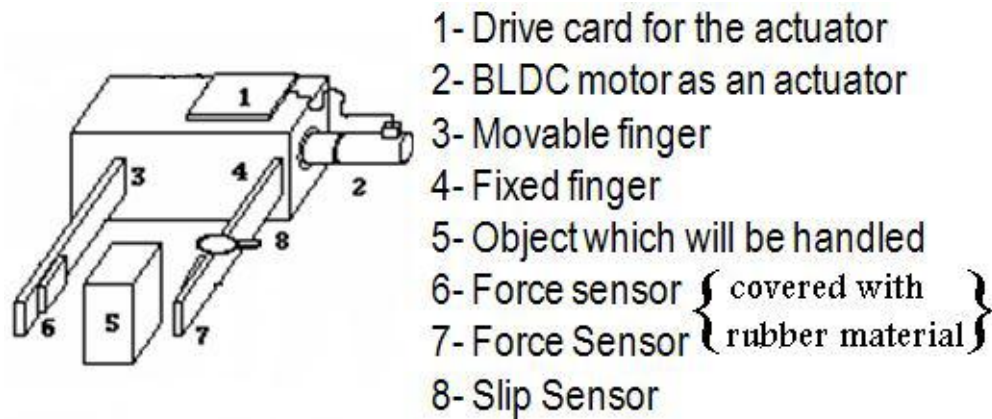


Figure 2.4: The mechanical design of the HPRG gripper (adopted from Christophe Leroux, et al, 2007)

2.3.1 Mechanical design

The mechanical design of the HPRG is simple to demonstrate the effectiveness of the sensors attached to its finger. Two flat plate fingers are used and the length of these two plate is 15 cm which requires high developpe torque from the dc motor. The width of these plates are fit to size of the sensors attached on it. The movement of the gripper is control by the lead screw, by rotating the proper direction will open or close the gripper.

2.3.2 Sensors

2.3.2.1 Force sensor

The force sensor being employed is A201 which is used to detect only force employed on it. The force sensors are covered with rubber to increase the friction coefficient μ so the object gripped will be sticking on the rubber surface. Voltage

generated from the force sensor will be used to measure the force applied onto the finger.

2.3.2.2 Slip sensor

The slip sensor being used is the Phidget vibrator sensor which is used to detect the vibration on the gripper. Since the object is in steady position in the gripped position, any external force will tend to break this steady state. Once the external force is applied, the vibrator will detect the vibration of the gripper and the object might slip away from the gripper finger. Then, the gripper will apply more force onto the object to ensure the object does not fall out.

2.3.2.3 Evaluation

The design of the gripper is simple and matching with its objective. However, the finger designed is lacking of flexibility with detecting the force only on two points. There is a high chance of rotation motion occurring on the object while gripping.

2.4 Design and Construction of a Robotic Gripper for Activities of Daily Living for People with Disabilities

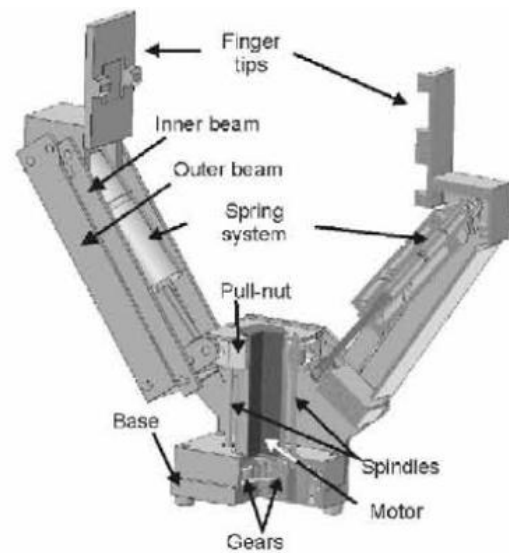


Figure 2.5: Manus gripper internal mechanical part (adopted from Redwan Alqasemi, et al, 2007)

Design and Construction of a Robotic Gripper for Activities of Daily Living for People with Disabilities (Redwan Alqasemi, et al, 2007) uses the Manus gripper which consist 2 fingers gripper to grip the object. The purpose of building this gripper is serving the disabled person at home. This gripper fully employs mechanical components to enforce gripping performance and controled using one motor. The fingers' tip can be changed to suit the daily activities of the disabled. Using the lead screw, the motion of close and open can be controlled by attaching the screw to the motor and the motor spins. The gripping operation is depending on the machine vision system, which controlled directly from user's sight.

2.4.1 Mechanical Design

2.4.1.1 Mechanical Movement

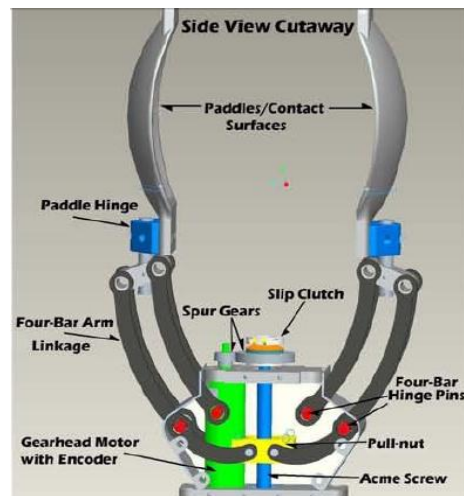


Figure 2.6: Manus gripper internal mechanical part movement (adopted from Redwan Alqasemi, et al, 2007)

The Manus gripper movement in figure 2.6 is summarized below:

- I. The motor turns the gears which turns the acme screw.
- II. The acme screw will be turned and move the pull-nut which turns the four bars hinge pins.
- III. The spur gear is turned in the same time as the acme screw turn to open up the fingers.
- IV. The spring will be pulled which put the gripper fingers in tension form and grip the objects.
- V. When the motor turn in different direction, the acme screw will turn in opposite way to make all the components back to initial state.

Design of the Fingers' Tip

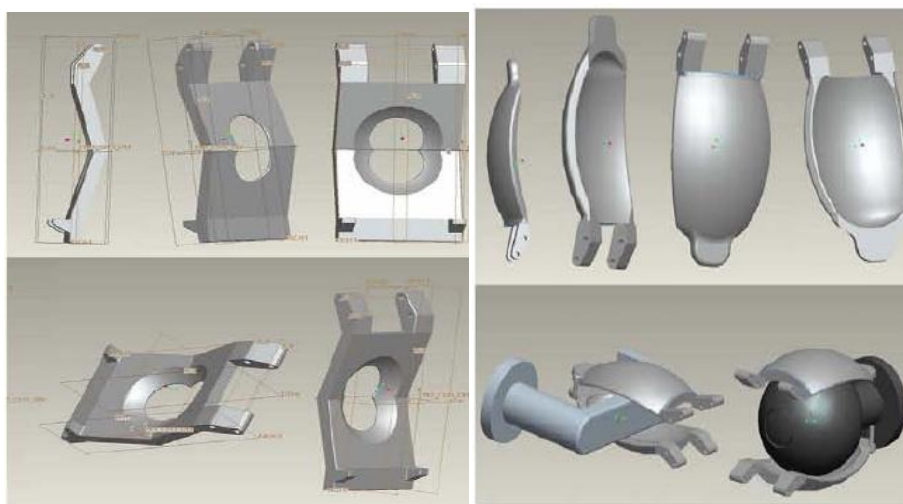


Figure 2.7: Various finger tip of the Manus Gripper (adopted from Redwan Alqasemi, et al, 2007)

The finger tip in this gripper is designed to be universal, which means the finger tip can be in any shape. The purpose of making it universal is due to under different circumstances, the finger tip can be changed to achieve the objective.

2.4.2 Evaluation

The Manus gripper is a good design which fully utilize the mechanical structure. However, its flexibility is not so high because the gripper's finger has one rotation motion. The surface of the finger cannot be attached with any force sensors due to lack of space. The force of gripping can only be estimated via the machine vision system it has stated early. Each angle of finger's joint is not controlled independently. One motor's movement will define the all angle of the joint.

CHAPTER 3

METHODOLOGIES

3.1 Project Design Overview

The primary concern of this project is the **design procedure of electronic circuit system design** and **search algorithm design** of the prototype. The workflow is shown in **figure 3.1** and **figure 3.2**.

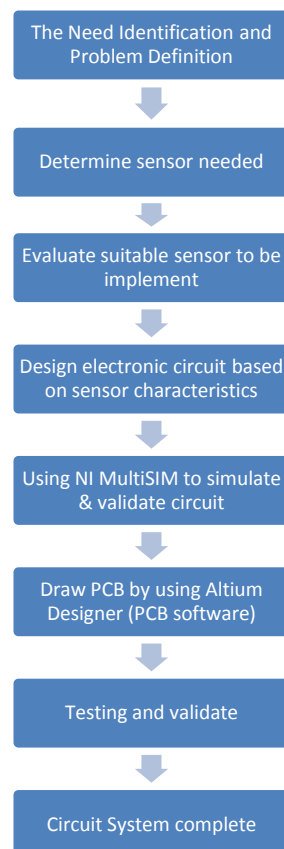


Figure 3.1: Flow chart of electronic circuit system design.

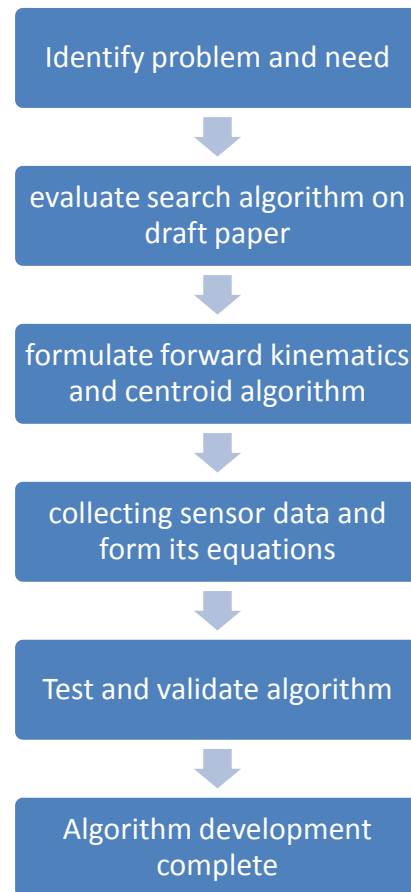


Figure 3.2: Flowchart of algorithm design

3.2 The System

After a Literature review is done in the Chapter 2 to gather some information and generate idea before planning the experiment layout. The overall system is named IVOARM, it has contained three sub system: mechanical parts, electronics system and algorithm development.

In mechanical parts section, it can separate into two components: Robotic Manipulator and Foundation Settlement. Robotic Manipulator is the main body of IVOARM, which is mechanical structure to perform object's detection and grasping object. Foundation Settlement is fixture stand use to holding the robotic manipulator in static environment.

Force control modelling is dynamic model of the IVOARM, with the aid of dynamic model of force control, , the advantages of adding dynamic model of force control into IVOARM is it able to grasping an object without reaches maximum grasping force. In this project, mechanical parts and sensor development has been assigned to Mr. Chia Kok Siang,

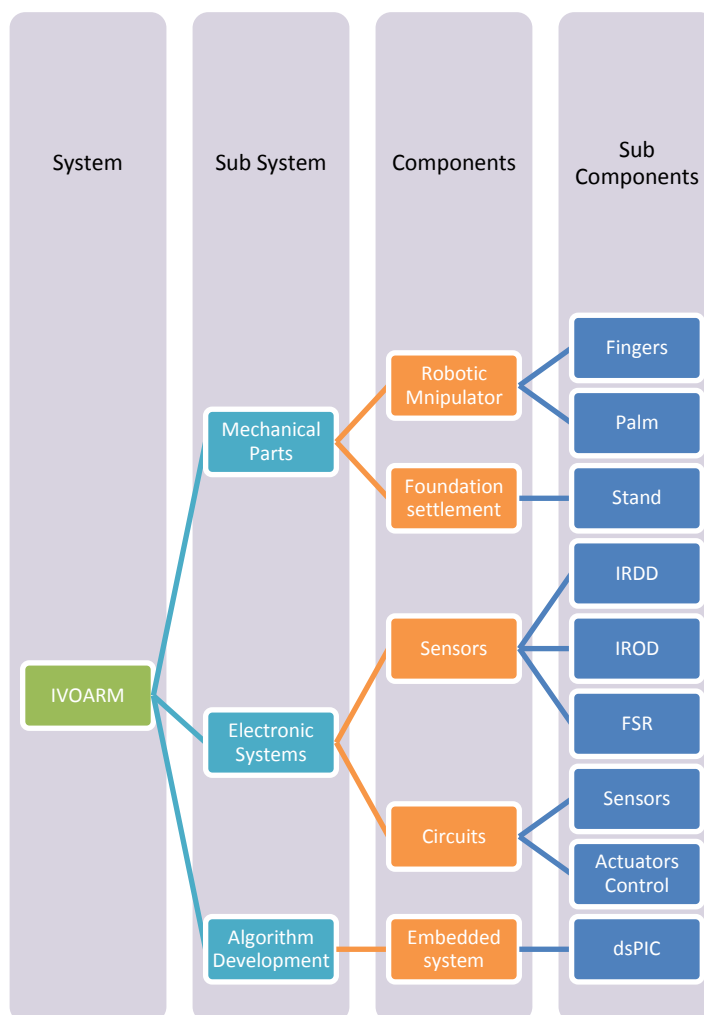


Figure 3.3: IVOARM system overview

3.3 Project Management

In a project, planning acts an important role, it might lead project to neither success nor failure. This project has lead by the four management function: Planning, Organising, Leading and Controlling (POLC) has stated in figure at below:



Figure 3.4: POLC process flow

According to New Era of Management (Richard L. Daft, 2008), Planning means identify goals and deciding tasks and use of resources needed to attain them. In planning stage,

Organising typically follow planning and way to accomplish the plan. Organising involves assigning tasks, grouping tasks, allocating resources for tasks. Examples like Gantt chart, design procedure for each sub systems, allocating resources and tasks scheduling. This project has involves mechanical parts, electronics circuit and algorithm development. Hence author has separated tasks respect to ability of team members and assigning tasks details to each of them.

Leading is the use of influence to motivate team members to achieving goals. A good leader must able to create a shared cultures and values, communicating goals and influence employees to perform at higher level.

Finally is Controlling, controlling is fourth function in the management process. It means monitoring team members activities, determining whether the project team is on target toward its goals, and make correction as necessary. Example is every two weeks our Project Supervisor will give guidance and coaching to ensure the project keep on track.

3.3.1 Gantt chart

The Gantt Chart is planned to ensure all the sequences of the project are done on time. Appropriate assignment of time on each of the sequence is done by making it into Gantt chart management as shown in Appendix A. Literature review will use up to four days for analysis. The mechanical design of IVOARM will be plan first. The mechanical design will use up to 23 days to ensure the parts are able to be fabricated out. This 23 days includes the purchase of suitable electronic components to be used and this will takes around 1 week to gather all the components. The circuit design is then implemented to suit the usage of electronic components which drive the mechanical part.

Once the mechanical part is assembled, it is tested run with simple mechanical movement to ensure its reliability. Next, the algorithm is formulated to ensure the initial objective can be achieved in programming part. This formulation will take up to 4 days. The algorithm is then programmed into the electronic embedded system to test run the mechanical part. Additional time has been reserved to fine tune the program.

When the program is done, experiment will be done to ensure the objectives which is stated in aim and objectives in 1.2 will be achieved. The final step is the thesis preparation which compiles the whole project sequence. This project estimates to be completed within 44 days.

3.4 List of Tools

After completion of Root Cause Analysis, the project has stated from concept design into detail design, after discussion among team members, the author has listed all required tools into two sections, hardware's and software's.

3.4.1 List of hardware

Table 3.1: List of hardware's

List of Hardware	Name of components
Electronics hardware	Solder gun, solder stand, solder lead, crocodile clip, lead sucker, wire cutter, printed circuit board driller, wire
Embedded system	Explorer 16 development board and personal computer
Measurement Equipment	Agilent Digital Multimeter U2741A and Agilent Data Acquisition U2352A



Figure 3.5: part of hardware's in project

Due to the limitation of funding, allocating resources are important. Some the tools required can borrow or requested from university. This can reduce the unnecessary expenses and save fund for other purpose.

In this project, some of the equipment are loan or utilise from different places, like Agilent Technologies has loan a Precision Measurement Equipments to this project. Or some equipment can requested and use in workshop, like drilling machine and INSTRON 5582 for force testing experiment.

3.4.2 List of software

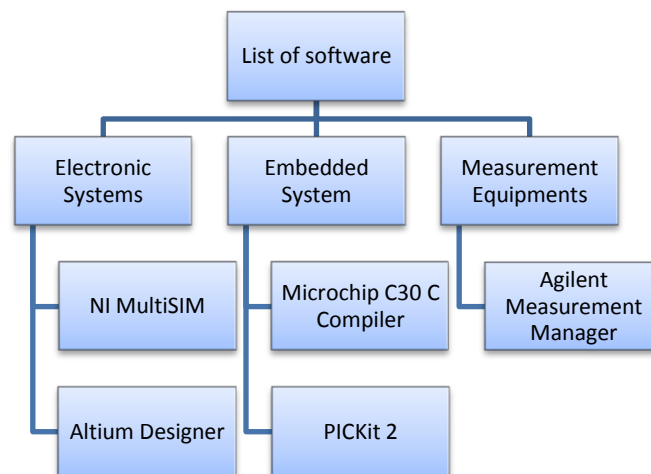


Figure 3.6: List of software

Table 3.2: Functions of software

Name of software	Functions
SolidWorks	Modelling parts, assemblies, verify and simulate in 3D environment, to make a
NI Multisim	Construct and simulate circuit in software before actual system was build
Altium Designer	Design and develop a PCB circuit layout
Microchip C30 C Compiler	Programming dsPIC in C language, Compiler will convert C language to machine language accordingly
PICKit 2	Firmware as programmer for dsPIC

CHAPTER 4

ELECTRONIC CIRCUIT SYSTEMS

4.1 Electronic Components Selection

4.1.1 Selection of distance detector

The sensors used in this project will be infra-red distance detector, infra-red object detector and force sensing resistor. These sensors will act as eyes for the gripper to obtain the data such as distance, force, and the presence of the object for the gripper's decision to grip the object with proper way.

The selection of distance detector in IVOARM must have reasonable range of detection. Since the distance detection in close range must be small, the selection of the distance detector sensor must have short detection range. The sensor resolution must be high so that the conversion into voltage must be high. Moreover, the size must be small so that it can be fit into the IVOARM and the cost must be low.

Table 4.1 shows the comparison of Ultrasonic Range Finder and the SHARP GP2D120. SHARP GP2D120 is chosen over Ultrasonic Range Finder due the fact that the media used by the Ultrasonic Range Finder is wavelength. The wavelength that emitted by Ultrasonic Range Finder will be easily deflect in the IVOARM since the finger gripper will rotate around and might deflect its wave to it while measuring.

Thus, it has high interference. SHARP GP2D120 has very fast refresh rate and its cost is much lower than Ultrasonic Range Finder

Table 4.1: Comparison of Ultrasonic Range Finder and the SHARP GP2D120

Specification	Ultrasonic Range Finder	SHARP GP2D120
Supply voltage	2.5v~5v	4.5~5.5v
Signal output	Analog or Discrete (UART)	Analog
Sensing distance	0~6.45m	4~0.4m
Size of sensor	medium	small
Sensor media	ultrasonic	Infrared
Interference	High	Moderate
Sensor refresh rate	50ms	36ms
Cost	Rm140	Rm60

4.1.2 Selection of force sensor

Table 4 shows the characteristic of different sensors. Force sensor selected must have small size, light, wide sensing range from around 100g above and have reasonable sensor resolution. FSR Part-402 is chosen over the others due to its tactile sensor type which is small and thin, sensing range of 100g and above and come in various size. It also has reasonable sensor resolution. Its cost is the lowest among the others.

Table 4.2: Comparison of Force Sensors' Characteristic

Specification	FSR Part-402	FS20	ENDEVCO Model 2312
Type of sensor	Tactile sensor	Low force compression load cell	Piezoelectric Force Sensor
Force sensing range	100g~10kg	750g~1500g	0~7kg
Size	medium	small	Small
Supply voltage	2~12v	3.3v~12v	5v~12v
Response time	fast	fast	fast
Sensor resolution	medium	high	high

4.2 Electronic circuit system design

4.2.1 Infra-Red Distance Detector

The Infra-Red Distance Detector (IRDD) is used to detect the presence of the object and aids in the calculation of the object's distance from the gripper. The IRDD used in this project will be SHARP GP2D120 which has very good object detection. However, its nearest object detection distance is 4cm. Its characteristic on object colour intensity is shown in figure 4.1. However, since the colour intensity and temperature will impact the performance of IRDD, several tests will be done to verify its characteristic.

Features of SHARP GP2D120:

- Analog output
- Effective range: 4 to 30 cm
- Typical response time: 39 ms
- Typical start up delay: 44 ms

Verification Tools:

In the verification process the result is obtained using the selected measurement tools below:

- I. Agilent U2352A Digital Acquisition device
- II. Agilent U2741A Digital Multimeter device

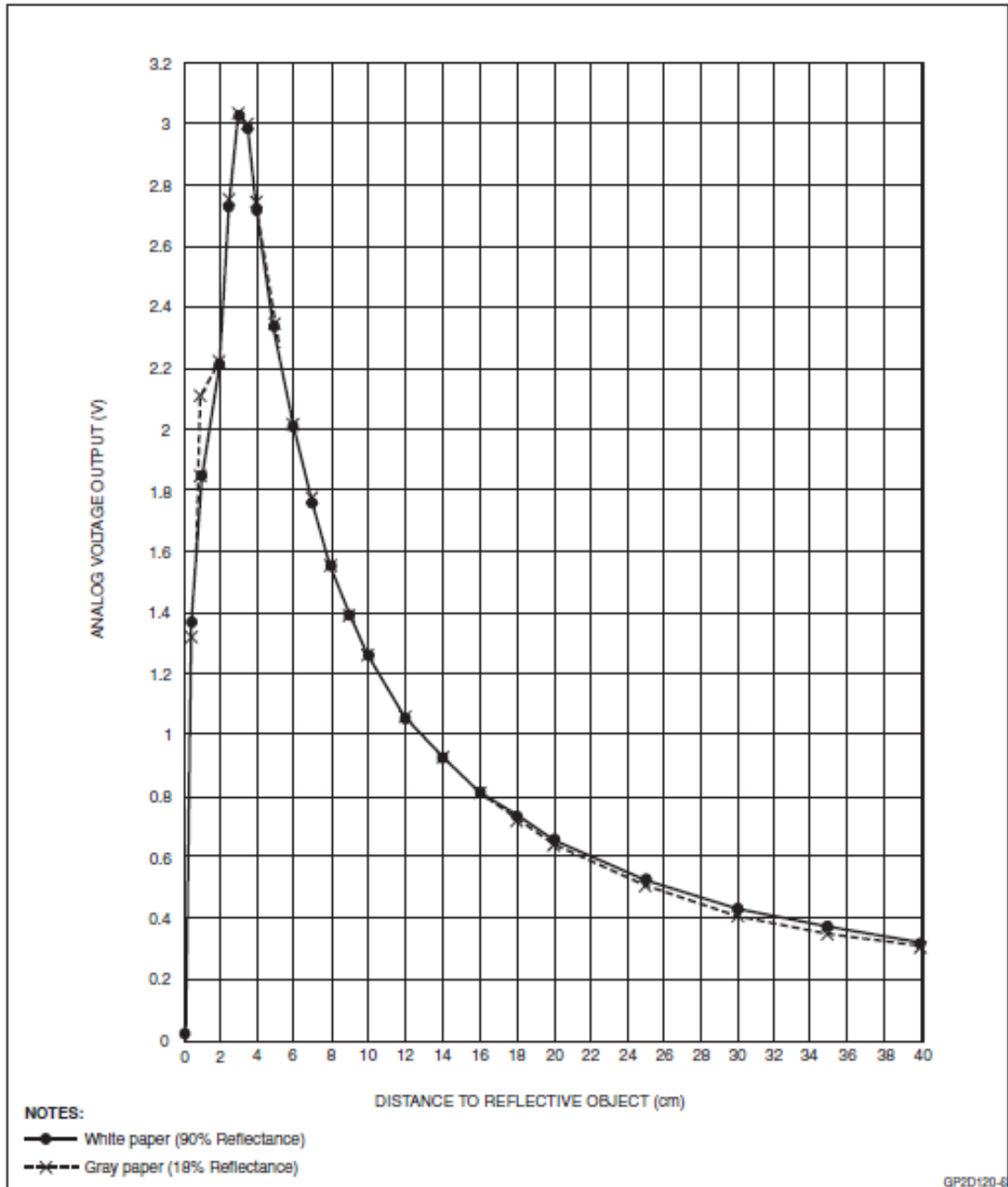


Figure 4.1: Distance detection on object's colour intensity (Adopted from *Sharpsma, 2011*)

4.2.2 Infra-Red Object Detector

The Infra-Red Object Detector (IROD) will be attached at the hole on the surface of the gripper's finger. The IROD is used to detect the presence of the object to aid in the calculation of the object's size.

The IROD industrial specification stated that maximum detection range is 15mm with peak operating distance is 2.5mm. However, the object's colour intensity will influence the detection range of the IROD in real situation. Figure 4.2 shows the internal diagram of the TCRT5000.

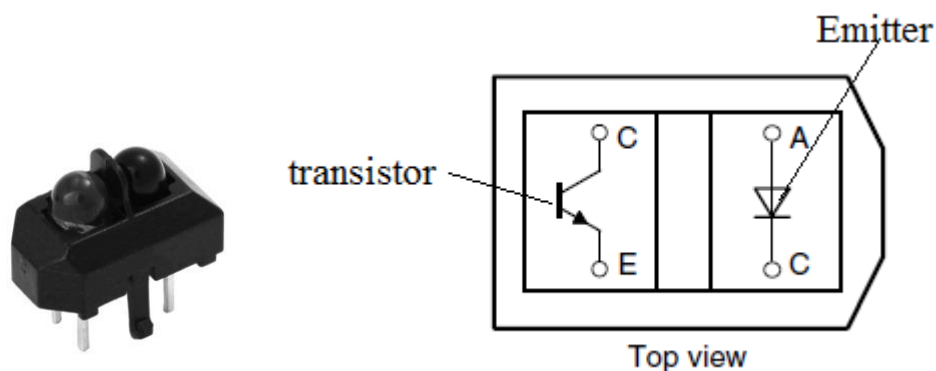


Figure 4.2: The TCRT5000 outlook and internal diagram (Adopted from Vishay Semiconductors, 2011)

Features:

- Detector type: phototransistor
- Dimensions (L x W x H in mm): 10.2 x 5.8 x 7
- Peak operating distance: 2.5 mm
- Operating range within > 20 % relative collector current: 0.2 mm to 15 mm
- Typical output current under test: $I_C = 1 \text{ mA}$
- Daylight blocking filter
- Emitter wavelength: 950 nm
- Lead (Pb)-free soldering released
- Compliant to RoHS directive 2002/95/EC and in accordance to WEEE 2002/96/EC

Verification Tools:

In the verification process, the maximum distance of using detection range of IROD will be obtained using the selected measurement tools below:

- I. Agilent U2741A Digital Multimeter device.

4.2.3 Force Sensing Resistor

The force sensors used in IVOARM gripper is Force Sensing Resistors (FSR) from Interlink Electronics which has the characteristic below. The structure of the FSR is shown in figure 4.3 below which has good protection on its connection and flexible. Its original characteristic is shown in figure 4.4. The force increment will decrease the resistance of the force resistor itself. However, when implement in certain circuit, its sensing resistance will change, depending on the design.

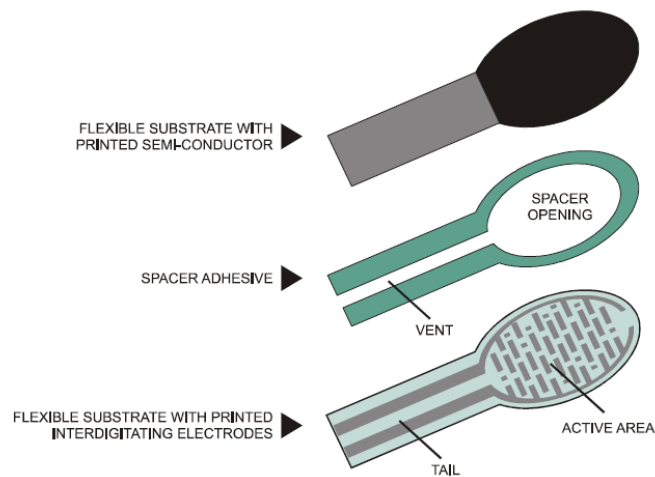


Figure 4.3: Force resistor internal layout structure (Versa Point Technology, 2011)

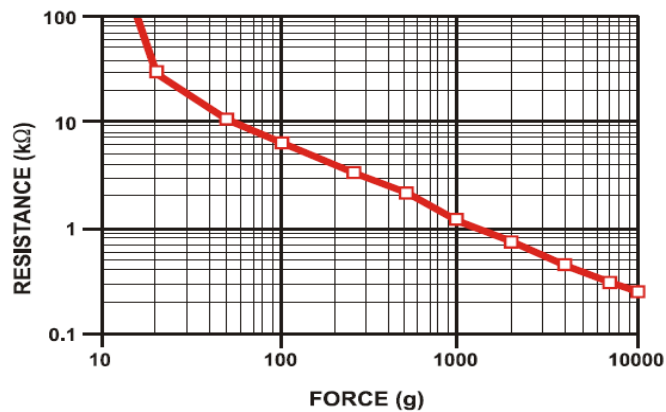


Figure 4.4: Force applied on the FSR (Adopted from Versa Point Technology, 2011)

4.3 Circuit Design

The circuit design for each of the sensors is implemented based on their characteristic and the project requirement. Each of the design will take into consideration of their specification as review previously. There are three circuit boards with each of the board serves different purpose. However, dsPIC used in this project is a device that is ready to use from market.

Circuit Testing

After creating the circuit for each sensor, the circuits are virtually test run to ensure there is no error occurs. The test run is done by using the National Instrument's program 'Multisim'. This program will virtually run the circuit in real time to validate the design by output the virtual result to the users. Any error regarding the design can be traced at the output of the virtual test run. This can be used to trace back the error done.

4.3.1 Main Board

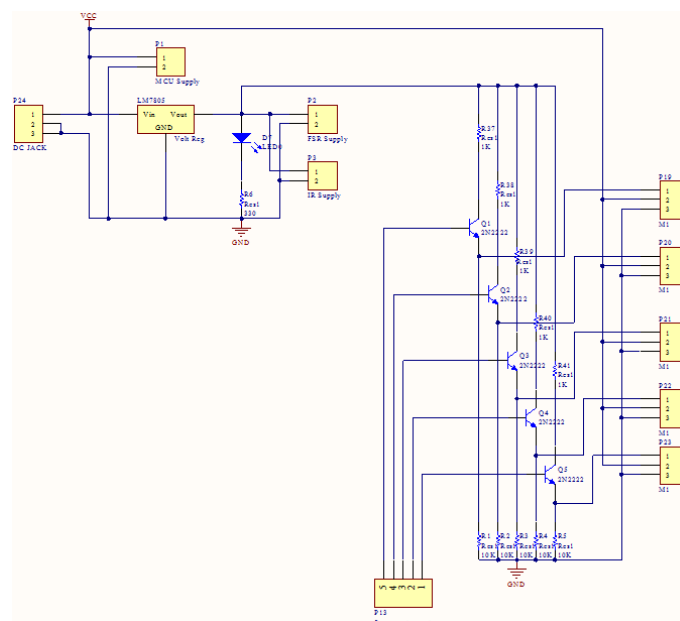


Figure 4.5: Complete schematic view of the main board.

Voltage regulator

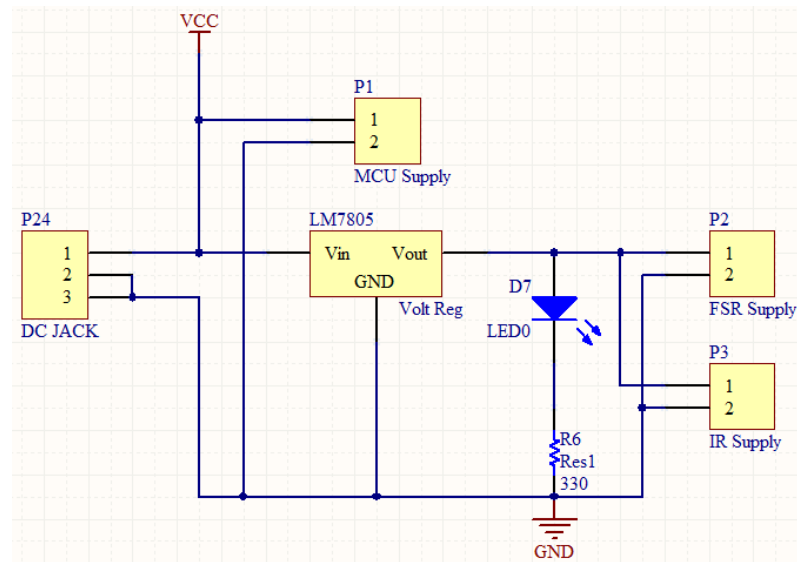


Figure 4.6: Voltage supply and voltage regulator in main board.

The features of the main board as shown in figure 4.6 are consisting:

- voltage regulator regulates the power supply received into 5 volt
- Regulated 5 volt will be supplied to other boards.
- LED in the circuit indicates if the voltage regulation is still in good condition.

4.3.1.1 Servo Controlling using the NPN Transistor

The transistor 2N2222A in the main board is functioning as voltage buffer between dsPIC and Servo Motor. The PWM signal acts as controller to control the flow of supply voltage into the servo motor as shown in figure 3.21. Using the NI Multisim simulation program, the measured voltage output is 2.707 V as shown in figure 4.8, which has fulfil minimum signal input voltage of servo motor and acts as a bridge between dsPIC and servo motor.

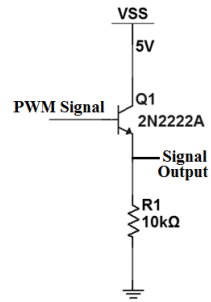


Figure 4.7: The simplified NPN working principle

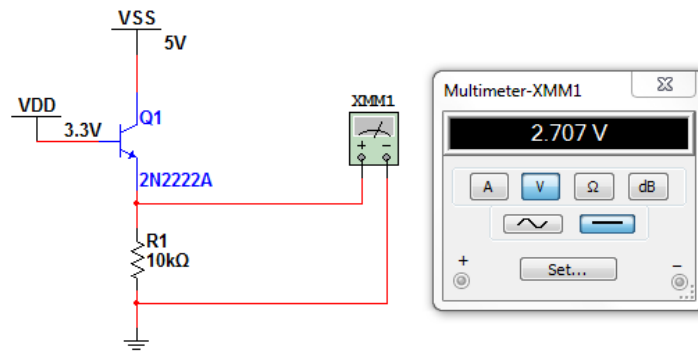


Figure 4.8: Virtual testing on the designed circuit using NI Multisim virtual multimeter

4.3.2 FSR Board

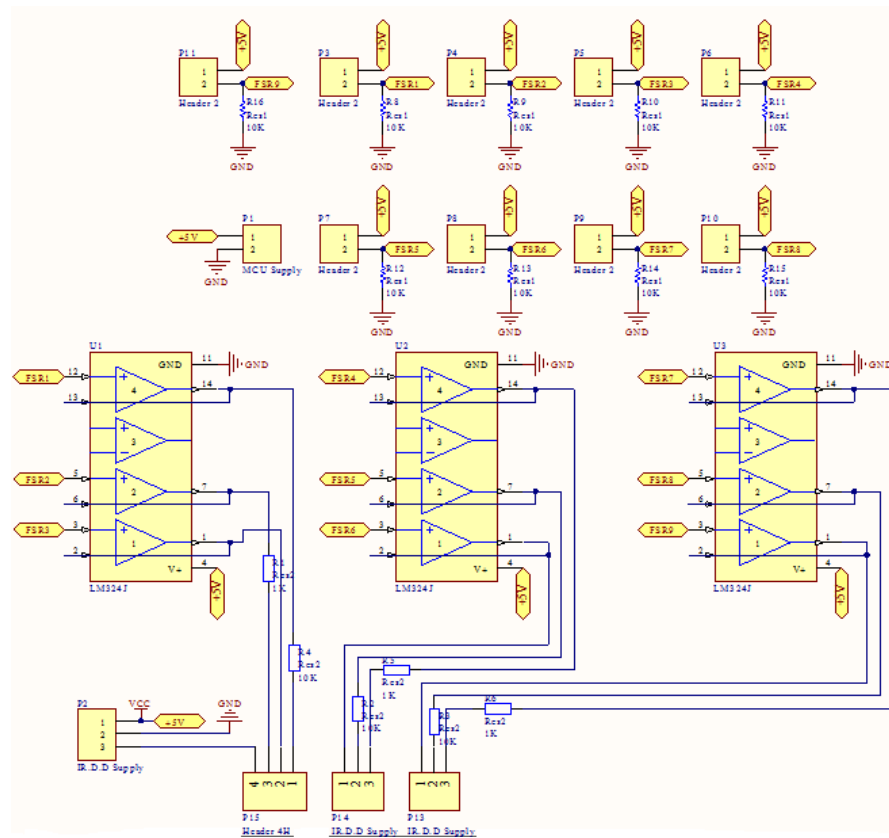


Figure 4.9: Complete schematic view of the FSR board

The feature of the FSR board is to obtain the FSR value by using the comparator LM324J. The FSR will value will be send into Agilent Measurement Manager to display its value.

4.3.2.1 Working principles of the FSR board

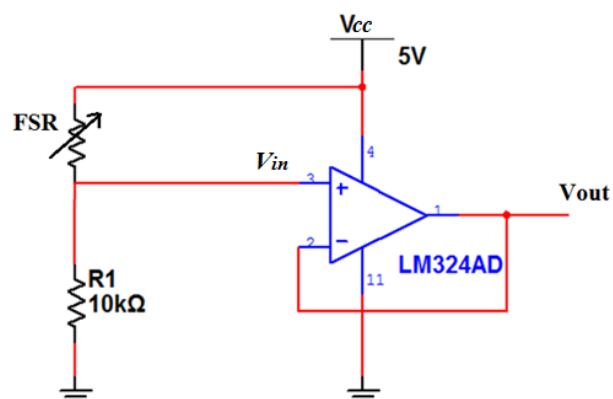


Figure 4.10: Voltage divider with voltage follower

Figure 4.10 shows the voltage complete view of the voltage divider in the FSR board. This voltage divider is used to input the FSR voltage value into the control system of Agilent Measurement Manager.

4.3.2.2 Voltage Divider Formula

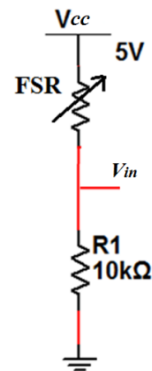


Figure 4.11: Simplified voltage divider

By applying Voltage divider rules:

$$V_{in} = \frac{R_1}{R_{FSR} + R_1} V_{CC}$$

4.3.2.3 Voltage follower

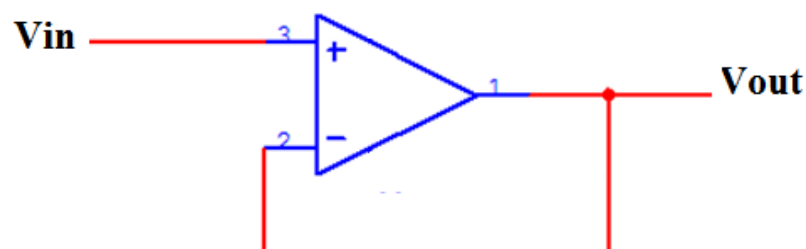


Figure 4.12: Simplified voltage follower

The voltage follower is used as a buffer amplifier to eliminate loading effects (e.g., connecting a device with high source impedance to a device with low input impedance).

The operational amplifier design applied is voltage follower, where gain of op amp are equal to 1, hence obtain:

$$V_{out} = V_{in}$$

By substitute (11) into (10),

$$V_{out} = \frac{R_1}{R_{FSR} + R_1} V_{CC}$$

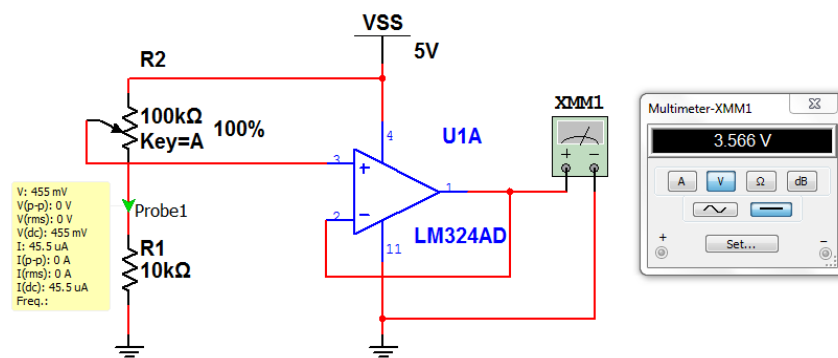


Figure 4.13: Virtual measurement on virtual circuit of FSR board using NI Multisim

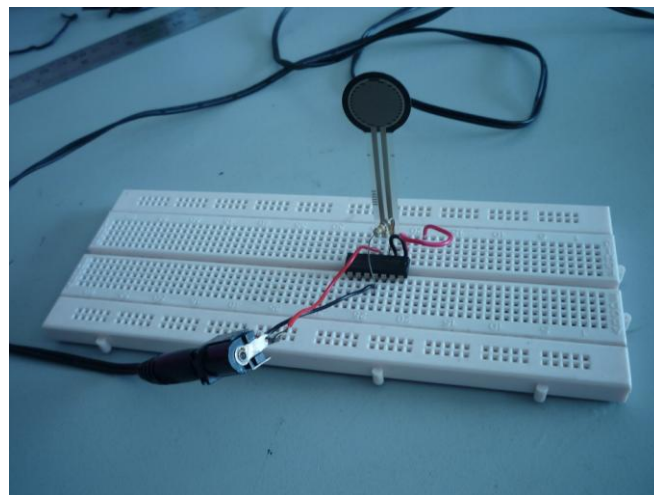


Figure 4.14: FSR circuit design with breadboard

4.3.3 Infra-Red Object Detector Board

Function of Infrared Object Detector in IVOARM is determine the presence of object, to sense the object, the design of IROD is combination of Infra-Red Sensor and LM339 low voltage quad comparator, Infra-Red emitter transmit Infra-Red light and phototransistor will decrease or increase its resistance depends on reflected Infra-Red light received, LM339 comparator will trigger output refer to the compare voltage difference between voltage input and voltage reference.

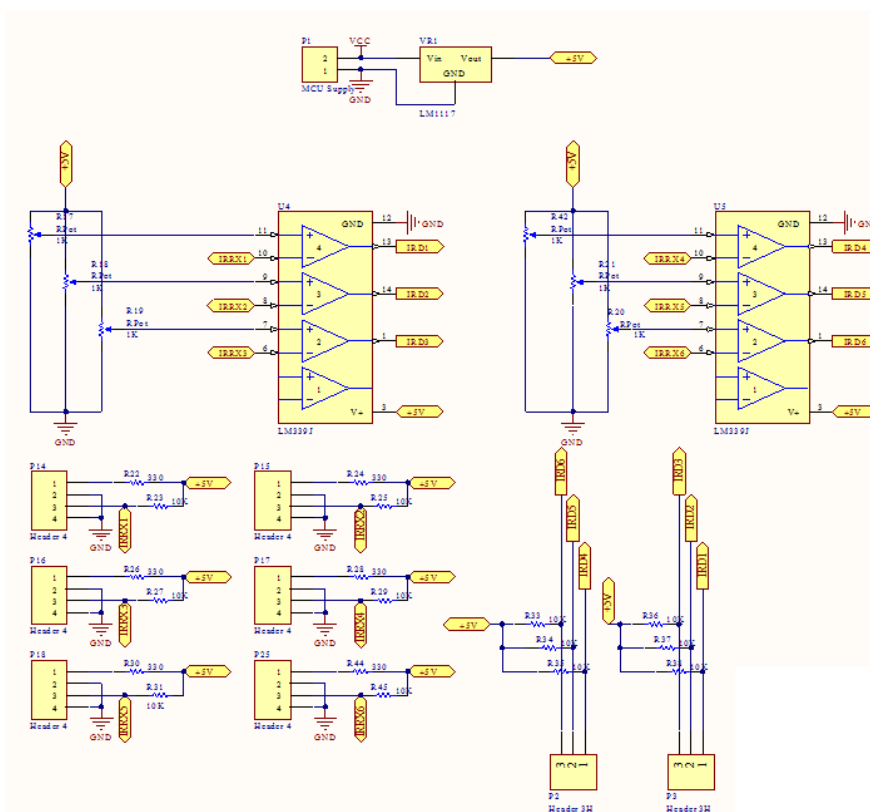


Figure 4.15: Complete schematic view of Infra-Red Object Detector board

4.3.3.1 Working Principle of IROD board

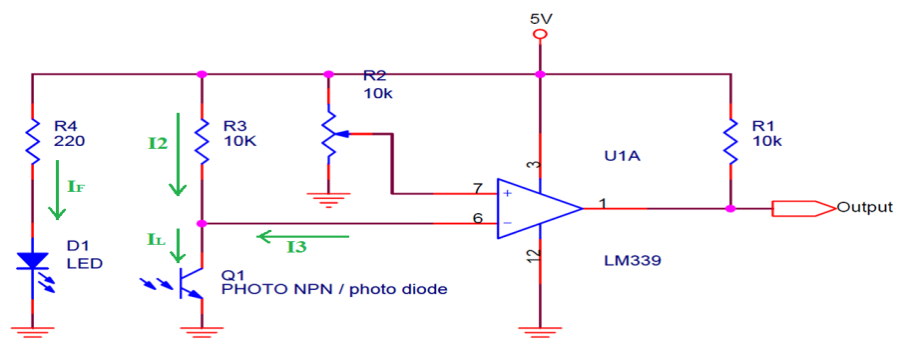


Figure 4.16: Working principle of Infra-Red Object Detector circuit

First, calculate forward voltage drop at LED are V_F , the current I_F flowing to the LED is given by:

$$I_F = \frac{V_{CC} - V_{D1}}{R_4}$$

Where

V_{CC} = input voltage, V

V_{D1} = forward voltage drop of an LED, V

R_4 = resistor to LED, Ω

In this circuit design, the minimum requirement of voltage supply to op-amp is 2v and dsPIC33F only can receive 3.3v signal, hence the supply voltage, V_{CC} set as 3.3v.

Hence, obtain the resistor. From figure 3.27, is current flow from R3 until Q1 when input voltage is low. The formula is given as:

$$I_2 + I_3 = \frac{V_{CC} - V_{CE(sat)}}{R_3} + I_3$$

$$I_L = I_2 + I_3$$

I_L = light current (phototransistor), A

V_{CC} = input voltage, V

$V_{CE(sat)}$ = saturation voltage, V

General, the phototransistor system will anticipating with nearly 50% reduction from the initial value of I_L with consideration of temperature characteristics. Hence settings of system must be made so that $I_L \times 0.5 > I_2 + I_3$

4.4 Imprint on PCB Board

Having the circuit design in virtual will not be able to run the actual sensors. The circuit design needed to be imprint on the Printed Circuit Board (PCB) to run the system. The circuit designed will be drawn into PCB circuit format using Altium Designer program. This program will aid in arrangement of the circuit line and make it into PCB circuit. Once the PCB circuit is printed on the PCB board, components will be soldered on this board. All PCB and schematic layout has listed in Appendix C.

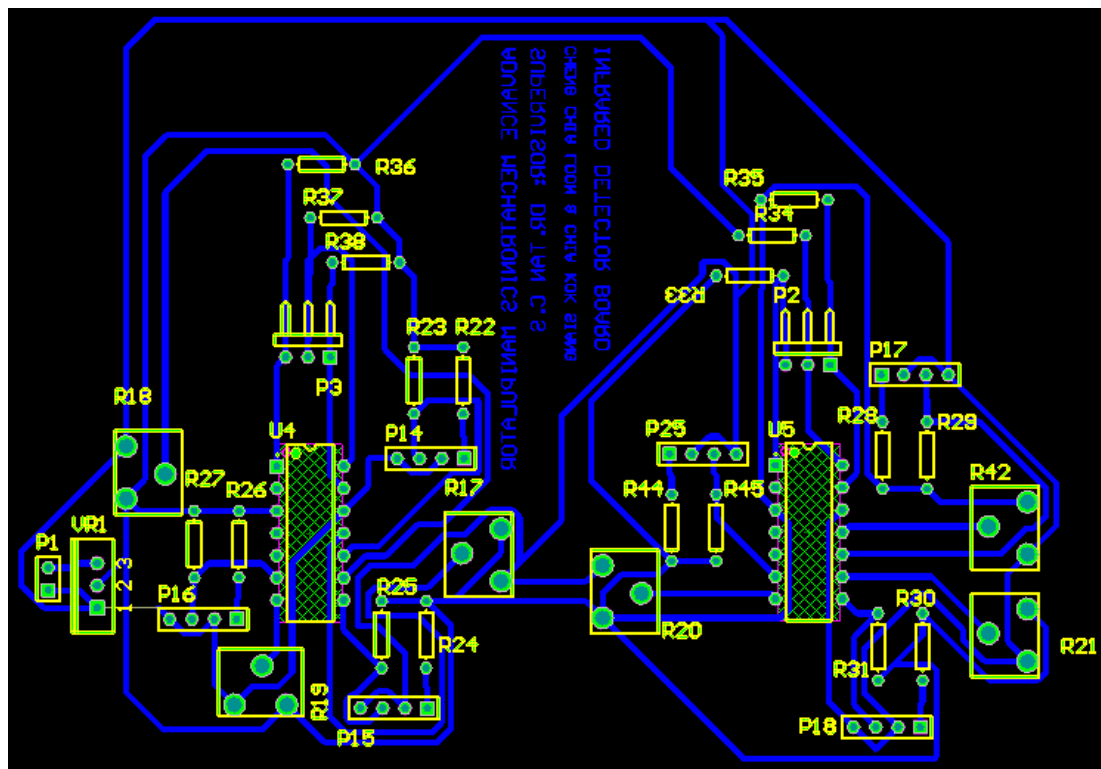


Figure 4.17: PCB design in Altium Designer, blue colour indicates connection routes, yellow colour indicates components and green colour indicates components pin holes

4.4.1 Fabrication Process of PCB:

1) Send PCB layout to UTAR Electronic Lab Technician

When the PCB layouts complete, design can send to UTAR Electronics Lab Officer, Mr. Ho for the fabrication.

2) Receive complete PCB board from technician

After 3 working days, Lab officer will list the complete PCB in Electronics Lab and ready for collection.

3) Using drilling machine to drilling all holes

The fabricated PCB board is comes without drilling holes, beside the Lab has Project workshop which provide PCB drilling machine for students to drilling holes as shown in figure 4.18.

4) Insert components into PCB board

When all components and PCB are prepared, the components needed insert with referring PCB schematic.

5) Using solder kits from SD101 to solder PCB

Soldering PCB with solder kits provided from Mechatronics Lab SD101,

6) Real Board Testing and Validation

After soldering the components onto PCB board, the board now will be validated using Agilent U2352A DAQ and Agilent U2741A Digital Multimeter. By confirming the output, the PCB boards will be now ready for use.

7) PCB complete and ready for use

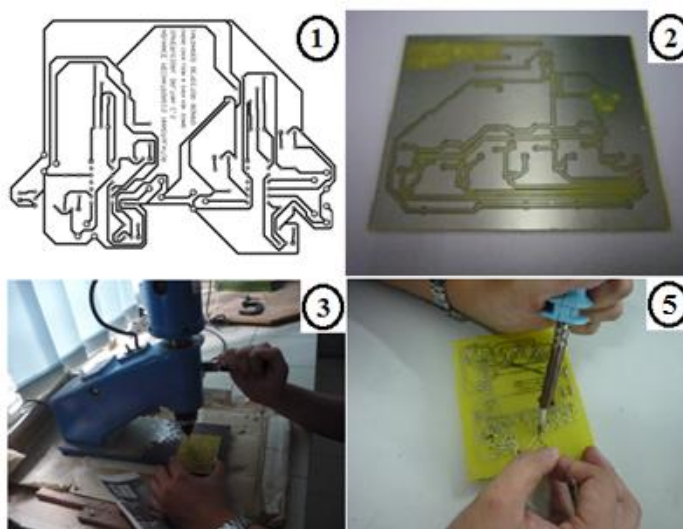


Figure 4.18: procedure of PCB fabrication process

CHAPTER 5

ALGORITHM DEVELOPMENT

5.1 Problem Identification

In creating the algorithm, an objective will be set as guidance in leading to the right path during formulation. In this project, search and calculating the object size will be focused to develop out the suitable algorithm.

5.2 Selection of embedded system

Table 5.1: The Comparison of Embedded System

Name	SH7705	dsPIC33F256 GP710	ST10F273
Manufacturer	Renesas	Microchip	ST Microelectronics
Processing speed	133MHz	80MHz	64MHz
DSP multiplier	32 bit	40 bit	40 bit
ALU	-	16 bit	16 bit
Timer	CMT, RTC	RTC	RTC
Channel of ADC	24 pins	32 pins	24 pins

10 bit A/D	4 channels	4 channels	24 channels
12 bit A/D	-	1 channel	-
On chip peripherals	USB	UART, SPI, CAN	UART, I2C, CAN
Cost	RM60	RM25	RM120

There are some considerations to select a good embedded system: processing speed can run IVOARM smoothly, function required has included on chip, e.g. ADC & RTC, programming compiler available, Timer for PWM control servo motor, and most important, the cost of embedded system.

After evaluation of embedded system, the author has selected Explorer 16 Development Board for dsPIC as the embedded system for IVOARM. It's named Digital Signal Controller (DSC). it runs in 16 bit ALU which has higher speed than normal 8 bit microcontroller, inside chip architecture, it has contains 40 bit multiplier DSP engine for better mathematics performance, besides that, it has included on chip peripherals 10 bit ADC, Digital I/O, RTC and ease to program source code from Personal Computer (PC) to dsPIC.



Figure 5.1: Explorer 16 Development Board for dsPIC

Architecturally, although they share the PIC moniker, they are very different from the 8-bit PICs. The most notable differences are:

- bank switching is not required to access RAM or special function registers
- data stored in program memory can be accessed directly using a feature called Program Space Visibility
- interrupt sources may be assigned to distinct handlers using an interrupt vector table
- Compatible with high level language programming, capable to use C language to do complex system programming.

5.2.1 Selection of Compiler

The language of programming are important, it will affect the performance of embedded system, a good programmer need a lot of practice to enhance their code be short, ease to debugging, save cost of instruction to increase performance time.

In this project, Microchip C30 C Compiler has been chosen as compiler for embedded system dsPIC. This is because it has consists:

- High efficiency compilation
- Ease to debug and error tracking
- Provided sufficient source codes and libraries

5.3 System Architecture

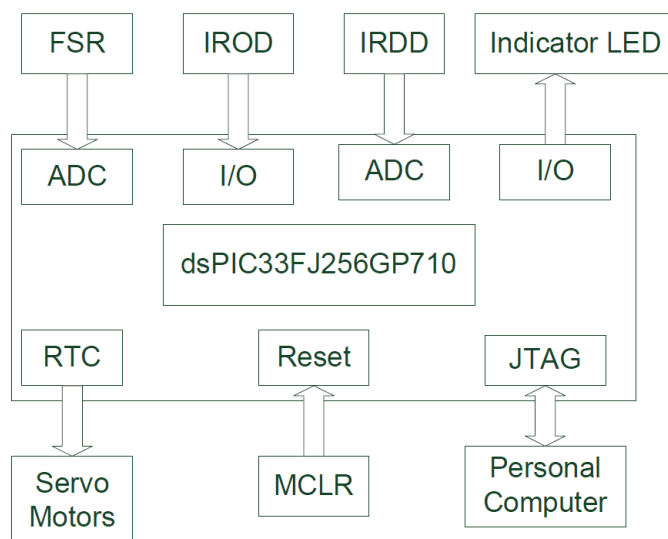


Figure 5.2: System Architecture of IVOARM

As the figure shown as above, system architecture of IVOARM consist ADC, Digital I/O Input, indicator LED, MCLR reset button, RTC PWM Generator and communication port for programmer

5.4 Algorithm

5.4.1 Search Algorithm

The algorithm of IVOARM will be integrated into Microchip C30 C Compiler. Firstly, the system will operate in three modes: Exploring mode and Grasping mode. the algorithm has shown in figure 5.3 & work flow has shown in table 5.2

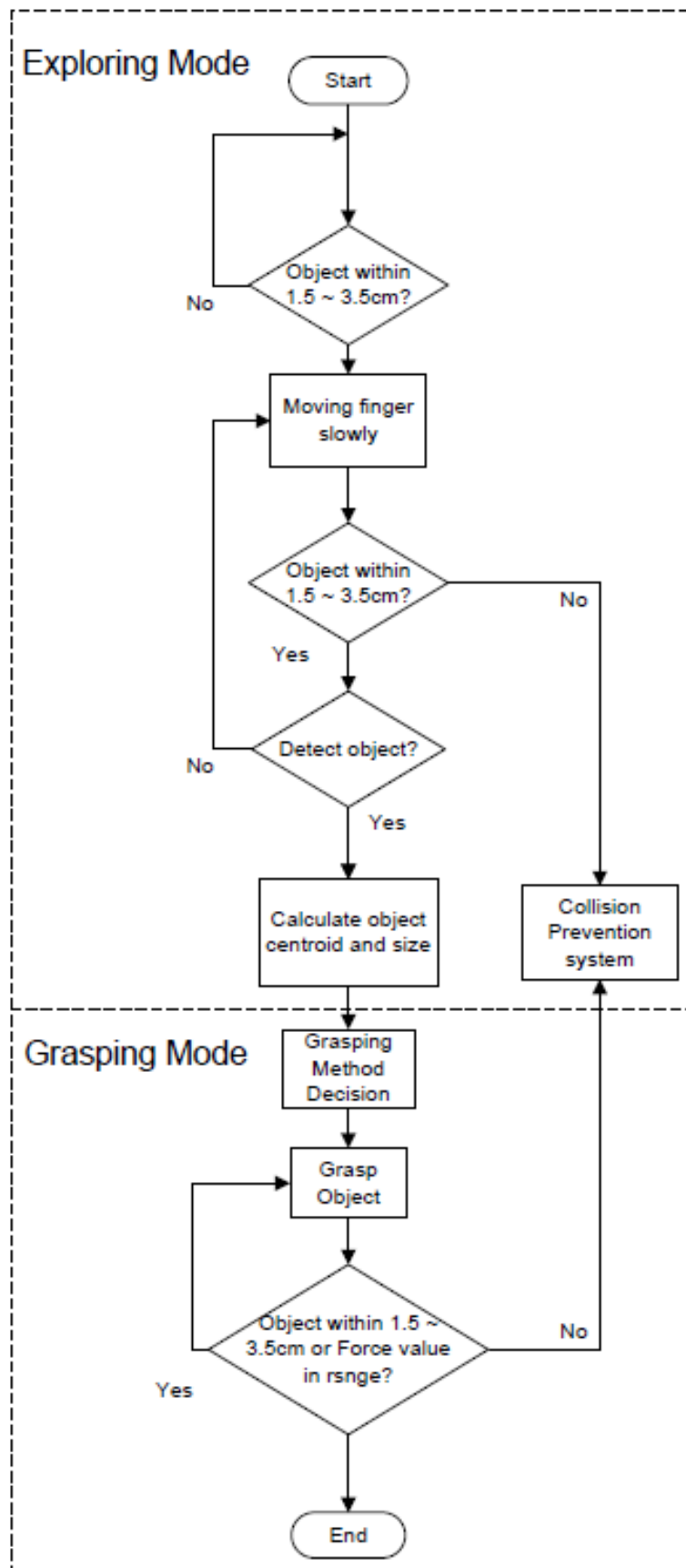


Figure 5.3: Algorithm of IVOARM

5.4.1.1 Exploring Mode

When the size of the object has been defined by the user, the gripper will explore the surrounding and locate the target object. Infrared sensor is used to obtain the distance between the object and gripper. When the object is within range, the infrared detector mounted on the gripper will swing to estimate the basic size of the object.

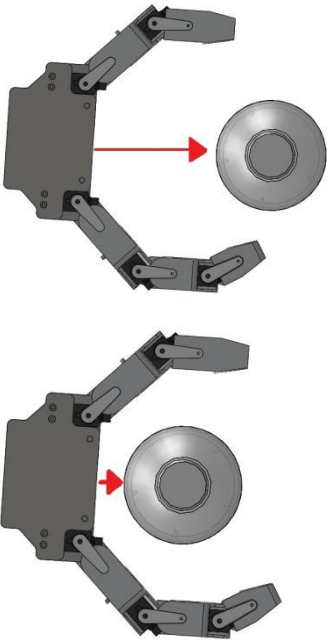
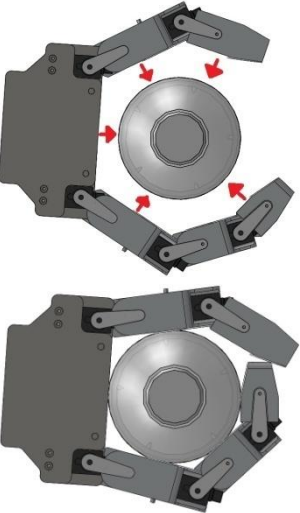
When the object size is determined, dsPIC Digital Signal Controller will start to calculate the centre of gravity of object. Based on this data, it will decide on a suitable grasping method and perform it in grasping mode.

5.4.1.2 Grasping Mode

When the grasping method has been decided, the object is grasped, while force sensing method is applied. The method used is to sum the force applied on the object by using force sensing resistors (FSR).

When the applied force has reached the desired range, the gripper needs to maintain the applied force, in the meantime if objects was happened object slippage or out of grasping range, IVOARM will release object to prevent collisions between manipulator joints.

Table 5.2: Mode descriptions

Method		Description
Exploring mode		<ul style="list-style-type: none"> - Infrared Distance Detector (IRDD) measures distance between gripper and object - When object is within desired range, Infrared Distance Detector (IRDD) and Infrared Object Detectors (IROD) located around the joints will determine the centroid of object - If centroid has been calculated, IVOARM will start grasping object in grasping mode
Grasping mode		<ul style="list-style-type: none"> - In grasping mode, the motion of servo motor will be affected by force sensing values obtained by Force Sensing Resistors (FSR) - When the force sensing value reaches the desired range, it will maintain joint motion of IVOARM

5.4.2 Formulate the Searching Algorithm on Draft Paper

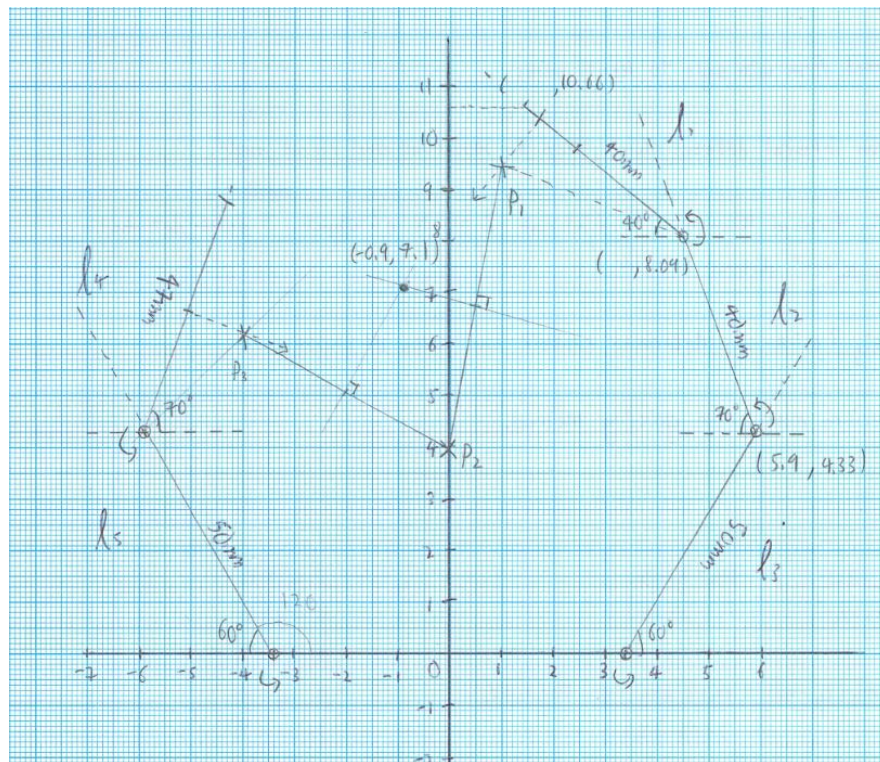


Figure 5.4: Draft and proof the algorithm concept on graph paper

Once the problem is indentified, the objective's working principle will be map out into the draft paper. In this project, the working principle of the searching and calculating the object's size will be draft on a piece paper. Once the draft complete, analysis will be done on this drafted works to formulate the theoretical algorithm that will be used into this project. The theoretical algorithm will be developed using the existing knowledge or formula. In this project, the knowledge of forward kinematic is applied.

5.4.3 Object Centroid and Diameter Calculation by using Forward Kinematics

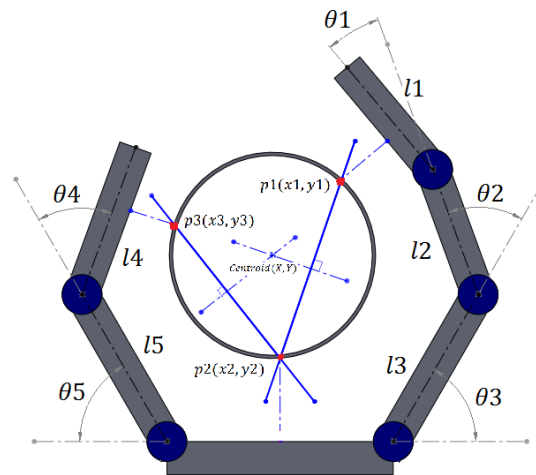


Figure 5.5: Centroid calculation method

Searching equation:

$$ma = \frac{y2-y1}{x2-x1}$$

$$mb = \frac{y3-y2}{x3-x2}$$

Centroid, (X , Y):

$$X = \frac{ma.mb.(y1-y3)+mb.(x1+x2)-ma.(x2+x3)}{2(mb-ma)}$$

$$Y = -\left(\frac{X - \left(\frac{x1+x2}{2}\right)}{ma}\right) + \frac{y1+y2}{2}$$

$$radius, r = \sqrt{(X - x1)^2 + (Y - y1)^2}$$

The figure 5.5 shows the basic idea on how to plot the line to find the size of the object using 3 point circulation method. 3 point circulation is a method to find out centroid with 3 points needed only.

P2 can be determining by IRDD equation which will be discuss at later on. P1 and P3 can be determined by using forward kinematics. From the forward kinematics derived by Mr. Chia Kok Siang, the equation for P1 is:

$$P_{x1} = l_1 \cos\theta_1 + l_2 \cos(\theta_1 + \theta_2) + l_3 \cos(\theta_1 + \theta_2 + \theta_3)$$

$$P_{y1} = l_1 \sin\theta_1 + l_2 \sin(\theta_1 + \theta_2) + l_3 \sin(\theta_1 + \theta_2 + \theta_3)$$

And the equation for P3 is:

$$P_{x3} = l_5 \cos \theta_5 + l_3 \cos(\theta_4 + \theta_5)$$

$$P_{y3} = l_5 \sin \theta_5 + l_3 \sin(\theta_4 + \theta_5)$$

When the sensors have determined the surface of the object, the gripper finger will halt. Based on the angle of the motor position halt, the point of P1, P2 and P3 on the surface of the object will be determined. This will pave the way to determine the P1 and P3 distance with the P2. Then, the middle of the distance between P1 and P2, P3 and P2 will be determined to plot a normal line. Both of the normal lines will be extended to the centre of the object where these lines will intersect. This will give the centroid of the object. When the coordinate of the centroid point is determined, the distance between the centroid with P1, P2 or P3 will be used to determine radius. This will estimate the size of the object and the gradient between P1, P2 and P3

5.5 Equations Formulation

5.5.1 FSR Equation Formulation

Since the electronic control system of the IVOARM can only accept the voltage and current, force applied is needed to be converted into voltage. This can be done by formulating a formula based on the experimented result of each of the FSR. With the assist of equation, IVOARM can receive more accurate force response and precise detection on object slippage.

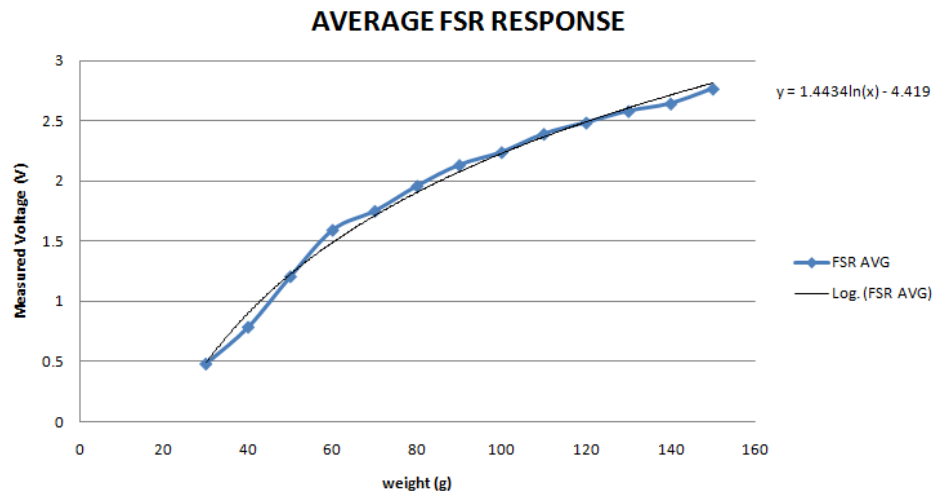


Figure 5.6: Average FSR response

From the figure shown at above, the FSR response equation can be formulate with using Microsoft Excel.

The equation formulated is:

$$V = 1.4434 \ln(g) - 4.419$$

Where,

V = Voltage output

g = force response respect with grams

To compute the force (g) based on voltage, inverse the equation respect with g :

$$g = e^{\left(\frac{V+4.419}{1.4434}\right)}$$

5.5.2 IRDD Equation Formulation

From figure 3.15, the dependence between voltage output and corresponding distance for SHARP GP2D120 is not linear. In order to make it can be read by embedded system dsPIC, equations for measured voltage to distance conversion are needed.

The MS Excel can be used to find out the equation of trend line for the graph as same method with finding FSR equation. In the case of GP2D120 sensor, the power interpolation function is:

$$V = 10.49D^{-0.9283}$$

Where V is the output voltage in volts and D is the corresponding distance in centimeters. To compute distance based on voltage, it is necessary to make inverse function, which has the following form:

$$D = \left(\frac{10.49}{V} \right)^{1.077}$$

5.6 Servo Motor Control

In order to make the formulated method to work in real situation, the relevant component's data will be collected. Sensors such as IRDD and IROD's detection range will be determined so that the formula can include their specification.

The servo motor implemented into this project is HITEC Servo HS-56HB, it small in size but produced moderate torque enough for grasping experiment object. Servo motor usually has three wires: control, positive and ground. The control wire communicates servo angle and speed to turn through Pulse Width Modulation (PWM) signal. In order to maintain servo position, servo motor needed position commanded in continuous time.

5.6.1 Initial Design of Servo Control Signal

The motor control is also needed to be known since every angle and method to control it will affect the result of the calculation. Figure 5.7 shows the initial servo control signal into the servo motor.

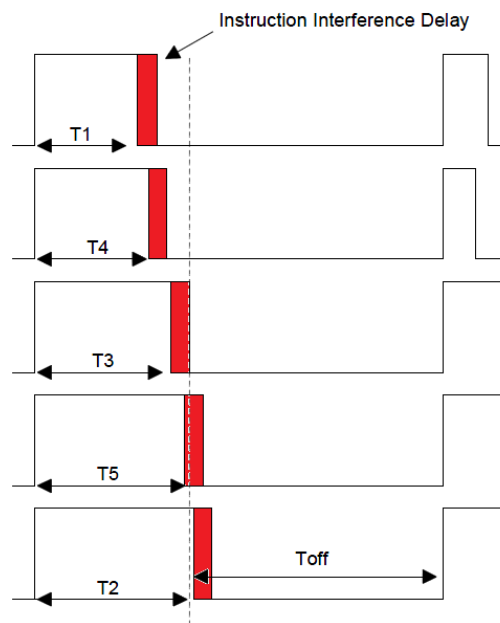


Figure 5.7: Initial servo control signal

The origin servo control pulse was control by “delay” function in C language, which use oscillator of dsPIC to count the servo pulse. With the test of single servo was success, When more servos was added into program, Instruction Interference Delay may occur, the reason is when digital sampling function like ADC trigger and receive information, the delay will stop until ADC sampling has end it sampling and it will continue delay counts and affect continuous delay as shown at figure 5.7. If the Instruction Interference Delay may also affect the resulting delay in dsPIC. To overcome this problem, RTC PWM Generator was suggested by Mr. Lim See Wei, an experienced Engineer from DDMan Sdn Bhd.

5.6.2 RTC PWM Generator

RTC PWM Generator is a programming technique which able to control multiple servos in real time. Since the signal is input into the servo motor feed by a 32KHz RTC Timer at one time, the sequence of each signal input will be arranged in sequential way so that no error will occurs and each of the signal input can be executed at one time. This cycle will repeat itself to maintain the position of the servo motor’s angle. The control algorithm has shown in figure 5.8.

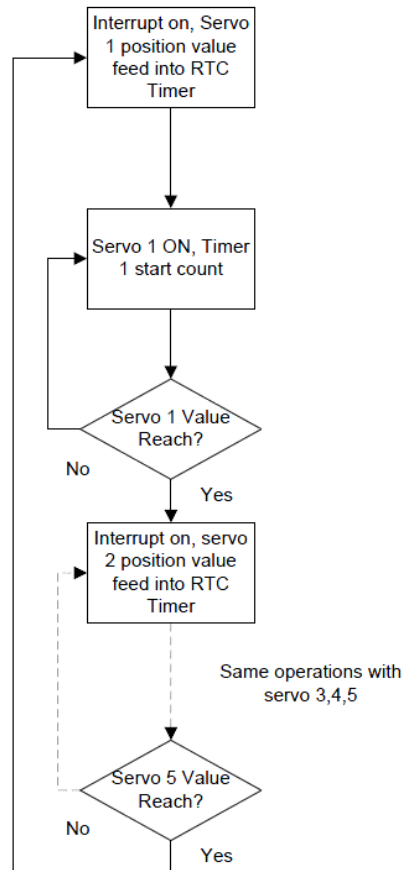


Figure 5.8: RTC PWM servo control

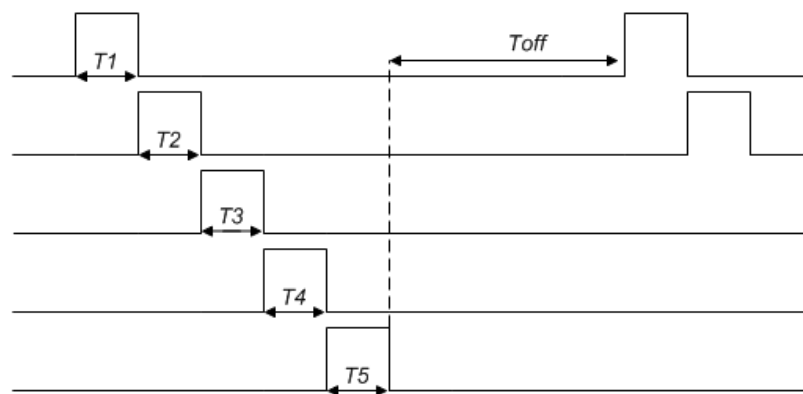


Figure 5.9: The signal sequence input controlled by RTC timer

To control servos with RTC Timer, each servo pulse can be control with equation shown as below:

$$T_n = \frac{Value_n}{32KHz}$$

Where,

T_n = pulse period for servo n,

$Value_n$ = value n to be substitute into RTC Timer for generates servo n pulse

n indicates servo number, e.g. servo 1, servo2, ...

For HS-56HB servo datasheet, the pulse period is fixed at 20ms. Hence the servo time off signal can derive as:

$$T_{off} = 20ms - (T_1 + T_2 + T_3 + T_4 + T_5)$$

5.7 Collision Prevention System

Collision Prevention System (CPS) is designed to prevent the collision may occurred during the exploring mode and grasping mode. With the aid of CPS, the collision between joints has eliminated. The collision will trigger when:

- 1) The object has suddenly disappear during the exploring mode
- 2) The object has force out or broken/damaged from manipulator during grasping mode

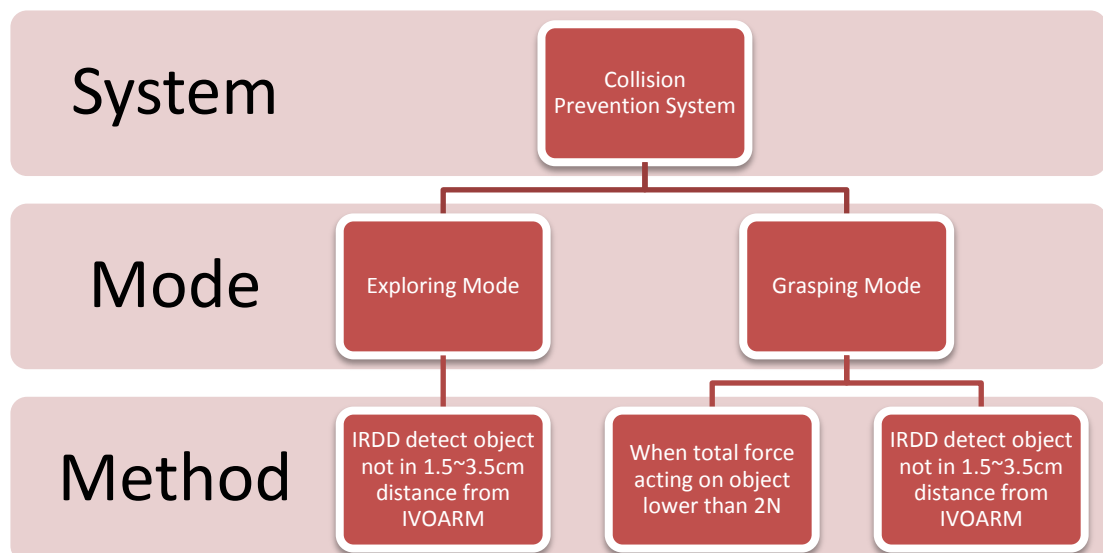


Figure 5.10: Collision Prevention System algorithm

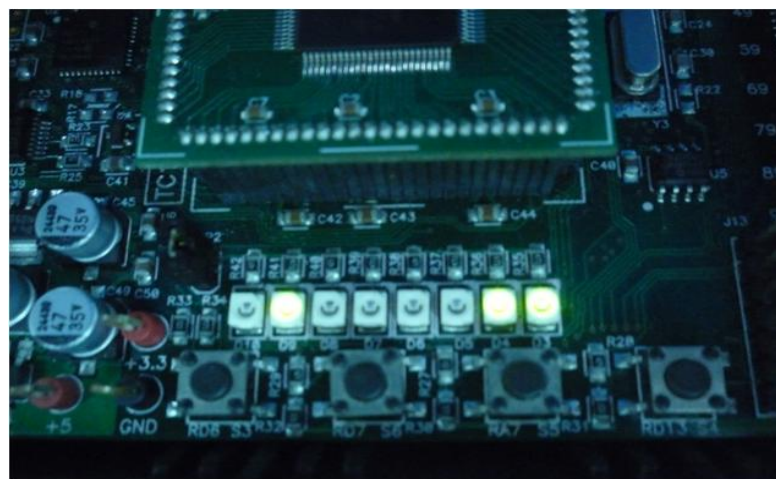
From figure 5.10, the Collision Prevention System (CPS) will occur in Exploring Mode when the sensing distance of object was not in desired distance. During Grasping Mode, the system will triggered by IRDD and FSR both. When IRDD detected object not in distance and/or when force response onto the system was lower than 2N.

5.7 Test and Validate

Once the algorithm formula is formulated out, it will be programming into the dsPIC to test run its function. If the objective of searching and determining the size of the object can be achieved, this algorithm will be put into the system.

Result Display

All result can be display through LED in IVOARM, example like the diameter calculated in IVOARM can display with LED in binary form, figure 5.11 shown the result of diameter are 1000011_2 , convert to decimal form will be 67mm.



$$01000011_2 = 67_{10}$$

$$\text{Diameter of Can} = 67\text{mm}$$

Figure 5.11: Diameter of object display through LED

CHAPTER 6

RESULT AND DISCUSSION

6.1 Results

Result verification on IRDD SHARP GP2D120 at different colour intensity and different colour.

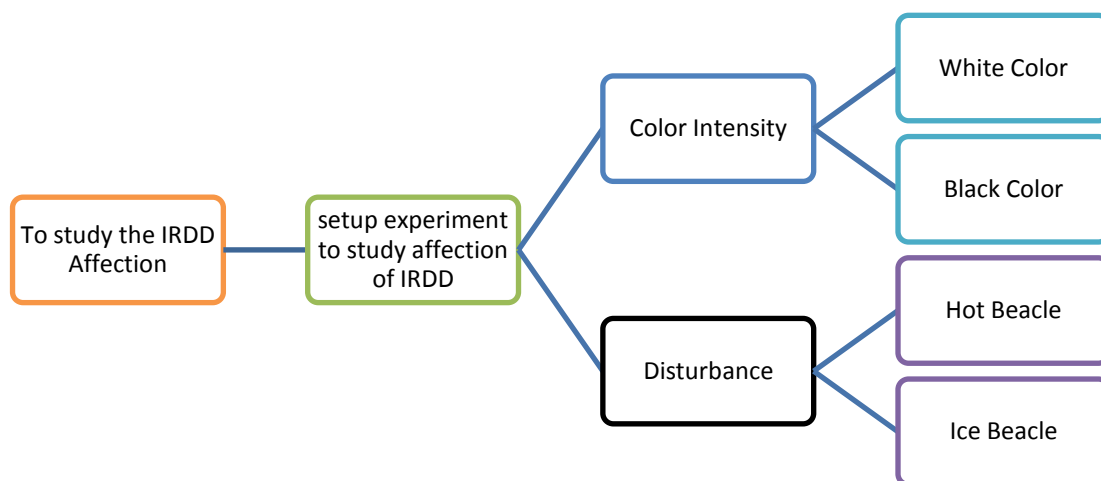


Figure 6.1: Study affection of IRDD

6.1.1 Object's Colour Detection

Objective: This experiment is study the affection of object colour to Infrared Distance Detector

Hypothesis: The colour of object do not cause much affection on reflection of Infra-Red light from IRDD



Figure 6.2: White colour detection

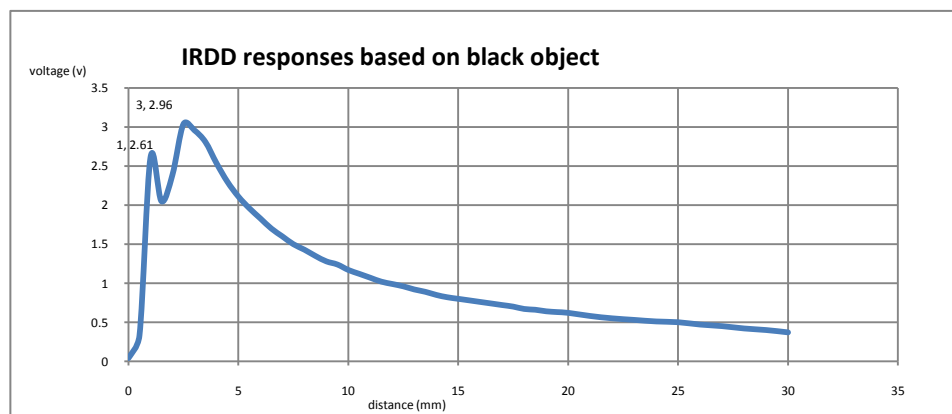


Figure 6.3: Black colour detection

Using the Agilent U2741A Digital Multimeter, the voltage is measured at different distance from the gripper palm. The peak voltage shown in figure 6.2 and figure 6.3 are both 3V. However, the white colour can be detected by the SHARP GP2D120 at 4cm while the black colour is detected at the close range of 2cm. This

indicates the SHARP GP2D120 can detect white colour objects due to its high reflection compare to the black colour objects. However, there is a spike voltage between 0 and 0.03m. Therefore, the IRDD is offset inward the base of the gripper to eliminate this effect.

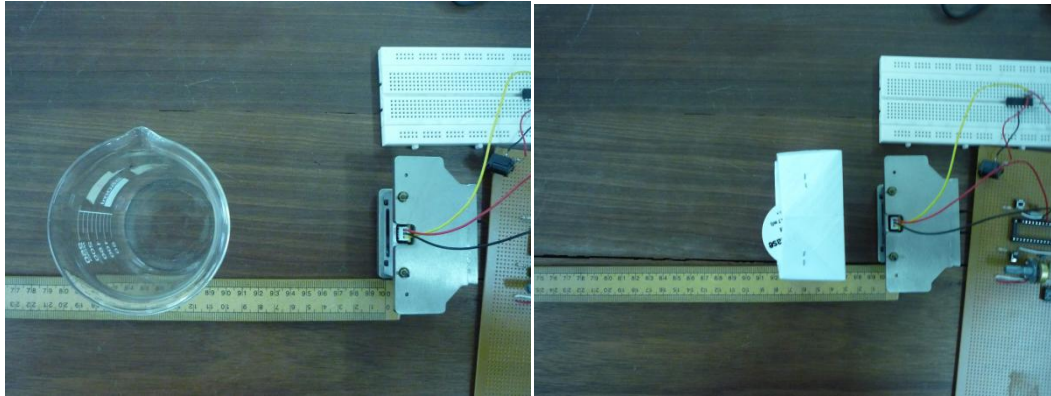


Figure 6.4: The photo taken during experiment

Discussion:

The result shown in figure 6.2 and figure 6.3 has little different in when subject to different colour of detection. The maximum voltage that can be reached in both experiment is nearly 2.96v and their minimum voltage is 0.47v. The result obtained through experiment is proven to have same characteristics with the datasheet provided by SHARP.

The sensing accuracy of IRDD does not affected by colour intensity of the object compares to IROD is because it has signal processing unit inside the sensor.

Conclusion: the colour of object does not affect much for Infra-red Distance Detector range detection. Hypothesis has proven.

6.1.2 Detection of Objects at Different Temperatures

Objective: This experiment is to study the affection of object at different temperature

Hypothesis: The more heat conducted in object, the more infra-red light will be generated and transmitted from object to IRDD.

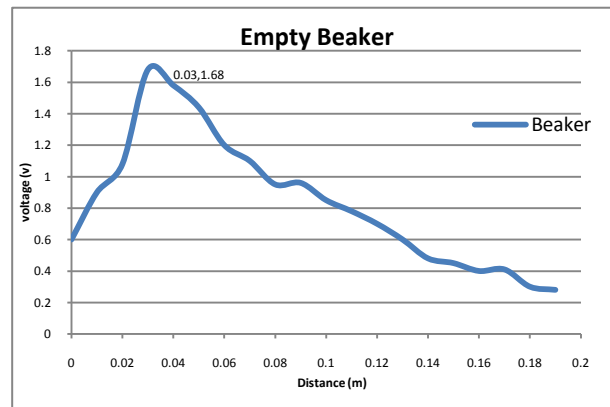


Figure 6.5: Detection of empty beaker at normal temperature

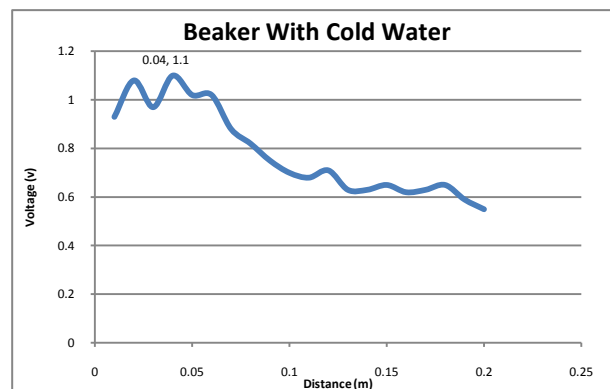


Figure 6.6: Detection of beaker filled with cold water of 0 degree Celsius

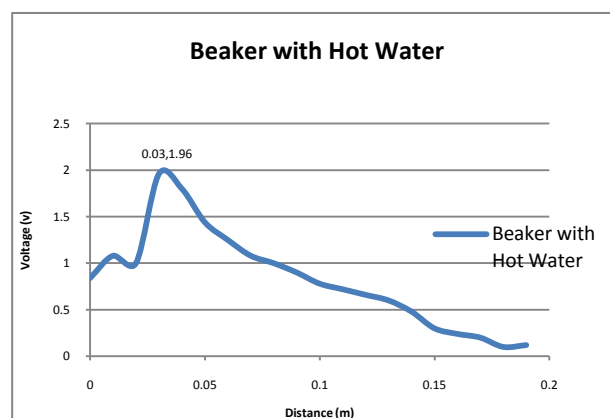


Figure 6.7: Detection of Beaker filled with hot water of 76 degree Celsius

Beakers with various conditions such as empty, filled with hot water and filled with cold water have been tested for the range detection using the infrared distance detector. It is noted that voltage resulted in IRDD for empty and cold water detection is lower than the hot water as shown in Fig. 6.5 and Fig. 6.6. This experiment also helps in possibility indication of voltage in different object temperature.

Discussion:

The experiment shown in figure 6.5, is used to examine the reflection of Infra-Red wavelength on empty beaker. From the result obtained, the maximum measured voltage of the empty beaker is 1.88v. The measured voltage from empty beaker is much lower than the white colour and black colour object. The peak sensing distance for the empty beaker experiment is 3cm. This is due to the light from Infra-Red detector has been refracted when it detects transparent object.

In figure 6.6, the cold water resulted in a splint with a curve. This is because the mist formed on the beaker is caused by low temperature. This has caused the diffraction of infra-Red light emitted from IRDD. From the observation in this experiment, it is found that cold water does not reflect Infra-Red. The reflection is only caused by mist on the object.

In figure 6.7, the maximum measured voltage is at a distance of 3cm. By comparing the result with an empty beaker, heated water has the same voltage peak which is 1.98v at a distance of 3cm. It is shown that heated water will not affect the accuracy of IRDD.

In order to get precise data, the experiment is conducted in SD101 Mechatronics Lab. IRDD has to avoid high ambient light, especially **direct sun light or artificial light** which may cause disturbance to the sensor.

Conclusion: Temperature of object will not cause much affection IRDD accuracy. Affection of IRDD accuracy can be affect by other elements like mist. Hypothesis has proven.

6.1.3 Colour Intensity response on Infra-Red Object Detector

Objective: To determine the affection of reflection by colour on IROD

Hypothesis: The higher colour intensity of object, the longer distance determined by IROD

The reflective sensor mounted on the surface of the gripper finger is to detect the presence of the object to ensure the object is placed within the grasping range. The reflective sensor range of detection is based on the colour intensity of the object. Table 6.1 are the results of the reflective sensor sensing the objects with different colours.

Table 6.1: Distance detected on different colour

Color	Detected Range (cm)
White	1.5
Black	0.5
Mirror	2.6

Discussion:

From Table 6.1, the mirror can be detected at greater distance of 2.8cm compare to white at 1.7cm and black at 1.5cm. This is due to the mirror's high reflective. The black colour detection needs closest range due to its dark colour intensity which absorbs incoming emitted light and low in reflection back to emitter.

Conclusion: the higher colour intensity, the farer distance detected by IROD. Hypothesis has proven.

6.1.4 Experiment and Result of Object Diameter Estimation

Objective: To study the object diameter estimation with different colour

Hypothesis: The lighter colour intensity, the accuracy of estimation will be higher

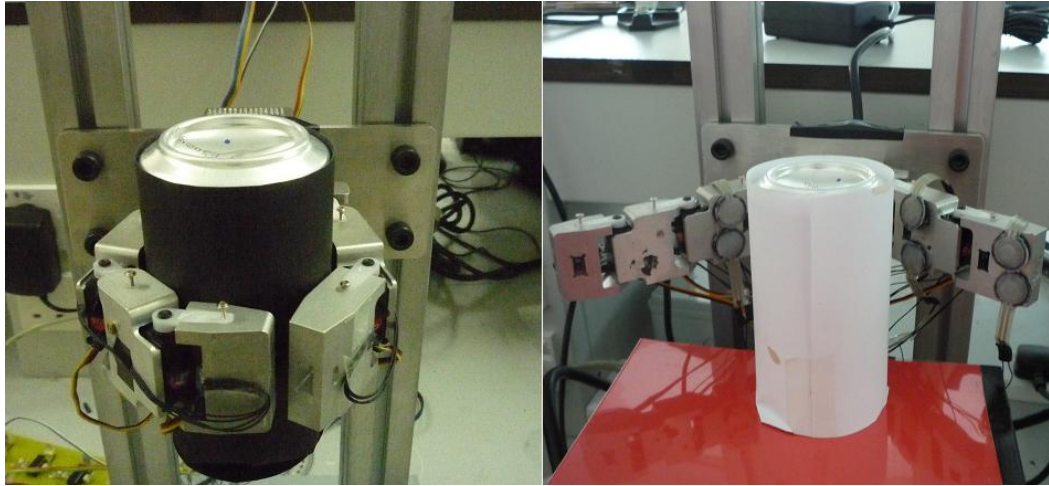


Figure 6.8: Screenshot of Exploring Mode and Grasping Mode

The result in table 6.2 and table 6.3 shows the result of the algorithm used to determine the diameter. In this experiment, a white and a black cans with a diameter of 6.4cm is used. It is noted that the SHARP GP2D120 need to be offset at least 2.5cm distance from the base of the gripper. The purpose of offsetting the Infrared Distance Detector to 2.5cm is to eliminate the present of spike voltage from 0 to 3cm in the IRDD as shown in Figure 6.2 and Figure 6.3.

Table 6.2: Experimental results on White Can Diameter

Distance (cm)	Diameter Detected (cm)
1.5	6.7
2.0	6.3
2.5	6.0
3.0	5.9
3.5	5.8

Table 6.3: Experimental results on Black Can Diameter

Distance (cm)	Diameter Detected (cm)
1.5	6.9
2.0	6.6
2.5	6.2
3.0	5.7
3.5	5.3

Discussion:

As shown in the Table 6.2, the near to zero error percentage in diameter calculation for white can is occurred at the distance of 2cm from the base of the gripper.

However, for black can calculation shown in table 6.3, the diameter at 2cm is 6.6cm which is less accurate compare to the white can due to the black surface which has absorbed part of the emitter light from reflecting back to the receiver diode in infrared distance detector. Therefore, the gripper is programmed to detect the object at 2cm before start to estimating the object size. This is used to obtain the near accurate information.

Conclusion: colour intensity of object will affect the object estimation, the higher colour intensity, the more accurate object estimation. Hypothesis has proven.

6.2 Discussions

6.2.1 FSR Respond

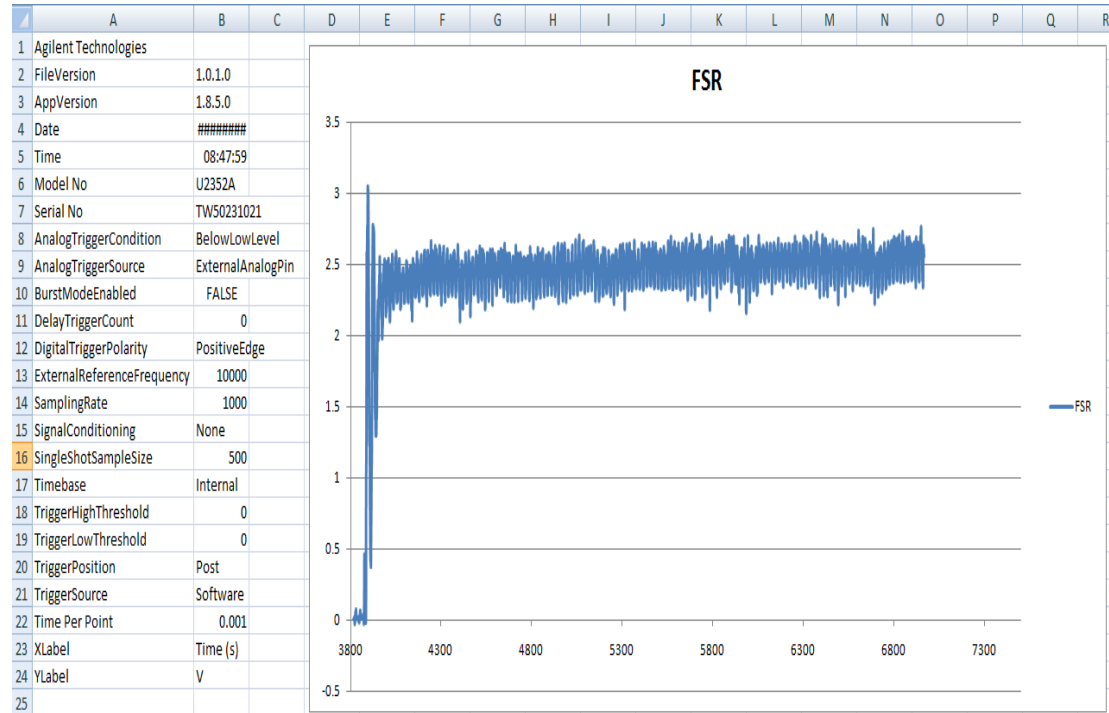


Figure 6.9: Force respond of the IVOARM finger gripper on the surface object

The force respond in the figure 6.9 is measured using the Agilent U2352A DAQ and the Agilent Measurement Manager. The force respond in figure 6.9 is obtained by summing all the respond from all the FSR's respond in the gripper. From the graph, the steady state which the force is equilibrium with the force respond from the tin is at 2.5v. When converted into force using the figure 5.6, 2.5v gives the force of 0.03N

It is noted that a spike voltage has occurred at the 3v at 4000 millisecond. This is a damping effect of the gripper's finger and the object surface. The initial contact of the gripper's finger with the object has causes the gripper's finger to bound upon the impact.

The vibrating line which can be seen at the steady state is actually caused by the noise of the surrounding. It can be filtered out to obtain a pure steady respond.

However, other factors that contribute to such vibration is the servo motor control is constantly switch to on and off due to the repeating signal sent into it.

6.2.2 Suggestion of Noise Filtering

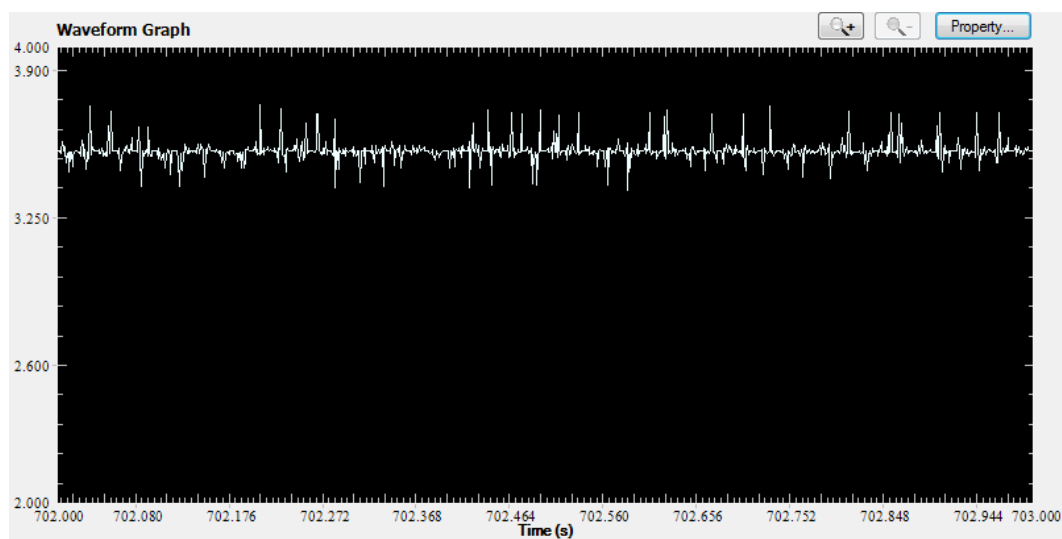


Figure 6.10: Noise disturbance in force response

The force response obtained by Agilent U2352A has significant noise plotted by PC. This force response noise might but it might cause the problem to IVOARM when manipulator needed more precise force data in future development. The noise disturbance shown in figure can be removed by implement some filtering techniques like wavelet transform into dsPIC. With the wavelet transform filtering, noise received can be eliminate and smoothen force response signal.

6.2.3 Problem of circuits constructed with Veroboard

In initial stage of project development, the author tries to construct the circuit with donut board as the base to solder. After the circuit constructed, many of the problems was appear. First, the connectivity between Veroboard (known as prototype board)

and sensors always loose, the reason is the contact point between pin and holder are small. Second, tight soldering route has because some signal disturbance.

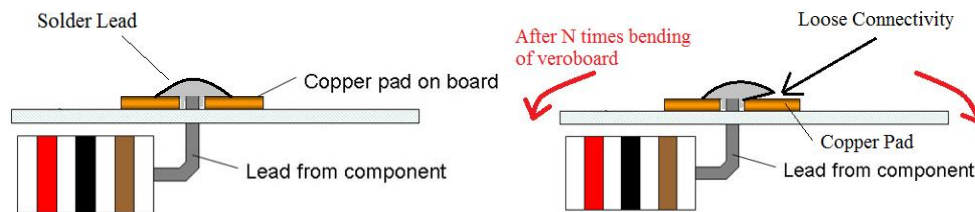


Figure 6.11: Loose connectivity of Veroboard

With some investigation, the reason is bending of Veroboard. The figure 6.8 has shown the loose connectivity caused by Veroboard. Commonly the Veroboard can perform circuits perfectly, the solder connection of Veroboard is construct with solder lead, it is solid and fragile. With many times of bending up and down, the solder route has formed a crack. This crack might cause the connectivity problem between Veroboard and components.

To overcome this problem, the author has decided to redesign circuit system and fabricate into PCB and problem discussed has been solved.

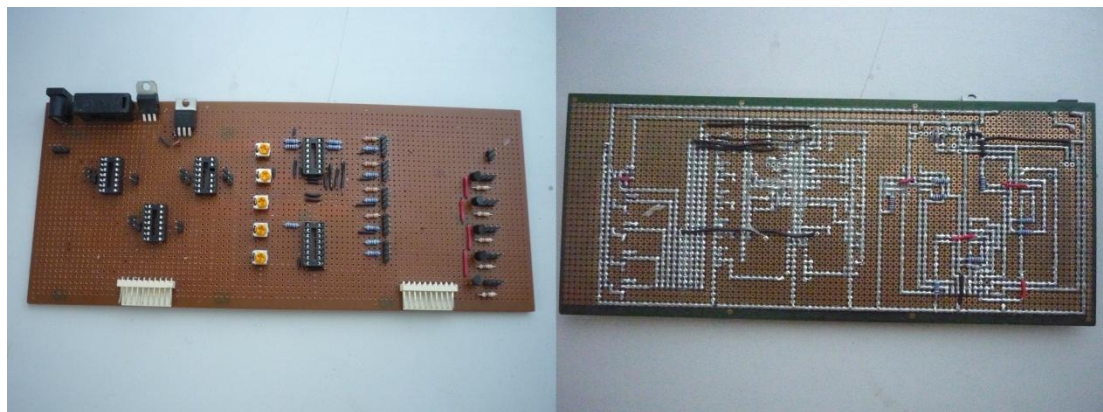


Figure 6.12: Electronic circuit soldered in Veroboard

6.2.4 Problem of using Agilent VEE Pro

In the initial development stage, the estimated diameter of object and force responses are proposed to displayed with Agilent Virtual Engineering Environment Professional (Agilent VEE Pro), a engineering software design function with flow diagram, can interface with MATLAB and able to communicate with instrument hence display results in Graphical User Interface (GUI).

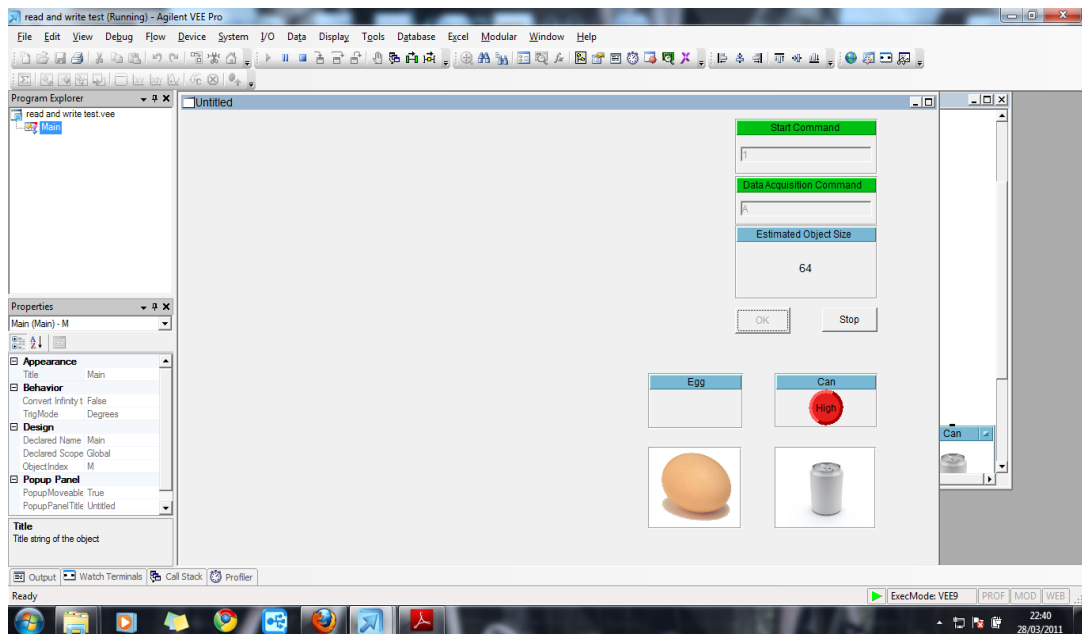


Figure 6.13: Development of program in Agilent VEE Pro

During the development of Agilent VEE Pro, the author has develop a serial communication between Agilent VEE Pro and dsPIC. To communicate with other instruments, Agilent VEE Pro need communication configurations like IVI-COM, Direct I/O, VISA and other configurations. The communication used during project development is Agilent Virtual Instrument Soft Architecture (VISA). The VISA address in Agilent is called ASRL3::INSTR, its mean ASRL communication in port 3, INSTR stand for instrument, the communication problem between Agilent VEE Pro and dsPIC is communication between may able to communicate but sometimes may not. Hence an investigation has been tested:

- 1) Transmit a set of data from PC to dsPIC
- 2) Transmit a set of data from Agilent to dsPIC
- 3) Transmit a set of data from dsPIC to PC
- 4) Transmit a set of data from dsPIC to Agilent VEE Pro

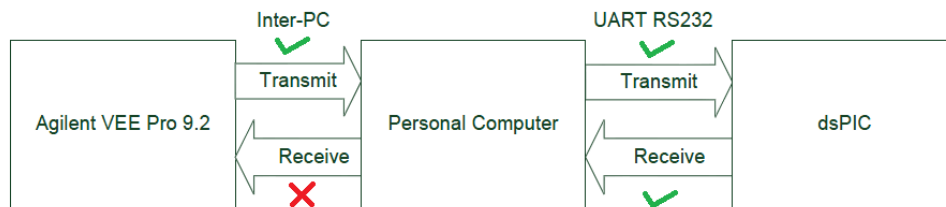


Figure 6.14: suspected problem of Agilent VEE Pro serial communication

From the investigation has tested, the transmission from dsPIC Explorer 16 Development board to Agilent VEE Pro has been suspected. Problem suspected was occurred by the VISA configurations, VISA configuration in Agilent VEE Pro might has some bugs and not operates well anytime.

6.3 Precautions

6.3.1 Wire Selection

in circuit design, power transmission between system need o consider power loss and signal noise may bring problem to obtain good result.

In this project, two main wire are consider to be implement in circuit: solid core wire use for power transmission and stranded wire for signal transmission. solid core wire apply in static condition like PCB inter route. Stranded wire is used when high cable flexibility is required, such situations like connection between device and

Print Circuit Board, where rigidity of solid wire would produce much stress in movement.

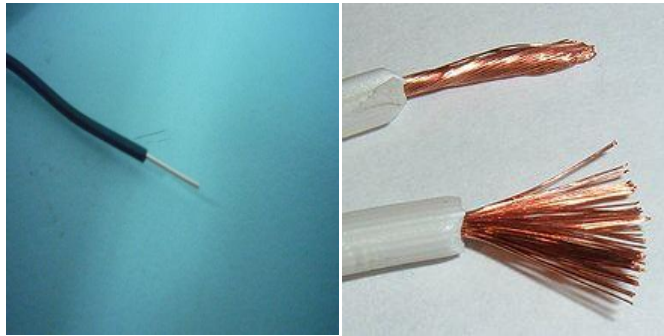


Figure 6.15: Solid Core wire (left) and Stranded wire (right)

6.3.2 Wiring covered by Cable Protector

When all wiring are arranged, the cable need to categorized into related groups to minimise the human errors.

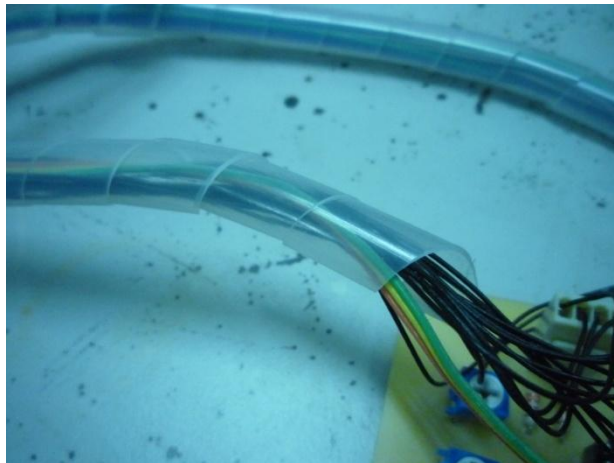


Figure 6.16: Wire covered by cable protector

6.3.3 Labelling each wire with suitable name

The main function to label the cables is to determine wire function, cut down the time to connecting wire and minimize error of connecting wrong wire

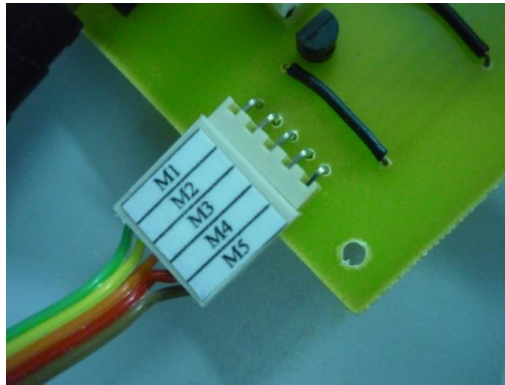


Figure 6.17: Labelling wire with suitable name

6.3.4 Programming separate into main program and sub program

In programming, the author need to separate their source code into main program and sub program, this programming practice can make programmer easier to track and troubleshooting the problems when error comes out. Example: when the ADC function has some problem, programmer no need to check line by line from the whole code, programmer only need to tracking error from the separated source files (e.g. `int_ADC.c` and `isr_ADC.c`) which shown in figure 6.18.

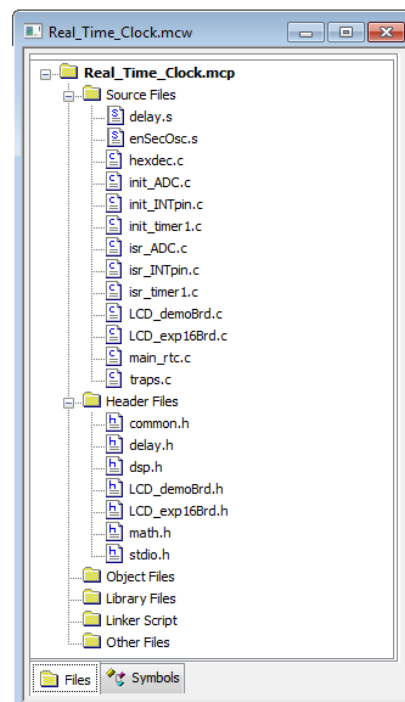


Figure 6.18: separate program into main program and sub program

6.3.5 Soldering Techniques

Soldering techniques are important because incorrect soldering may cause the open circuit or partial connectivity between the PCB and the component pin soldered. Figure 6.19 shows proper soldering techniques and Figure 6.20 shows improper soldering techniques.

Some components can be damaged by heat when soldering period too long or soldering temperature has over temperature can handle by components characteristics. So, the solder time to solder the pin onto the PCB must be quick as longer solder time may generate more heat and cause components damage.

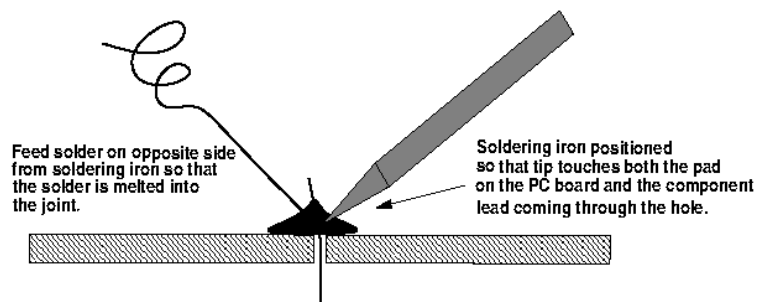


Figure 6.19: Proper soldering techniques (adopted from Fred Martin, 1998)

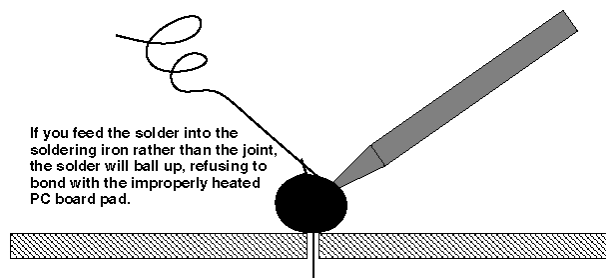


Figure 6.20: Improper soldering techniques (adopted from Fred Martin, 1998)

6.3.6 Component selection

Some of the components used in this project has to be select carefully, especially those components which may affect accuracy of system. One of the examples in this project is the selection of resistor for FSR. Different value and tolerance of resistor may result different accuracy of value sensed by sensor. By considering the sensor

characteristics, the resistor value has selected with moderate resistance value and low tolerance which makes system has high accuracy.

6.3.7 Power Supply Management

The input power to the IVOARM system is design with well calculation of power consumption. Before the Switch Mode Power Supply (SMPS), the high performance power supply purchased, the power consumption of whole system has been estimated with referring all datasheet. Total current of IVOARM can be estimated as 1.5A, the final SMPS purchased is 6V/2A and it has fulfils all requirements of IVOARM needed.

6.3.8 Testing and Troubleshooting

All the circuits are tested by Multisim and breadboard to ensure the design is working properly before implement the circuit into the Printed Circuit Board. The function of the hardware is tested using dsPIC explorer 16 development board. Testing is important because it helps to discover problem in an early stage. To solve the problem happen during testing, troubleshooting plays an important role in solving the cause of the problems and modified the design if necessary.

CHAPTER 7

CONCLUSION

7.1 Conclusion

As the conclusion, the design of IVOARM gripper has achieved all the objectives stated in the aims and objectives. The IVOARM's angle for each of the joint can be controlled independently from others,

The sensors such as IRDD, IROD and FSR can be integrated into IVOARM. The detection using sensors are achieved and able to be measured using U2352A DAQ and monitored using Agilent Measurement Manager.

Experiment for measuring the centroid and radius size of the object has been achieved and the result is matching with the actual radius size of the object.

Finally, this final thesis is completed with an IVOARM and the design is proven feasible with information collected from embedded system dsPIC and Agilent U2352A Data Acquisition module.

7.2 Recommendations

7.2.1 High Speed Grasping with Force Control

The IVOARM research can be further improved where the impact of high speed grasping upon the surface of the object which is force control can be focused on.

7.2.2 Implement a Colour Sensor

Existing design of IVOARM only able to perform search algorithm with fixed colour of object, the reason is defined as IROD in the system cannot differentiate colour of objects and change IROD sensor value for calculation and detection, improvement is recommend to implement a colour sensor which able to recognise object colour and adjust IROD sensing range, the illustration shown in figure 7.1.

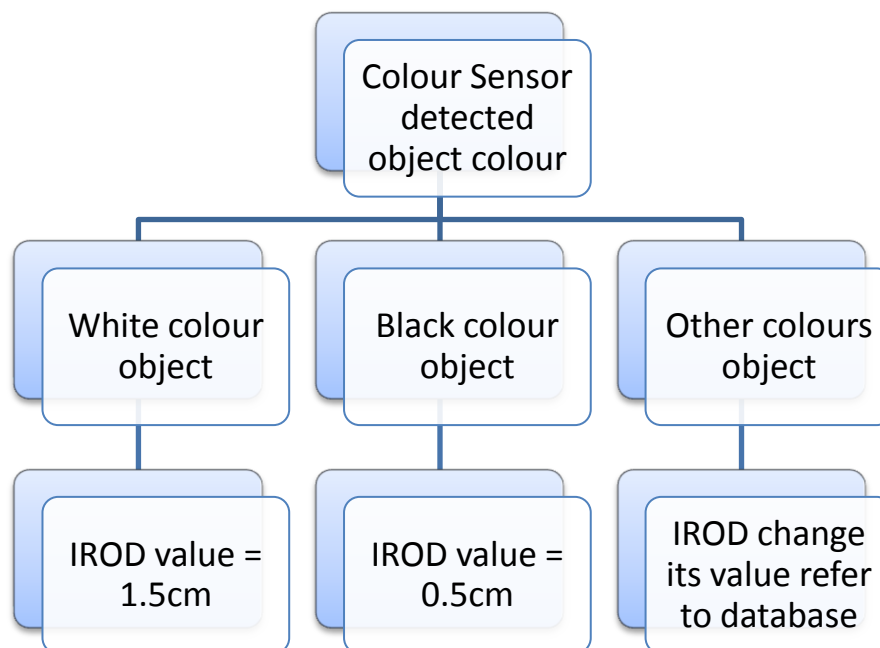


Figure 7.1: Implement colour response to IVOARM

7.2.3 Implement Artificial Intelligent (AI) on search algorithm

The IVOARM can search object in fixed pattern, in algorithm design, the joint control and control by series, e.g. joint3->joint2->joint1->joint5->joint4. In order to perform a better object estimation, a good search is a must. The AI is one of the best approaches to enable the search mission.

7.2.4 Shape recognition for IVOARM

The IVOARM can be attached onto robot arm as end-effector to perform new research which is shape recognition. The IRDD can be used to scan on the surface of the object to extract its shape. The movement of the arm holding the IVOARM can aid the IRDD to scan on the surface at various place, saving each point it scanned and combine all the points together to form a line which represent the extrude and intrude of the object's surface.

7.3 Publication on Symposium (6th MCSoCs) and finalist in competition

At the end of this project, the project team has submitted a symposium paper to IEEE 6th International Symposium on Embedded Multicore SoCs (MCSoCs) in Japan, the paper has attached with the thesis. The project also shortlisted into finalist of Innovate Malaysia Competiton 2011 – Agilent Track and results will announce at 11 June 2011.

Embedded System Application - In-Vitro Optically Aided Robotic Manipulation

ChingSeong Tan, ChiaLoon Cheng, KokSiang Chia

Department of Mechatronic & Biomedical Engineering

Faculty of Engineering & Science

Universiti Tunku Abdul Rahman

Kuala Lumpur Campus

Jalan Genting Kelang, Setapak 53300, Kuala Lumpur

Email: tancs@utar.edu.my, chialoon@ieee.org, cks_999@hotmail.com

Abstract— This paper demonstrates the embedded application of a novel manipulator design. The In-Vitro Optically Aided Robotic Manipulation (IVOARM) constitutes a blind grasping concept using two anthropomorphic fingers with the aid of the directional force sensors and infra-red sensors mounted on it. This manipulator is controlled by an embedded system with high DSP compatibility. The infra-red sensors are mounted on the surface of the finger gripper to detect the presence of the object in the area of the grasping. The size and centroid of the object is determined with the aid of the in-vitro embedded infra red sensors. The centroid estimation is to determine the size and initiate the grasping configuration of the object. The result of the object size determination using the IVOARM is presented.

Keywords - Infrared Distance Sensor, Embedded System, In-Vitro Optical Aid

I. INTRODUCTION

Most of the industrial robot today employs unique method to grab and grip the object with the specific gripper, depending on the requirements and working constraints. Most of them have actively employed the external vision system to aid the gripping process. These give the information such as size, location, orientation, and object type to the gripper. However, not all situations can employ the use of machine vision.

The main component used by NASA for the assembly of the International Space Station is the space machine vision. Video camera based system, are attractive because of their ease of use, low maintenance and simplicity of integration to existing equipment [1]. However, not all the external machine vision can be employed to supervise the gripper. Presence of sun and other strong source of light adversely affect the quality of the conventional methods that rely on standard video images, e.g. the camera on board the Space Shuttle [1]. This has given poor disadvantage to the machine vision where light reflection on the surface of the components or material captured in the video will gives poor view to the engineer when assembling

because the engineer need to uses the gripper to move the components at exact location.

The Northern Digital Incorporate [2], a company specialize in medical field has stated machine vision looks appealing from the perspective of minimal impact (with the exception of line-of-sight), there are many difficult implementation and environmental problems. These problems prevent machine vision from being broadly applicable. It is rare to find a machine vision solution that considers usability and minimizes application interference.” The interferences that stated by the Northern Digital Incorporate are the weakness of the machine vision such as line of sight between tracker and target, A less intrusive system typically means a less robust or flexible system, lighting conditions and background interference (complexity) can cause tracking problems [2].

In determining the location of the object, there is a method known as visual odometry in machine vision which analyze the camera images to obtain the robot movement or location. However, the precision of the visual odometry system depends, among other things, on the resolution of the camera images. If the resolution is high, the precision can become better but the system has to handle more information. More information can lead to more errors in the object matching process, due to problems with more noise in the image [3].

Thus, unsupervised gripper is needed to grip the unknown object randomly with or without the aid of the machine vision. The IVOARM is a design that integrates with force sensors and infra-red sensors to enforce blind (non-machine vision) grasping. The blind grasping operation is done with the aid of the infra-red sensors detector to locate the object with or without the presence of the machine vision.

The object is first detected by the distance detector to ensure it is in the envelope of gripping area. Then, both of the fingers gripper will start to move closer to the object at fast speed. When the infra red sensor mounted on the surface of the finger gripper detects the object, the gripper movement will be halted. The size of the object is calculated using the angle position of the motor which is in

halt. Once the size of the object is known, the gripper will then slowly moves to the surface of the object, depending on the information calculated from the algorithm and apply small force.

II. MECHANICAL DESIGN

A. Kinematic of Gripper

The two fingers anthropomorphic gripper is chosen in the design due to the fact that this anthropomorphic has the highest percentage of gripping in term of envelope. Fig. 1 shows the percentage of envelope of a cylindrical object in percentage.

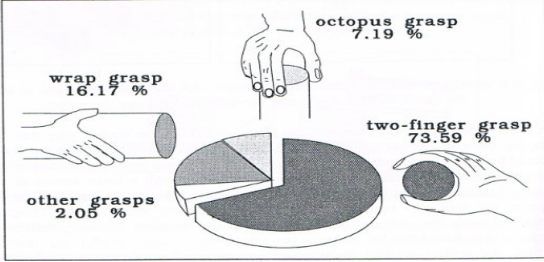


Figure 1. Percentage of envelope of a cylindrical object in percentage using anthropomorphic method [4]

The forward kinematic method [6], [7] is used to design the two joints gripper as displayed in Cartesian coordinate system shown in Fig. 2.

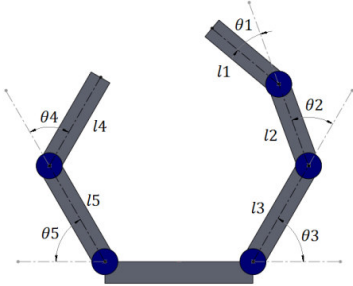


Figure 2. Free body diagram of a gripper designed

The free body diagram in Fig.2 can be expressed into forward kinematic equation of index finger as below:

$$T1(\theta1) = \begin{bmatrix} \cos(\theta1) & -\sin(\theta1) & 0 \\ \sin(\theta1) & \cos(\theta1) & 0 \\ 0 & 0 & 1 \end{bmatrix}, \quad (1)$$

$$T2(\theta2) = \begin{bmatrix} \cos(\theta2) & -\sin(\theta2) & l1 \\ \sin(\theta2) & \cos(\theta2) & 0 \\ 0 & 0 & 1 \end{bmatrix}, \quad (2)$$

$$T3(\theta3) = \begin{bmatrix} \cos(\theta3) & -\sin(\theta3) & l2 \\ \sin(\theta3) & \cos(\theta3) & 0 \\ 0 & 0 & 1 \end{bmatrix}, \quad (3)$$

$$T4 = \begin{bmatrix} 1 & 0 & l3 \\ 0 & 1 & 0 \\ 0 & 0 & 1 \end{bmatrix}, \quad (4)$$

$${}^{ee}_bT = {}^4_0T(\theta1 \ \theta2 \ \theta3). \quad (5)$$

Where ee is end effector and the b is the base.

Then,

$$\begin{bmatrix} x \\ y \\ 0 \end{bmatrix} = T \begin{bmatrix} 0 \\ 0 \\ 1 \end{bmatrix}. \quad (6)$$

Thus, the forward kinematic complete equation of the index finger is

$$x1 = l_3 \cos \theta_3 + l_2 \cos(\theta_2 + \theta_3) + l_1 \cos(\theta_1 + \theta_2 + \theta_3), \quad (7)$$

$$y1 = l_3 \sin \theta_3 + l_2 \sin(\theta_2 + \theta_3) + l_1 \sin(\theta_1 + \theta_2 + \theta_3). \quad (8)$$

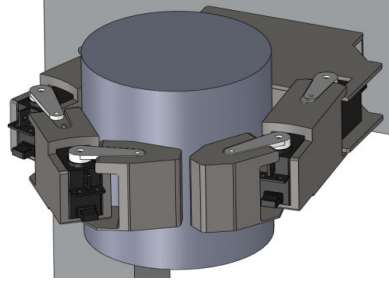


Figure 3. Grasping Simulation of IVOARM in Solidwork.

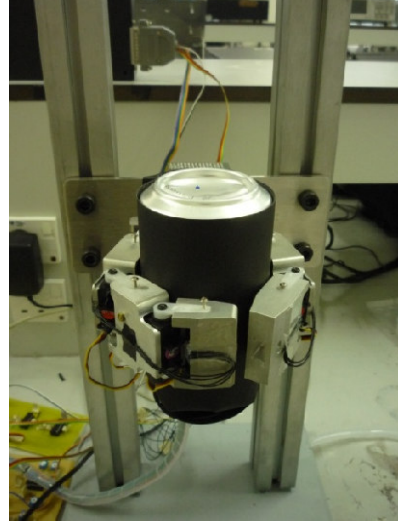


Figure 4. The IVOARM grasping black can in real world.

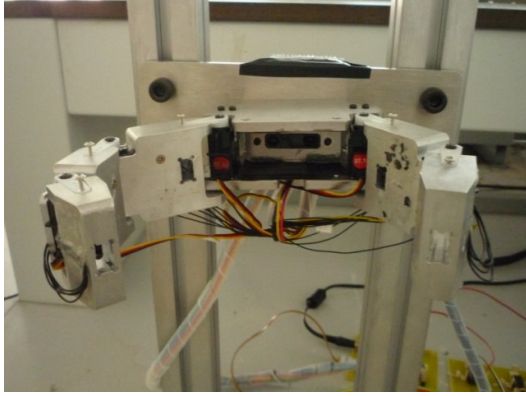


Figure 5. The Infrared distance detector is offset inward the base of the gripper

The infrared distance detector in Fig. 5 is built beyond the base of the palm. The purpose of offset the infrared distance detector inward is to eliminate the voltage spike which will be discussed in Section IV.

For the thumb finger, the final equation is

$$x_4 = l_5 \cos \theta_5 + l_4 \cos(\theta_4 + \theta_5), \quad (9)$$

$$y_4 = l_5 \sin \theta_5 + l_4 \sin(\theta_4 + \theta_5), \quad (10)$$

Simulation of IVOARM is shown in Fig. 3 while the Fig.4 shows the gripping of bottle by ARM in real world.

III. SYSTEM ARCHITECTURE

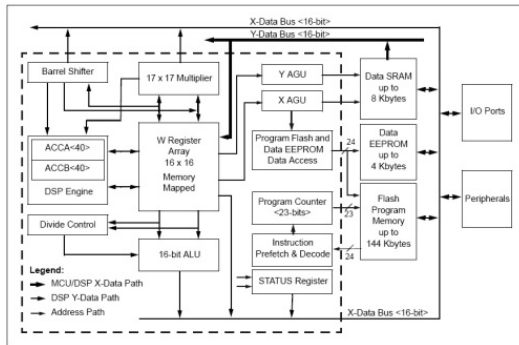


Figure 6. IVOARM's dsPIC 33F256GP710 architecture structure [5]

The IVOARM system architecture is fully displayed in Fig. 6. The dsPIC is used in IVOARM because its architecture system inside has a built in DSP Engine which is used to perform the control in high speed and lower cost. It has the advantage of high speed which is up to 30 MIPS and faster than the normal 16 bit microcontroller. This can stamp out any slowdown to the respond system.

IV. EXPERIMENT RESULT OF THE SENSORS

A. Infra-red Distance Detector

The function of the infrared distance detector (IRDD) is to detect the distance of the object from the gripper inner base of the gripper hand. The infra red sensor distant detector used in this project is SHARP GP2D120 where the detection ranges' results on different object with different colours and temperature.

1) Object's Colour Detection

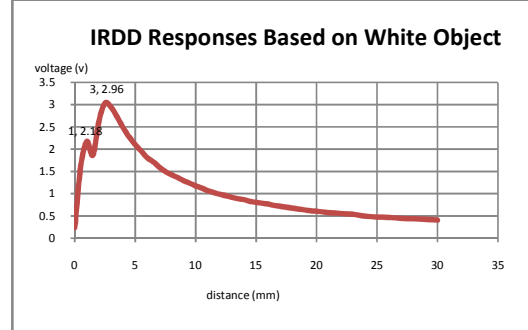


Figure 7. White colour detection

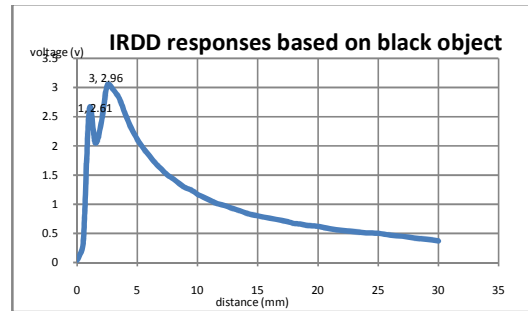


Figure 8. Black colour detection

The calibration [8], [9] of the sensor can done using Fig. 7 & Fig. 8. The peak voltage shown in Fig. 7 and Fig. 8 are both 3V. However, the white colour can be detected by the SHARP GP2D120 at 4cm while the black colour is detected at the close range of 2cm. This indicates the SHARP GP2D120 can detect white colour objects due to its high reflection compare to the black colour objects. However, there is a spike voltage between 0 and 0.03m. Therefore, the IRDD is offset inward the base of the gripper to eliminate this effect.

2) *Detection of Objects at Different Temperature*

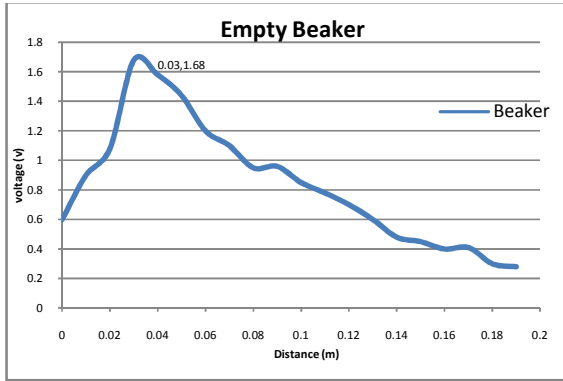


Figure 9. Detection of Empty Beaker at normal temperature

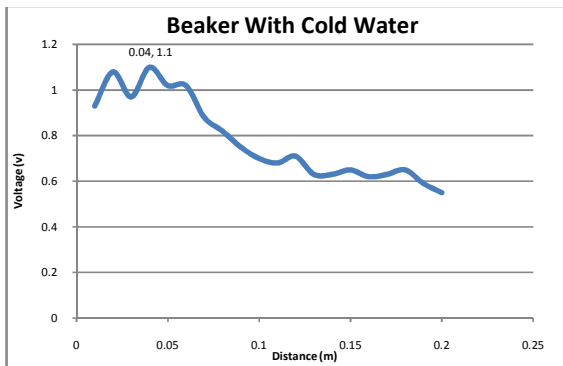


Figure 10. Detection of Beaker filled with cold water of 0 Celcius

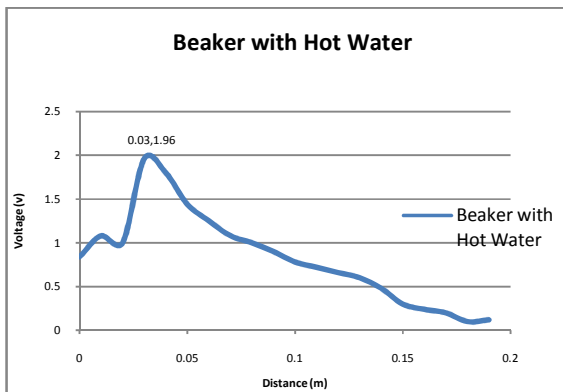


Figure 11. Detection of Beaker filled with hot water of 76 degree Celcius

Beakers with various conditions such as empty, filled with hot water and filled with cold water have been tested for the range detection using the infrared distance detector. It is noted that voltage resulted in IRDD for empty and cold water detection is lower than the hot water as shown in Fig. 9 and Fig. 10. This experiment also helps in

possibility indication of voltage in different object temperature.

B. Reflective Optical Sensor with Transistor

The reflective sensor mounted on the surface of the gripper finger is to detect the presence of the object to ensure the object is placed within the grasping range. The reflective sensor range of detection is based on the colour intensity of the object. Table I are the results of the reflective sensor sensing the objects with different colours.

TABLE I. DISTANCE DETECTED ON DIFFERENT COLOUR

Color	Detected Range (cm)
White	1.5
Black	0.5
Mirror	2.6

From Table I, we found out that mirror can be detected at greater distance of 2.8cm compare to white at 1.7cm and black at 1.5cm. This is due to the mirror's high reflective. The black colour detection needs closest range due to its dark colour intensity which absorbs incoming emitted light and low in reflection back to emitter.

V. THE EMBEDDED CONTROL SYSTEM

A. IVOARM's Closed Loop System

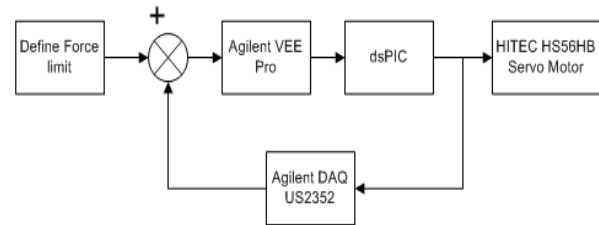


Figure 12. Closed loop system of Advanced Robotic Arm gripper.

The control system in Fig. 12 will be used to dictate the behavior of the gripper. At first, user will define the estimated force. Then, this force estimation will be keyed in to the Agilent VEE Pro. The Agilent VEE Pro serves as the graphic user interface between the dsPIC and Agilent DAQ. The dsPIC is used to control the movement of the servo motor based on the data sent from Agilent VEE Pro. The servo motor will position itself to the defined place and the sensors will send feedback to the Agilent VEE Pro via Agilent DAQ US352. The Agilent will minimize error of the feedback data with the defined data. The loop continues until suitable level is reached.

B. In-Vitro 's Flow Chart Diagram

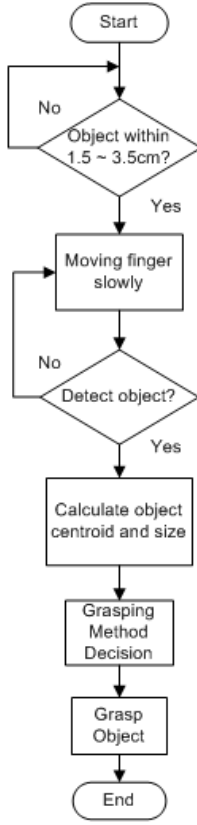


Figure 13. Flow chart of the Advanced Robotic Arm gripper

The flow chart in Fig. 12 starts with the detection of the object within the range of 1.5 cm and 3.5cm from the base of gripper. This is to ensure the presence of the object. Next, the finger gripper will move in slow motion towards the surface of the target object. The infra red detectors on the surface of the finger gripper will sense if the surface of the object is detected. If yes, decision making stage will be executed based on the calculation of the target object size. The method will be included such as grasping bottle, grasping egg or grasping pen method [10]. After the decision has been made, the object will be grasped accordingly.

The maximum distance for object detection for this gripper will be up to 0.035m which is in the boundary location of the reflective sensor. Any object outside this range will not trigger any respond from the gripper.

If the object is removed from the gripper during the process of estimating its size, the gripper will reset to its home position.

VI. CENTROID SIZE AND CALCULATION

A. Mathematic Formulation

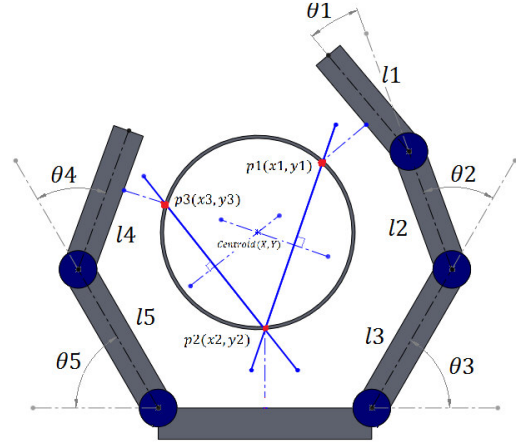


Figure 14. Centroid calculation method

The Fig. 14 shows the basic idea on how to plot the line to find the size of the object. When the sensors have determined the surface of the object, the gripper finger will halt. Based on the angle of the motor position halt, the point of P1, P2 and P3 on the surface of the object will be determined. This will pave the way to determine the P1 and P3 distance with the P2. Then, the middle of the distance between P1 and P2, P3 and P2 will be determined to plot a normal line. Both of the normal lines will be extend to the center of the object where these lines will intersect. This will give the centroid of the object. When the coordinate of the centroid point is determined, the distance between the centroid with P1, P2 or P3 will be used to determine radius. This will estimate the size of the object and the gradient between P1, P2 and P3

Searching equation:

$$ma = \frac{y2-y1}{x2-x1}, \quad (11)$$

$$mb = \frac{y3-y2}{x3-x2}. \quad (12)$$

Centroid, (X, Y);

$$X = \frac{ma.mb.(y1-y3)+mb.(x1+x2)-ma.(x2+x3)}{2(mb-ma)}, \quad (13)$$

$$Y = -\left(\frac{X - \frac{x1+x2}{2}}{ma}\right) + \frac{y1+y2}{2}, \quad (12)$$

$$radius, r = \sqrt{(X - x1)^2 + (Y - y1)^2} \quad (14)$$

VII. EXPERIMENT AND RESULT OF RADIUS CALCULATION

The result in Table II shows the result of the algorithm used to determine the radius. In this experiment, a white and a black cans with a diameter of 0.064m is used. It is noted that the SHARP GP2D120 need to be offset at least 0.025m distance from the base of the gripper. The purpose of offsetting the infrared distance detector to 0.025m is to eliminate the present of spike voltage from 0 to 0.03m in the IRDD as shown in Fig.7 and Fig 8.

TABLE II. EXPERIMENTAL WHITE CAN DIAMETER

<i>Distance (m)</i>	<i>Diameter Detected (m)</i>
0.015	0.067
0.020	0.063
0.025	0.060
0.030	0.059
0.035	0.058

TABLE III. EXPERIMENTAL BLACK CAN DIAMETER

<i>Distance (m)</i>	<i>Diameter Detected (m)</i>
0.015	0.069
0.02	0.066
0.025	0.062
0.03	0.057
0.035	0.053

As shown in the Table II, the near to zero error percentage in diameter calculation for white can is occurred at the distance of 0.02m from the base of the gripper. However, for black can calculation, the diameter at 0.02m is 0.066m which is less accurate compare to the white can due to the black surface which has absorbed part of the emitter light from reflecting back to the receiver diode in infrared distance detector. Therefore, the gripper is programed to detect the object at 0.02m before start to estimating the object size. This is used to obtain the near accurate information.

VIII. CONCLUSION

The use of embedded system in IVOARM is a new idea to enhance the capability of gripping process with or without the presence of the machine vision. Any weakness of the machine vision such as trouble of locating the object exactly or presence of ambient light that will cause the interference can be minimize by the sensors that mounted on the gripper. The infrared sensors mounted on the gripper

can be used to estimate the size of the object to acknowledge the system on proper method to grasp it.

IX. ACKNOWLEDGMENT

We would like to express our gratitude to for IPE Automation Sdn. Bhd. for funding us to complete mechanical design of IVOARM in order to achieve our objective. We would also like to thanks Agilent Technologies for lending us appropriate measurement equipments to obtain the data and result. We would like to express our special thanks to Universiti Tunku Abdul Rahman for nurturing and their relentless support toward us in completing this IVOARM.

X. REFERENCES

- [1] Blais, François; Beraldin, Jean-Angelo; Cournoyer, Luc; El-Hakim, Sabry; Picard, Michel; Domey, Jacques; Rioux, Marc, "The NRC 3-D Laser Tracking System: IIT's Contribution to the International Space Station Project" Proceedings of the 2001 Workshop of Italy-Canada on 3D Digital Imaging and Modeling Application, Italy April 2001.
- [2] Northern Digital Industry, "Machine Vision Technology," NDI website, 2011.
- [3] Anders Hagnelius , Supervisor Cs-umu , Niclas Börlin, "Visual Odometry," in CVPR IEEE Computer Society, pp. 652-659, Conference on Computer Vision and Pattern Recognition, 2004.
- [4] Marco Ceccarelli, "Fundamentals of Mechanics of Robotic Manipulation", Kluwer Academic Publishers, vol. XXVII, pp 246, 2004
- [5] Dlab, "Selection of DSPs" Dlab website, 2010, <http://www.dlab.ch/competences/selection-of-dsps.html>
- [6] Dean C.Karnopp, Donald L.Margolis, Ronald C. Rosenberg, "System Dynamics" in Modeling and Simulation of Mechatronics System, John Wiley & Sons Inc. vol. IV, 2006
- [7] Caihua Xiong, Han Ding, Youlun Xiong, "Fundamentals of Robotiv Grasping and Fixturing" World Scientific Publishers, vol. III, 2007
- [8] Václav KRYŠ, Tomáš KOT, Ján BABJAK, Vladimír MOSTÝN, "Testing and Calibration of IR Proximity Sensors" Acta Mechanica Slovaca, March 2008.
- [9] Susan J.Hall "Basic Biomechanicals" McGraw-Hill Education (Asia) Publisher, pp.165, Fifth Edition, ,2007
- [10] Xu DeZhang , YunJian Ge , Shen Fei , Wu Zhong Cheng , Gao LiFu, Nie Yuman, Tactile Sensing for "Underwater Operation System Based on Multi Finger Sensors Information Fusion", Proceedings of the 2005 IEEE International Conference on Information Acquisition, Hong Kong and Macau, China June 27- July 3, 2005.

REFERENCES

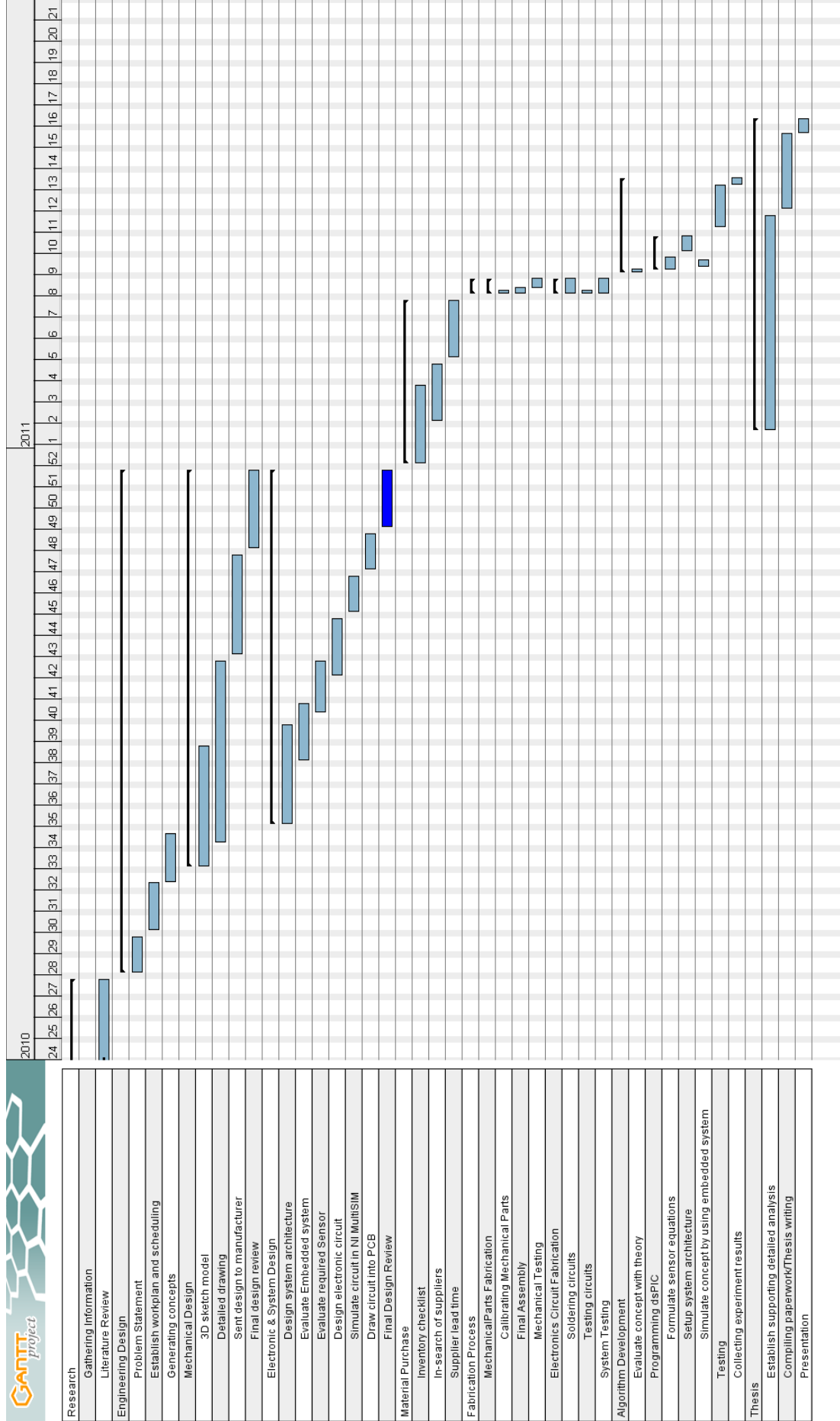
- 1) Blais, Fran çois; Beraldin, Jean-Angelo; Cournoyer, Luc; El-Hakim, Sabry; Picard, Michel; Domey, Jacques; Rioux, Marc. (2001). The NRC 3-D Laser Tracking System: IIT's Contribution to the International Space Station Project. Proceedings of the 2001 Workshop of Italy-Canada on 3D Digital Imaging and Modeling Application, Italy.
- 2) Northen Digital Industry. (2008). Machine Vision Technology. Retrieved October 2, 2010, from <http://www.ndigital.com/industrial/index.php>.
- 3) Anders Hagnelius, Supervisor Cs-umu, Niclas B örlin, Visual Odometry. (2004). in CVPR IEEE Computer Society, pp. 652-659, Conference on Computer Vision and Pattern Recognition.
- 4) Marco Ceccarelli. (2004). Fundamentals of Mechanics of Robotic Manipulation, Kluwer Academic Publishers, vol. XXVII, pp 246.
- 5) Dlab. (2010). Selection of DSPs. Dlab the digital laboratory website. retrieved August 6, 2010, from <http://www.dlab.ch/competences/selection-of-dsps.html>.
- 6) Dean C. Karnopp, Donald L. Margolis, Ronald C. Rosenberg. (2006). System Dynamics in Modeling and Simulation of Mechatronics System, John Wiley & Sons Inc. vol. IV.
- 7) Caihua Xiong, Han Ding, Youlun Xiong. (2007). Fundamentals of Robotic Grasping and Fixturing. World Scientific Publishers, vol. III.

- 8) Václav KRYS, Tomáš KOT, Ján BABJAK, Vladimír MOSTÝN. (2008). Testing and Calibration of IR Proximity Sensors. Acta Mechanica Slovaca.
- 9) Susan J.Hall. (2007). Basic Biomechanical. McGraw-Hill Education (Asia) Publisher, pp.165, Fifth Edition.
- 10) Xu DeZhang , YunJian Ge , Shen Fei , Wu Zhong Cheng , Gao LiFu, Nie Yuman. (2005). Tactile Sensing for Underwater Operation System Based on Multi Finger Sensors Information Fusion, Proceedings of the 2005 IEEE International Conference on Information Acquisition, Hong Kong and Macau, China June 27-July 3, 2005.
- 11) Zaki, A.M.; Soliman, A.M.; Mahgoub, O.A.; El-Shafei, A.M. (2010). High performance robotic gripper based on choice of feedback variables, Information and Automation (ICIA), 2010 IEEE International Conference on Conference on Digital Object Identifier: 10.1109/ICINFA.2010.5512336 , 54-59.
- 12) Anders Hagnelius, Supervisor Cs-umu , Niclas B örlin. (2004). Visual Odometry, CVPR IEEE Computer Society, 652-659, Conference on Computer Vision and Pattern Recognition.
- 13) Christophe Leroux, et al. (2007). Robot Grasping of Unknown Objects, Description and Validation of the Function with Quadriplegic People, Proceedings of the 2007 IEEE 10th International Conference on Rehabilitation Robotics.
- 14) Redwan Alqasemi, Sebastian Mahler, and Rajiv Dubey. (2007). Design and Construction of a Robotic Gripper for Activities of Daily Living for People with Disabilities. Proceedings of the 2007 IEEE 10th International Conference on Rehabilitation Robotics, June 12-15, Noordwijk, The Netherlands.
- 15) Marco Ceccarelli, (2004), Fundamentals of Mechanics of Robotic Manipulation, Kluwer Academic Publishers, vol. XXVII, pp 246, 2004.

- 16) SharpSMA. (2007). GP2D120 Data Sheet. Retrieved on March 21, 2011 from http://www.sharpsma.com/webfm_send/1205.
- 17) Vishay Semiconductors. (2011). Reflective Optical Sensor with Transistor Output. Retrieved March 21, 2011, from <http://www.vishay.com/docs/83760/tcrt5000.pdf>
- 18) Versa Point Technology. (2011). FSR 400 Data Sheet. Retrieved March 21, 2011 from http://www.drrobot.com/products/item_downloads/fsr400_2.pdf.
- 19) William A. Giovino. (2002). Microcontrollers and DSPs - Will the Two Worlds Intersect?. Microcontroller.com. retrieved April 07, 2011 from http://www.microcontroller.com/Microcontrollers_and_DSPs_Will_the_Two_Worlds_Intersect?.htm.
- 20) Richard L. Daft. (2008). "New Era of Management". South-Western Publisher. pg.76. 9th edition
- 21) H. M. Deitel, P. J. Deitel. (2005). C++: How To Program. Pearson International Edition. 5th edition.
- 22) Saeed B. Niku. (2006). Introduction to Robotics Analysis, Systems, Applications. Prentice Hall.
- 23) Drad Martin. (1998). Assembly Manual. Rice University. 2005. Retrieved April 05, 2011, from <http://www.clear.rice.edu/elec201/Book/assembly.html>.
- 24) Phil Loughhead. (2011). Tutorial - Getting Started with PCB Design. Altium Corporation. retrieved April 05, 2011, from <http://wiki.altium.com/display/ADOH/Tutorial+Getting+Started+with+PCB+Design>.

APPENDICE

APPENDIX A: Gantt Chart



APPENDIX B: PROGRAM SOURCE CODE OF IVOARM

MAIN PROGRAM

```

#if defined(__dsPIC33F__)
#include "p33fxxxx.h"
#endif

//-----math operation library-----
#include <stdio.h>
#include <math.h>
#include <dsp.h>
//-----

// Select the Board
#define __dsPICDEM1_1_BRD__ 0 // dsPICDEM Development Board
#define __EXPLORER16_BRD__ 1 // Explorer 16 Development Board

#include "LCD_demoBrd.h"
#include "LCD_exp16Brd.h"

#include "common.h"
#include "delay.h"

unsigned int valueA;
unsigned int valueB;
unsigned int valueC;
unsigned int valueD;
unsigned int valueE;

int end_indicator;

float IRDD_value, IRDD;

const int low_speed = 32000;
const int high_speed = 656;
unsigned int speed = 0;

//-----centroid configuration-----
double theta1;
double theta2;
double theta3;
double theta4;
double theta5;
double theta_p1 = 50; //fixed angle
double theta_p3 = 104; //fixed angle

double x1=0, x2=0, x3=0, x4=0, x5=0;
double y1=0, y2=0, y3=0, y4=0, y5=0;
double p1_x, p1_y, p3_x, p3_y;
double posx_origin = 34, negx_origin = -34;

//point 2 set as constant
double p2_x = 0, p2_y;
double ma = 0, mb = 0;
//define centroid x & y
double centroid_x=0, centroid_y=0;
double radius,diameter;

```

```

//robotic manipulator length configuration
double l1 = 40, l2 = 40, l3 = 50, l4 = 47, l5 = 50;

//-----

//Macros for Configuration Fuse Registers:
//Invoke macros to set up device configuration fuse registers.
//The fuses will select the oscillator source, power-up timers, watch-dog
//timers etc. The macros are defined within the device
//header files. The configuration fuse registers reside in Flash memory.

// Internal FRC Oscillator
_FOSCSEL(FNOSC_FRC);           // FRC Oscillator
_FOSC(FCKSM_CSECMD & OSCIOFNC_OFF & POSCMD_NONE);

// Clock Switching is Enabled and Fail Safe
Clock Monitor is disabled     // OSC2 Pin Function: OSC2 is Clock
Output                         // Primary Oscillator Mode: Disabled

_FWDT(FWDTEN_OFF);           // Watchdog Timer Enabled/disabled by user software

//----- main program -----
int main ( void )
{
// Configure Oscillator to operate the device at 40Mhz
// Fosc= Fin*M/(N1*N2), Fcy=Fosc/2
// Fosc= 8M*40/(2*2)=80Mhz for 8M input clock
    PLLFBD=38;                 // M=40
    CLKDIVbits.PLLPOST=0;      // N1=2
    CLKDIVbits.PLLPRE=0;      // N2=2
    OSCTUN=0;                  // Tune FRC oscillator, if FRC is used
    TRISE = 0X0000;
    TRISA = 0X0000;

// Disable Watch Dog Timer
    RCONbits.SWDTEN=0;

// Clock Switch to incorporate PLL
    __builtin_write_OSCCONH(0x01); // Initiate Clock Switch to

    // FRC with PLL (NOSC=0b001)
    __builtin_write_OSCCONL(0x01); // Start clock switching
    while (OSCCONbits.COSC != 0b001); // Wait for Clock switch to occur

// Wait for PLL to lock
    while(OSCCONbits.LOCK!=1) {};

//infrared detector input
    TRISDbits.TRISD0 = 1;
    TRISDbits.TRISD1 = 1;
    TRISDbits.TRISD6 = 1;
    TRISDbits.TRISD7 = 1;
    TRISDbits.TRISD8 = 1;
    TRISDbits.TRISD9 = 1;

//initialise ADC
    Init_ADC();

    /* Initialize Timer 1 for 32KHz real-time clock operation */
    Init_Timer1();
    /* Initialize INT1 pin used for setting Time-of-Day */
    Init_INTpin();

```

```

//-----main program run-----

while ( 1 )
{
    if(end_indicator==0)
    {
        initial_position();           //set position of IVOARM to initial position
        search_object();              //sub program to control IVOARM to search object
        calculation();                //sub program to calculate forward
        kinematic, centroid, radius adn diameter of object
        display_output();             //display diameter of object, commonly for experiment
        purpose
        grasping_method();           //sub program to perform different grasping method
        when the size of object has estimated
    }
    return 0;
}

void initial_position ()
{
    valueA = 49;                      //initial value of joint 1
    valueB = 49;                      //initial value of joint 2
    valueC = 68;                      //initial value of joint 3
    valueD = 49;                      //initial value of joint 4
    valueE = 30;                      //initial value of joint 5
    change_value1(valueA);           //substitutue value A into timer module
    change_value2(valueB);           //substitutue value B into timer module
    change_value3(valueC);           //substitutue value C into timer module
    change_value4(valueD);           //substitutue value D into timer module
    change_value5(valueE);           //substitutue value E into timer module
}

void search_object (void)
{
    // indicator for each search sequence
    int indicator1 = 1, indicator2 = 1, indicator3 = 1, indicator4 = 1, indicator5 = 1; //set all indicator to 1, indicator are use to stop servo
    when IROD detected object

    while(IRDD<50)                   //While Object are detected in range
    {
        while( PORTDbits.RD0 ==0 || PORTDbits.RD6==0)
        {
            int i,j,k,l,m;

            //-----right finger search -----
            for(i=65;i>49;i--);
            {
                if(indicator3==1)
                {
                    valueC = valueC - 1;
                    //if object not found, increase servo angle and keep searching
                    change_value3(valueC);
                    //M3 is move and search object
                    Delay(Delay_500mS_Cnt);
                }

                if(PORTDbits.RD1==1)
                {
                    PORTAbits.RA1=1;
                    indicator3=0;
                }
                else

```

```

    {
    PORTAbits.RA1=0;
    }

        if(valueC==59)
        {
            indicator3=0; //Trigger off indicator
        }
    IRDD_value = ADC1BUF0/124.0875;
    IRDD = 100*(pow((10.49/IRDD_value),1.0772379)); //equations for infrared distance detector
    if(IRDD>=50)
    {
        break;
    }
}

for(i=65;i>49;i--);
{
    if(indicator1==1 && indicator3==0)
    {
        valueA = valueA - 1;
        change_value1(valueA);
//M1 is move and search object
        Delay(Delay_500mS_Cnt);
    }

    if(indicator2==1 && indicator3==0)
    {
        valueB = valueB - 1;
        change_value2(valueB);
//M2 is move and search object
        Delay(Delay_500mS_Cnt);
    }

    if(PORTDbits.RD0==1 && indicator3==0)
    {
        PORTAbits.RA0=1;
        indicator1=0;
//Trigger off indicator
        indicator2=0;
    }
    else
    {
        PORTAbits.RA1=0;
    }

        if(valueA==30)
        {
            indicator1=0;
//Trigger off indicator
        }

        if(valueB==30)
        {
            indicator2=0;
//Trigger off indicator
        }
    IRDD_value = ADC1BUF0/124.0875;
    IRDD = 100*(pow((10.49/IRDD_value),1.0772379)); //equations for infrared distance detector
    if(IRDD>=50)
    {
        break;
    }
}

//----- left finger search -----

for(i=65;i>49;i--);
{

```

```

if(indicator4==1 && indicator1==0)
{
    valueD = valueD + 1;
    change_value4(valueD); //M1 is move and search object
    Delay(Delay_500mS_Cnt);
}

if(indicator5==1 && indicator1==0)
{
    valueE = valueE + 1;
    change_value5(valueE); //M2 is move and search object
    Delay(Delay_500mS_Cnt);
}

if(PORTDbits.RD6==1 && indicator1==0)
{
    PORTAbits.RA2=1;
    indicator4=0;
    indicator5=0;
}
else
{
    PORTAbits.RA2=0;
}

if(valueD==70)
{
    indicator4=0;
//Trigger off indicator
}

if(valueE==40)
{
    indicator5=0;
//Trigger off indicator
}

IRDD_value = ADC1BUF0/124.0875;
IRDD = 100*(pow((10.49/IRDD_value),1.0772379)); //equations for infrared distance detector
if(IRDD>=50)
{
    break;
}
end_indicator=1;
}

// for indicator purpose
if(PORTDbits.RD0==1)
{
    PORTAbits.RA0=1; // indicate presence of object on LED with ON
}
else
{
    PORTAbits.RA0=0; // indicate presence of object on LED with OFF
}

if(PORTDbits.RD1==1)
{
    PORTAbits.RA1=1; // indicate presence of object on LED with ON
}
else
{
    PORTAbits.RA1=0; // indicate presence of object on LED with OFF
}

if(PORTDbits.RD6==1)
{
    PORTAbits.RA2=1; // indicate presence of object on LED with ON
}
else

```

```

    {
        PORTAbits.RA2=0;                // indicate presence of object on LED with OFF
    }

//-----infrared distance detector-----
        IRDD_value = ADC1BUF0/124.0875;
        IRDD = 100*(pow((10.49/IRDD_value),1.0772379)); //equations for infrared distance detector
        p2_y = IRDD;
    }
if(end_indicator==1)
{
    break;
}
return;
}

//----- final output -----
void calculation (void)
{

theta1=(87-valueA)*2.368421053;        //convert value of each servo into angle
theta2=(87-valueB)*2.368421053;
theta3=(87-valueC)*2.368421053;
theta4=(87-valueD)*2.368421053;
theta5=(87-valueE)*2.368421053;

//-----MATH OPERATION-----

//all the value computed will be in ISO standrd (mm)

        theta1 = theta1 *(PI/180);        //convert degree into radian mode, use for calculation
        theta2 = theta2 *(PI/180);
        theta3 = theta3 *(PI/180);
        theta4 = theta4 *(PI/180);
        theta5 = theta5 *(PI/180);
        theta_p1 = theta_p1*(PI/180);
        theta_p3 = theta_p3*(PI/180);

//right gripper equation
        x3 = 13*cos(theta3)+ posx_origin;    //forward kinematic equation for right hand
        y3 = 13*sin(theta3);
        x2 = 12*cos(theta3+theta2) + x3;
        y2 = 12*sin(theta3+theta2) + y3;
        x1 = 11*cos(theta1+theta2+theta3) + x2;
        y1 = 11*sin(theta1+theta2+theta3) + y2;

//left gripper equation
        x5 = 15*cos(theta5)+ negx_origin;    //forward kinematic equation for left hand
        x4 = 14*cos(theta4+theta5) + x5;
        y5 = 15*sin(theta5);
        y4 = (14*sin(theta4+theta5)) + y5;

//three points to find centroid

        p1_x = 38*cos(theta3+theta2+theta_p1) + x2;
        p1_y = 38*sin(theta3+theta2+theta_p1) + y2;

        p3_x = -(27*cos(theta5+theta_p3) - x5);
        p3_y = (-27*sin(theta5+theta_p3)) + y5;

        ma = (p2_y - p1_y)/(p2_x - p1_x);

```

```

        mb = (p3_y - p2_y)/(p3_x - p2_x);

/*centroid calculation*/
centroid_x = (((ma*mb)*(p1_y-p3_y))+((mb)*(p1_x+p2_x))-((ma)*(p2_x+p3_x)))/(2*(mb-ma));
centroid_y = ((-1)*(centroid_x-(p1_x+p2_x)/2))/(ma)+((p1_y+p2_y)/2);

/*radius and diameter calculation*/
radius = sqrt((centroid_x - p1_x)*(centroid_x - p1_x) + (centroid_y - p1_y)*(centroid_y - p1_y));
diameter = radius*2;

//-----
return 0;
}

void display_output (void)
{
PORTA = radius*2;
}

void grasping_method()
{
    while(IRDD<50)
    {
        diameter = radius*2;
        if(diameter>=56) //grasping can method
        {
            valueA = 26;
            valueB = 36;
            valueC = 52;
            valueD = 76;
            valueE = 42;

            change_value1(valueA);
            change_value2(valueB);
            change_value3(valueC);
            change_value4(valueD);
            change_value5(valueE);

        }
        else if(diameter>40 && diameter<56) //grasping egg method
        {
            valueA = 65;
            valueB = 23;
            valueC = 49;
            valueD = 58;
            valueE = 49;

            change_value1(valueA);
            change_value2(valueB);
            change_value3(valueC);
            change_value4(valueD);
            change_value5(valueE);

        }
        IRDD_value = ADC1BUF0/124.0875;
        IRDD = 100*(pow((10.49/IRDD_value),1.0772379)); //equations for infrared distance detector
    }

//release object to prevent mechanical collision
    valueA = 49;//35
    valueB = 49;//42
    valueC = 68;//65
    valueD = 49;//65
    valueE = 30;//30

    change_value1(valueA);
    change_value2(valueB);
    change_value3(valueC);
    change_value4(valueD);
    change_value5(valueE);
}

```

SUB PROGRAM 1

SERVO CONTROL - INITIALISE TIMER

```

#if defined(__dsPIC33F__)
#include "p33fxxxx.h"
#endif

extern void enSecOsc();
unsigned int value1 = 26;           //M1 servo
unsigned int value2 = 36;           //M2 servo
unsigned int value3 = 49;           //M3 servo
unsigned int value4 = 76;           //M4 servo
unsigned int value5 = 42;           //M5 servo
unsigned int value6 = 0;
unsigned int value_new = 0;

//-----SAFETY VALUE-----
int min_value = 27;                // Program limit on servo control, make servo wont turn lesser or more than limitation
int max_value = 72;

//-----

/*-----
Function Name: Init_Timer1
Description: Initialize Timer1 for 1 second intervals
-----*/
void Init_Timer1( void )
{
    if(value1<min_value)            //limit at left angle
    {
        value1=min_value;
    }
    if(value1>max_value)           //limit at right angle
    {
        value1=max_value;
    }

    TICON = 0;                    // Timer reset
    IFS0bits.T1IF = 0;             // Reset Timer1 interrupt flag
    IPC0bits.T1IP = 4;             // Timer1 Interrupt priority level=4
    IEC0bits.T1IE = 1;            // Enable Timer1 interrupt

    PR1 = value1;                  // Timer1 period register = 32768
    T1CONbits.TCS = 1;            // Timer1 Clock= External

    enSecOsc();                    // Enable Secondary Osc
    T1CONbits.TON = 1;            // Enable Timer1 and start the counter
}

void Init_Timer2( void )
{
    if(value2<min_value)           //limit at left angle
    {
        value2=min_value;
    }
    if(value2>max_value)           //limit at right angle
    {
        value2=max_value;
    }

    TICON = 0;                    // Timer reset

```



```

        IFS0bits.T1IF = 0;           // Reset Timer1 interrupt flag
        IPC0bits.T1IP = 4;         // Timer1 Interrupt priority level=4
        IEC0bits.T1IE = 1;        // Enable Timer1 interrupt

        PR1 = value2;             // Timer1 period register = 32768
        T1CONbits.TCS = 1;        // Timer1 Clock= External

    enSecOsc();                   // Enable Secondary Osc
    T1CONbits.TON = 1;           // Enable Timer1 and start the counter
}

void Init_Timer3( void )
{
    if(value3<min_value)          //limit at left angle
    {
        value3=min_value;
    }
    if(value3>max_value)          //limit at right angle
    {
        value3=max_value;
    }

    T1CON = 0;                    // Timer reset
    IFS0bits.T1IF = 0;           // Reset Timer1 interrupt flag
    IPC0bits.T1IP = 4;           // Timer1 Interrupt priority level=4
    IEC0bits.T1IE = 1;           // Enable Timer1 interrupt

    PR1 = value3;                // Timer1 period register = 32768
    T1CONbits.TCS = 1;           // Timer1 Clock= External

    enSecOsc();                   // Enable Secondary Osc
    T1CONbits.TON = 1;           // Enable Timer1 and start the counter
}

void Init_Timer4( void )
{
    if(value4<min_value)          //limit at left angle
    {
        value4=min_value;
    }
    if(value4>max_value)          //limit at right angle
    {
        value4=max_value;
    }

    T1CON = 0;                    // Timer reset
    IFS0bits.T1IF = 0;           // Reset Timer1 interrupt flag
    IPC0bits.T1IP = 4;           // Timer1 Interrupt priority level=4
    IEC0bits.T1IE = 1;           // Enable Timer1 interrupt

    PR1 = value4;                // Timer1 period register = 32768
    T1CONbits.TCS = 1;           // Timer1 Clock= External

    enSecOsc();                   // Enable Secondary Osc
    T1CONbits.TON = 1;           // Enable Timer1 and start the counter
}

void Init_Timer5( void )
{
    if(value5<min_value)          //limit at left angle
    {
        value5=min_value;
    }

```

```

        if(value5>max_value)           //limit at right angle
        {
            value5=max_value;
        }

TICON = 0;                             // Timer reset
IFS0bits.T1IF = 0;                     // Reset Timer1 interrupt flag
IPC0bits.T1IP = 4;                      // Timer1 Interrupt priority level=4
IEC0bits.T1IE = 1;                     // Enable Timer1 interrupt

PR1 = value5;                           // Timer1 period register = 32768
T1CONbits.TCS = 1;                      // Timer1 Clock= External

enSecOsc();                             // Enable Secondary Osc
T1CONbits.TON = 1;                      // Enable Timer1 and start the counter
}

void Init_Timer6( int value6 )
{
    TICON = 0;                           // Timer reset
    IFS0bits.T1IF = 0;                   // Reset Timer1 interrupt flag
    IPC0bits.T1IP = 4;                   // Timer1 Interrupt priority level=4
    IEC0bits.T1IE = 1;                   // Enable Timer1 interrupt
    value_new = 656 - (value1 + value2 + value3 + value4 + value5); //3277 for low speed, 656 for high torque
    PR1 = value_new;                     // Timer1 period register = 32768
    T1CONbits.TCS = 1;                   // Timer1 Clock= External

    enSecOsc();                           // Enable Secondary Osc
    T1CONbits.TON = 1;                   // Enable Timer1 and start the counter
}

void change_value1( int valueA )
{
    value1 = valueA;
}
void change_value2( int valueB )
{
    value2 = valueB;
}
void change_value3( int valueC )
{
    value3 = valueC;
}
void change_value4( int valueD )
{
    value4 = valueD;
}
void change_value5( int valueE )
{
    value5 = valueE;
}

```

SUB PROGRAM

SERVO CONTROL –TIMER INTERRUPT

```

#if defined(__dsPIC33F__)
#include "p33fxxxx.h"
#endif

unsigned char indicator = 1;

/*-----
Function Name: _T1Interrupt
Description: Timer1 Interrupt Handler
-----*/

switch (indicator)
{
    case 1:
        PORTE = 0X01;//01 TIMER1
        Init_Timer2();
        indicator = 2;
        break;

    case 2:
        PORTE = 0X02;//02 TIMER2
        Init_Timer3();
        indicator = 3;
        break;

    case 3:
        PORTE = 0X04;//04 TIMER3
        Init_Timer4();
        indicator = 4;
        break;

    case 4:
        PORTE = 0X08;//08 TIMER4
        Init_Timer5();
        indicator = 5;
        break;

    case 5:
        PORTE = 0X10;//10 TIMER5
        Init_Timer1();
        indicator = 6;
        break;

    case 6:
        PORTE = 0X00;
        Init_Timer6();
        indicator = 1;
        break;
}
/* reset Timer 1 interrupt flag */
IFS0bits.T1IF = 0;
}

```

SUB PROGRAM

ADC – INITIALISE ADC

```
#include "p33FJ256GP710.h"
```

```

/*-----
Function Name: Init_ADC
Description: Initialize ADC module
Inputs:      None
Returns:     None
-----*/
void Init_ADC( void )
{
    /* set port configuration here */
    AD1PCFGLbits.PCFG0 = 0;    // ensure AN0/RB0 is analog (IRDD)
    AD1PCFGLbits.PCFG1 = 0;    // ensure AN1/RB1 is analog (FSR1)
    AD1PCFGLbits.PCFG2 = 0;    // ensure AN2/RB2 is analog (FSR2)
    AD1PCFGLbits.PCFG3 = 0;    // ensure AN3/RB3 is analog (FSR3)
    AD1PCFGLbits.PCFG4 = 0;    // ensure AN4/RB4 is analog (FSR4)
    AD1PCFGLbits.PCFG5 = 0;    // ensure AN5/RB5 is analog (FSR5)

    /* set channel scanning here, auto sampling and convert,
    with default read-format mode */
    AD1CON1 = 0x00E4;
    /* select 10-bit, 1 channel ADC operation */
    AD1CON1bits.AD12B = 1;

    /* enable DMA mode (ADC module sends all results
    to ADBUF0 and interrupts on each result */
    // AD1CON1bits.ADDMAEN = 1;

    /* No channel scan for CH0+, Use MUX A,
    SMP1 = 1 per interrupt, Vref = AVdd/AVss */
    AD1CON2 = 0x0000;

    /* Set Samples and bit conversion time */
    AD1CON3 = 0x032F;

    /* channel select*/
    AD1CHS0 = 0x0000;

    /* reset ADC interrupt flag */
    IFS0bits.AD1IF = 0;

    /* enable ADC interrupts, disable this interrupt if the DMA is enabled */
    IEC0bits.AD1IE = 1;

    /* turn on ADC module */
    AD1CON1bits.ADON = 1;
}

```

SUB PROGRAM

ISR ADC

```

#include "p33FJ256GP710.h"
#include "common.h"

volatile unsigned int temp1;
volatile unsigned char adc_update;

/*-----
Function Name: ADCInterrupt
Description:  ADC Interrupt Handler
-----*/
void __attribute__((__interrupt__)) _ADC1Interrupt( void )
{
    int count;

    /* Save off the data */
    temp1 = ADC1BUF0;

    /* set flag to update */
    adc_update = 1;

    /* reset ADC interrupt flag */
    IFS0bits.AD1IF = 0;
}

```

DELAY

```

#ifndef __DELAY_H__
#define __DELAY_H__

void Delay( unsigned int delay_count );
void Delay_Us( unsigned int delayUs_count );

#define Delay200uS_count 200
#define Delay_1mS_Cnt    1
#define Delay_2mS_Cnt    2
#define Delay_5mS_Cnt    5
#define Delay_15mS_Cnt   15
#define Delay_500mS_Cnt  500
#define Delay_1S_Cnt     1000

#endif

#ifdef __dsPIC33F
#include "p33fxxxx.inc"
#endif

.set Fcy,    40000000

.set US_K,   Fcy/1000000
.set MS_K,   Fcy/10000

    .global _Delay
    .global _Delay_Us

;=====
; ms Delay Function
;=====
_Delay:

ms_olloop:
    mov #MS_K,w1
ms_illoop:

```

```
nop
nop
nop
nop
nop
```

```
nop
nop
```

```
dec  w1,w1
bra  nz,ms_iloop
```

```
dec  w0,w0
bra  nz,ms_oloop
```

```
return
```

```
=====
; us Delay Function
;=====
```

```
_Delay_Us:
```

```
us_oloop:
```

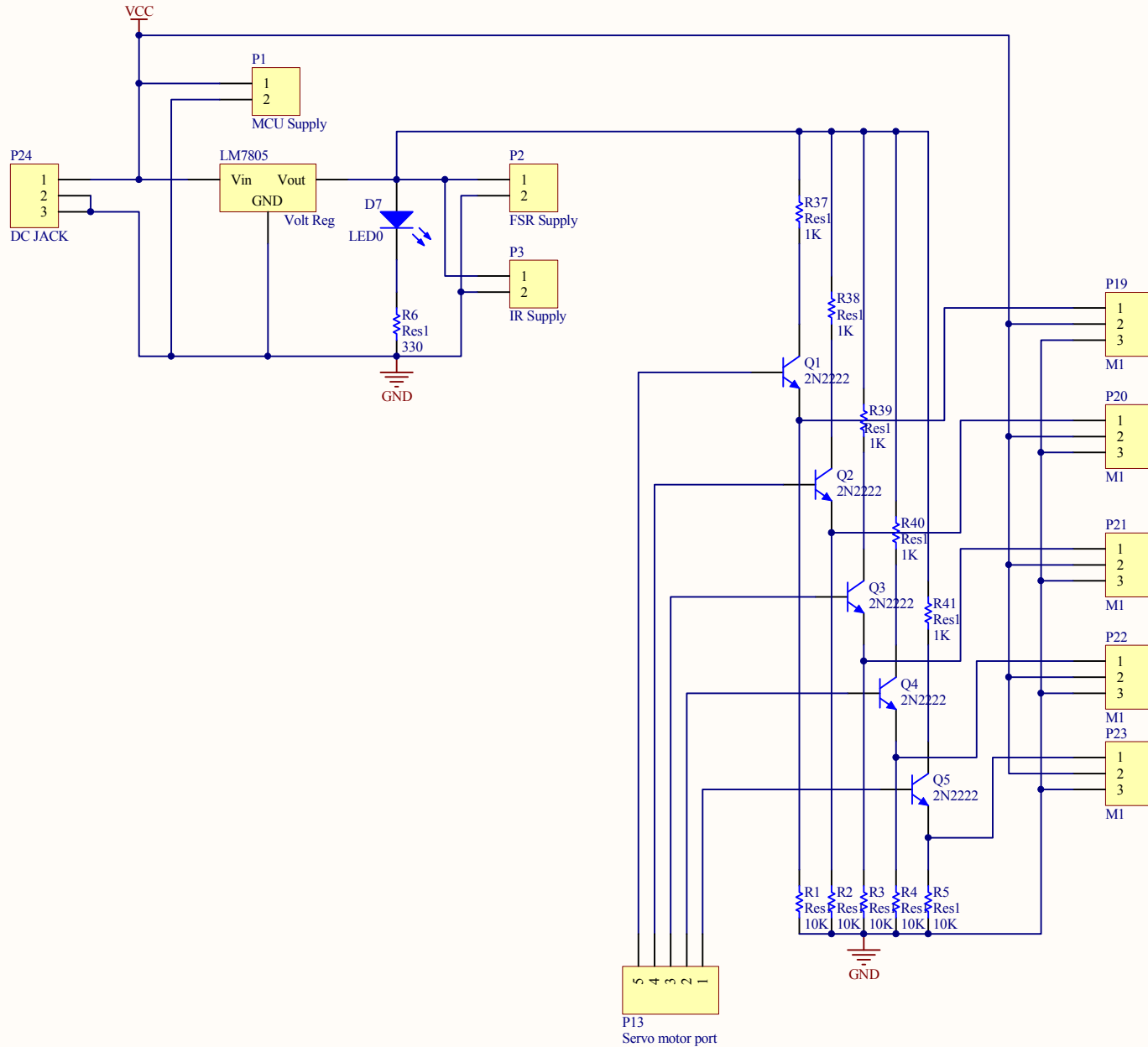
```
.rept (US_K-3)
nop
.endr
```

```
dec  w0,w0
bra  nz,us_oloop
```

```
return
```

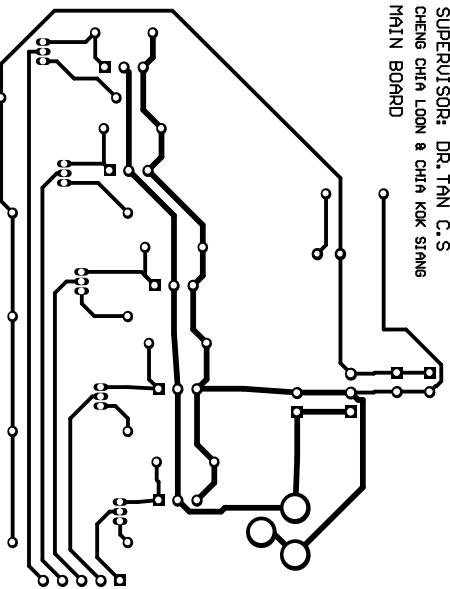
APPENDIX C

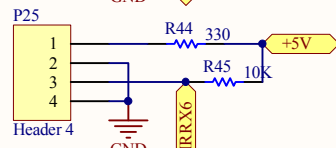
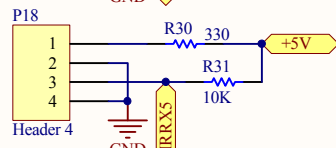
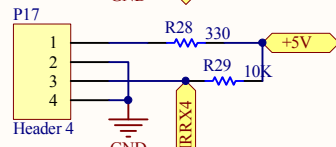
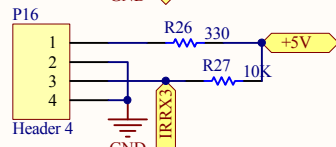
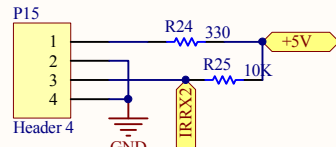
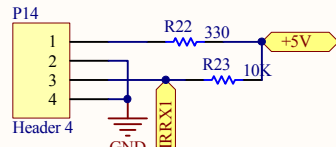
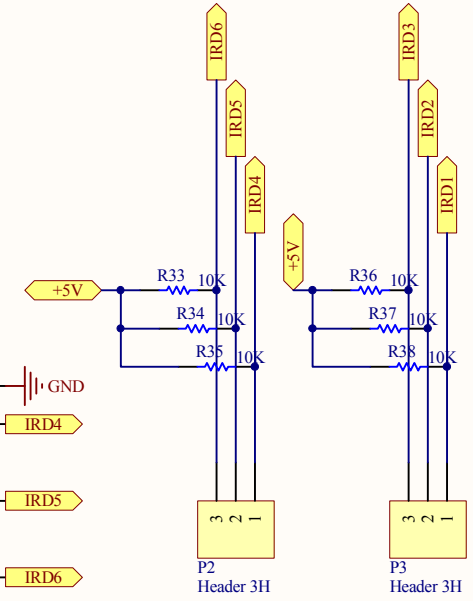
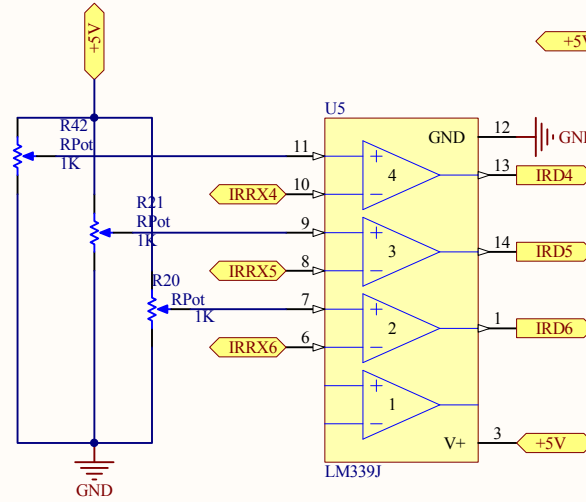
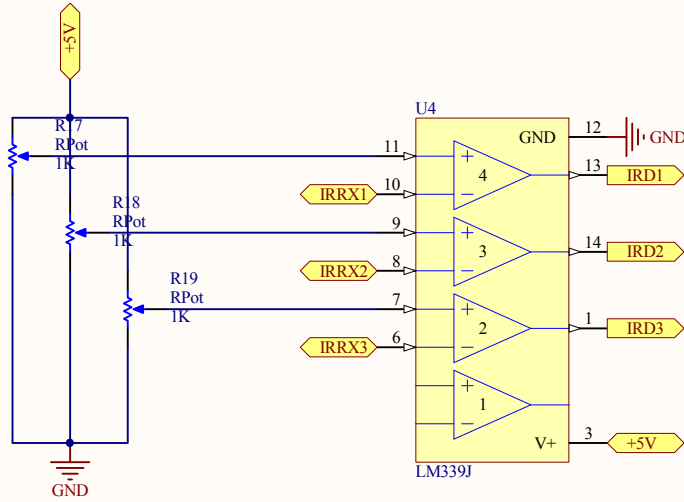
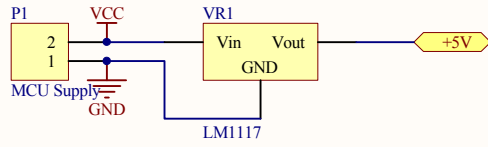
PCB Layout



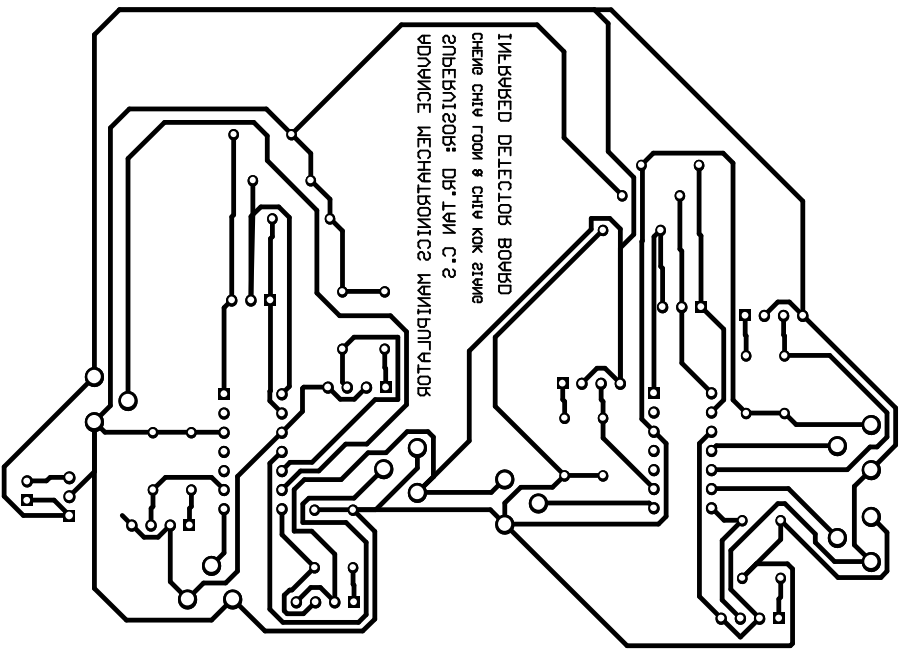
Title		
MAIN BOARD		
Size	Number	Revision
A4		
Date:	14/04/2011	Sheet of
File:	C:\Users\...\Main.SchDoc	Drawn By: CHENG CHIA LOON

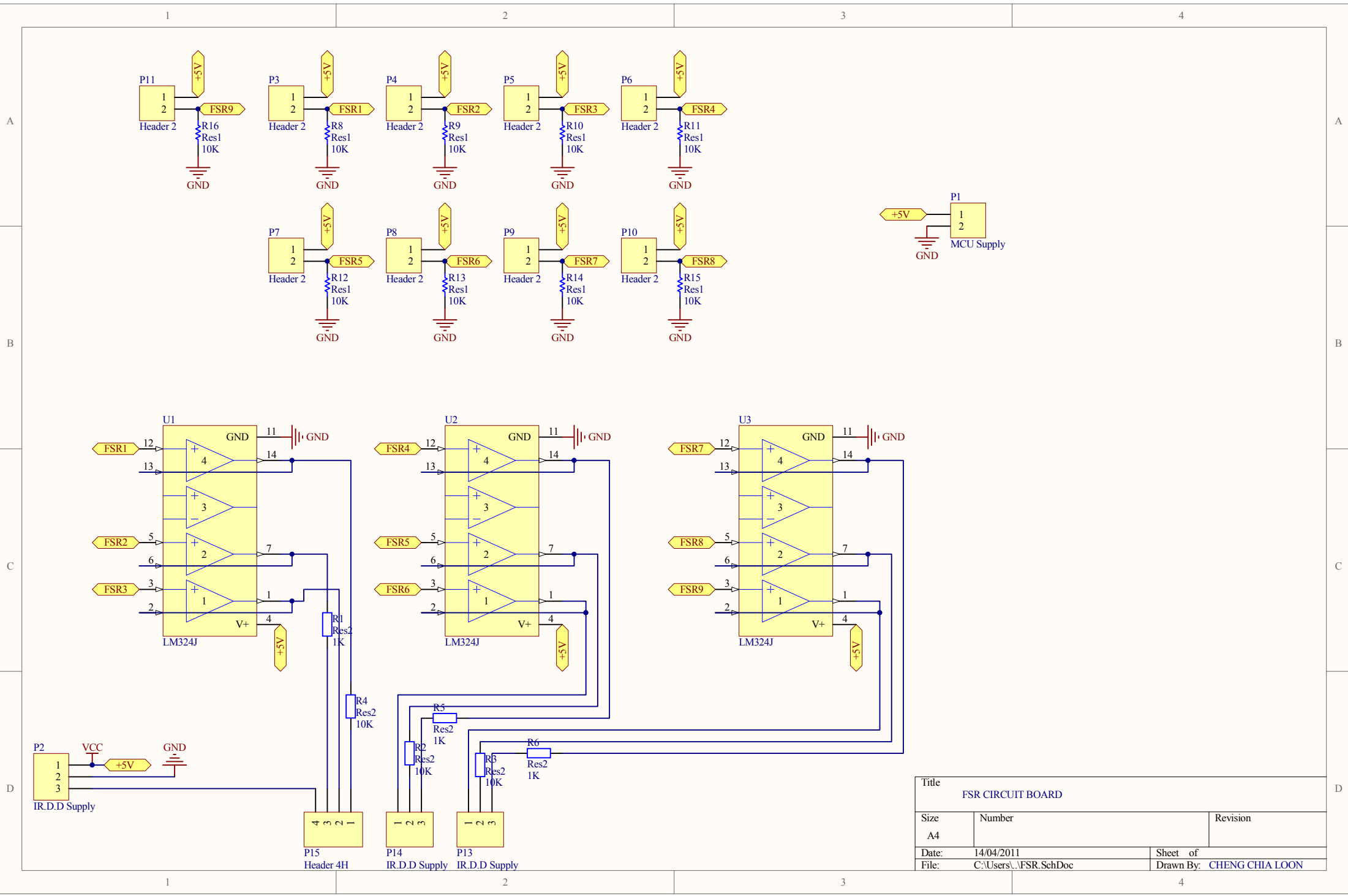
ADVANCE MECHATRONICS MANIPULATOR
SUPERVISOR: DR. TAN C.S
CHENG CHIA LOON & CHIA KOK SIANG
MAIN BOARD



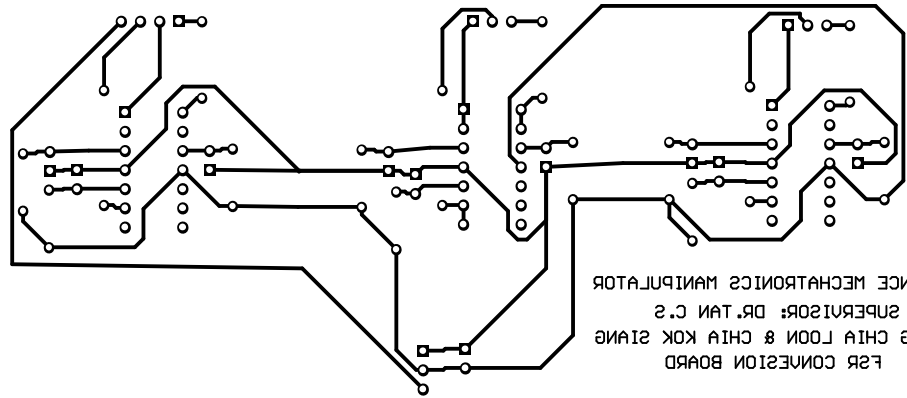


Title		
INFRA-RED OBJECT DETECTOR BOARD		
Size	Number	Revision
A4		
Date:	14/04/2011	Sheet of
File:	C:\Users\... \IRD.SchDoc	Drawn By: CHENG CHIA LOON





Title		
FSR CIRCUIT BOARD		
Size	Number	Revision
A4		
Date:	14/04/2011	Sheet of
File:	C:\Users\...\FSR.SchDoc	Drawn By: CHENG CHIA LOON



ADVANCE MECHATRONICS MANIPULATOR
SUPERVISOR: DR. TAN C.S.
CHENG CHIA LOON & CHIA KOK SIANG
FSR CONVERSION BOARD